



Norwegian University of
Science and Technology

Small scale experiments on severe slugging in flexible risers.

Eyamba Ita

Natural Gas Technology

Submission date: June 2011

Supervisor: Ole Jørgen Nydal, EPT

MASTEROPPGAVE

for

Student Eyamba Ita

Våren 2011

Småskalaforsøk med gas-væske slug strøm i fleksible stigerør

Small scale experiments on severe slugging in flexible risers

Background

Department of Marine Technology has long experience in modelling the dynamics of flexible risers connecting pipelines at sea bed to floating structures. The risers will move according to external forces from the surface vessel and from the sea currents.

The research group at the multiphase flow laboratory at EPT has experience with computational methods for the internal two phase flow in risers, including non-diffusive slug tracking methods.

An existing PhD is working on the dynamic coupling between structure models and internal flow models.

Some initial studies have been made as part of a student project in 2010. It was demonstrated that a small scale experimental setup can show the dynamic coupling between the internal flow and the flexible pipe. This provides a good starting point for a more extensive experimental work in MSc project. The initial tests were made in a shallow pool (1-2 m depth), further work can be made in a deeper pool (5-10 m depth)

Objectives

The objective of the work is to perform small scale experiments which can provide data for comparisons with numerical simulations

Tasks

The following tasks are expected:

1. Based on the previous experience: construct a small scale setup for severe slugging in the pool at Marintek
2. Install and qualify instrumentation (force gauges, pressure sensors, video/photo)
3. Perform experiments
4. If time permits: compare with numerical simulations
5. Report in a MSc thesis

Within 14 days of receiving the written text on the master thesis, the candidate shall submit a research plan for his project to the department.

When the thesis is evaluated, emphasis is put on processing of the results, and that they are presented in tabular and/or graphic form in a clear manner, and that they are analyzed carefully.

The thesis should be formulated as a research report with summary both in English and Norwegian, conclusion, literature references, table of contents etc. During the preparation of the text, the candidate should make an effort to produce a well-structured and easily readable report. In order to ease the evaluation of the thesis, it is important that the cross-references are correct. In the making of the report, strong emphasis should be placed on both a thorough discussion of the results and an orderly presentation.

The candidate is requested to initiate and keep close contact with his/her academic supervisor(s) throughout the working period. The candidate must follow the rules and regulations of NTNU as well as passive directions given by the Department of Energy and Process Engineering.

Pursuant to “Regulations concerning the supplementary provisions to the technology study program/Master of Science” at NTNU §20, the Department reserves the permission to utilize all the results and data for teaching and research purposes as well as in future publications.


One – 1 complete original of the thesis shall be submitted to the authority that handed out the set subject. (A short summary including the author’s name and the title of the thesis should also be submitted, for use as reference in journals (max. 1 page with double spacing)).

Two – 2 – copies of the thesis shall be submitted to the Department. Upon request, additional copies shall be submitted directly to research advisors/companies. A CD-ROM (Word format or corresponding) containing the thesis, and including the short summary, must also be submitted to the Department of Energy and Process Engineering

Department of Energy and Process Engineering, 10. January 2011



Olav Bolland
Department Head



Ole Jørgen Nydal
Academic Supervisor

Research advisors:

Arturo Ortega (PhD), prof. Carl Martin Larsen (Dpt Marine Technology)

PREFACE

This masters thesis is written at the Department of Energy and Process Technology at the Norwegian University of Science and Technology (NTNU) in Trondheim, spring 2011.

The thesis has included laboratory work and computational simulations. In the course of this thesis I have learnt a lot, within and outside my area of specialization and have gotten to work with very intelligent, extremely talented and wonderful people. With the help of these people, I have been able to overcome the challenges I have encountered.

I would like to thank God and my family for the support they have shown me through my academic journey, my supervisor Professor Ole Nydal and Co-supervisor Professor Carl Larsen, for their encouragement, support, knowledge and time. They are true giants in their areas of specialization and I have been extremely privileged to know and work with them.

I also want to thank Torgeir Wahl and Sverre Langolf of MarinTek for their immense assistance in helping me to set up my experiments in the laboratory pool, they made the experience fun and for this I am very grateful.

Finally, I would like to thank Doctor of Philosophy (Phd) students Tor Kjeldby and Arturo Ortega for their help and support on simulations and theories



Eyamba Ita. NTNU, Trondheim

ABSTRACT

Severe slugging is an undesirable unsteady multiphase flow phenomenon which occurs in riser-pipeline systems. During the course of this masters thesis work, a dynamic coupling has been shown to exist between this flow phenomenon and the flexible riser in which it occurs. To analyse the influence of this coupling, the cyclic displacement of the riser and the loads exerted by this cyclic displacement on the risers attachment point to a topside vessel have been evaluated.

A small scale experiment has been set up of a flexible riser (L and S configurations) undergoing the severe slugging cycle. The flexible risers were produced from a flexible transparent hose of internal diameter 0.016 metres and a load cell was used to measure the loads on the riser attachment point to a topside vessel. Three accelerometers were attached along the riser to measure the acceleration of the riser at defined points. The experiment was video recorded and from this, video analysis was used to calculate the displacement of the flexible riser during the severe slugging cycle. Data from the experiments was logged by Catman analysis tool and was compared with numerical simulations from OLGA.

Substantial displacement of the flexible riser has been recorded on both configurations of the flexible riser. Displacements in the order of approximately 1 metre have been recorded on some riser points on both riser configurations. When this occurs, there is a cyclic loading on the attachment point of the flexible riser to the topside vessel and this loading in the long term could lead to fatigue of the riser and probable failure. This loading has been illustrated, and maximum and minimum values for both riser configurations have been recorded.

For the constructed L-riser, the displacement of the riser at the top, middle and bottom sections were found to be 0.8588, 0.9760 and 0.5856 metres respectively. The maximum and minimum loads on the attachment points of the L-riser to the topside vessel during the severe slugging cycle have been found to be 0.1 and 6.4 Newtons respectively.

For the constructed S-riser, the displacement of the riser at the top, middle and bottom section were found to be 0.112, 0.7760 and 0.957 metres respectively. The maximum and minimum loads on the attachment point of the S-riser to the topside vessel during the severe slugging cycle have been found to be 8.0 and 13.6 Newton respectively.

NOMENCLATURE

Parameters

Q_g	Volumetric flow rate of gas (m^3/s)
Q_l	Volumetric flow rate of liquid (m^3/s)
A	Cross sectional area of the pipe (m^2)
A_L	Pipe area occupied by the liquid phase (m^2)
A_g	Pipe area occupied by the gas phase (m^2)
v_{sg}	Superficial velocity of the gas (m/s)
v_{sl}	Superficial velocity of the liquid (m/s)
v_m	Mixture velocity of the gas (m/s)
v_g	Phase velocity of the gas (m/s)
v_l	Phase velocity of the liquid (m/s)
V_g	Volume fraction of gas (-)
V_l	Volume fraction of liquid (-)
V_d	Volume fraction of droplets (-)
ρ_g	Density of gas (kg/m^3)
ρ_l	Density of liquid (kg/m^3)
ψ_e	Entrainment rates (-)
ψ_d	Deposition rates (-)
ψ_g	Mass transfer rates between the phases (kg/s)
G_g	Mass source for gas phase (kg)
G_l	Mass source for liquid phases (kg)
G_d	Mass source for droplets phase (kg)
λ_g	Friction factor of the gas phase (-)
λ_l	Friction factor of the liquid phase (-)
S_i	Wetted perimeter of the interface (m)
S_g	Wetted perimeter of the gas (m)
S_l	Wetted perimeter of the liquid (m)
F_d	Gas droplet drag term (N)

θ	Pipe inclination with the vertical (degrees)
Π_{ss}	Pots dimensionless number (-)
Z	Gas compressibility factor (-)
R	Gas universal constant (J/mol K)
T	Pipeline temperature (K)
M_g	Gas molecular weight (mol)
L	Pipeline length (m)
g	Acceleration due to gravity (m/s^2)
H_l	Average liquid hold up in the pipeline (-)
α	Gas fraction in the pipeline (-)
X	Slip ratio between phase velocities (-)
m_g	Mass of the gas (kg)
m_l	Mass of liquid (kg)
m_D	Mass of the droplets (kg)
E_g	Internal energy per unit mass of the gas (kJ/kg)
E_l	Internal energy per unit mass of the liquid (kJ/kg)
E_D	Internal energy per unit mass of droplets (kJ/kg)
H_s	Enthalpy from mass sources (kJ/kg)
U	Heat transfer from pipe walls (watt/ (m^2K))

ABBREVIATIONS AND ANNOTATIONS

NTNU	Norwegian University of Science and Technology
MARINTEK	Norwegian Marine Technology Research Institute
SINTEF	The Foundation For Scientific and Industrial Research.
OLGA	Oil and Gas simulation tool
PVT	Pressure, Specific volume and Temperature
MAXDT	Maximum Change in Time
MINDT	Minimum Change in Time
Catman	Computer aided testing, measurement and analysis tool

Table of Contents

1	INTRODUCTION	7
1.1	OBJECTIVE	7
1.2	BACKGROUND	8
2	THEORY	9
2.1	BASIC DEFINITIONS OF MULTIPHASE FLOW PARAMETERS	9
2.2	MULTIPHASE FLOW	10
2.3	CLASSES AND TYPES OF FLOW REGIMES	11
2.4	TYPES OF FLOWS	11
2.5	FIGURES OF FLOW REGIMES IN VERTICAL AND HORIZONTAL PIPES	12
2.6	FLOW REGIME MAPS	13
2.7	COMPUTATIONAL SIMULATION OF MULTIPHASE FLOW	14
2.7.1	MASS CONSERVATION EQUATIONS	15
2.7.2	MOMENTUM CONSERVATION EQUATION	15
2.7.3	ENERGY CONSERVATION EQUATION	16
2.8	OFFSHORE MARINE STRUCTURES	18
2.8.1	STRUCTURE OF A FLEXIBLE MARINE RISER	19
2.8.2	TYPES OF FLEXIBLE MARINE RISER	20
2.8.3	COMPUTATIONAL SIMULATION OF FLEXIBLE RISERS	22
2.8.4	EQUATION OF RISER HORIZONTAL MOTION ¹⁷	23
2.9	SEVERE OR TERRAIN INDUCED SLUGGING	26
2.9.1	SEVERE SLUGGING MECHANISM	27
2.9.2	PREDICTING ONSET OF SEVERE SLUGGING	28
2.9.3	EFFECTS OF SEVERE SLUGGING:	28
3	EXPERIMENT	29
3.1	MODIFICATIONS FROM PRECEEDING PROJECTS	29
3.2	EXPERIMENT SET UP	30
3.2.1	GEOMETRY AND DIMENSIONS OF THE EXPERIMENT POOL	30
3.2.2	DIMENSIONS OF THE POOL	31
3.2.3	EQUIPMENTS AND INSTRUMENTATION	31
3.2.4	MOBILE TWO-PHASE FLOW LOOP	32
3.2.5	DATA ACQUISITION SYSTEM	32
3.2.6	GEOMETRY AND PROPERTIES OF THE FLEXIBLE HOSE	33

3.3	EXPERIMENT PROCEDURE	34
3.3.1	SAMPLING DIRECTION OF ACCELEROMETERS	35
3.3.2	RISER CONFIGURATIONS.....	36
3.3.3	SECTION A DIMENSIONS	39
3.3.4	S-CASE SECTION B DIMENSIONS	41
3.3.5	PRINCIPLE OF RESOLUTION OF FORCES ACTING ON POINT OF ATTACHMENT OF MARINE RISER TO TOPSIDE VESSEL.	43
4	OLGA VERIFICATION.....	44
4.1	OLGA CASE DESCRIPTION.....	44
4.1.1	OLGA L-RISER NUMERICAL SIMULATION	45
4.1.2	OLGA S RISER NUMERICAL SIMULATION.	47
5	RESULTS AND DISCUSSIONS.....	48
5.1	L-RISER RESULTS.....	48
5.1.1	SEVERE SLUGGING IN L-RISER EXPERIMENTAL RESULTS	49
5.1.2	SEVERE SLUGGING IN L-RISER OLGA SIMULATION RESULTS	53
5.1.3	RESULTS OBTAINED FROM CALCULATIONS FOR THE L- RISER.	59
5.2	LAZY S RISER RESULTS:	60
5.2.1	SEVERE SLUGGING IN S-RISER EXPERIMENTAL RESULT	61
5.2.2	SEVERE SLUGGING IN LAZY S-RISER OLGA SIMULATION RESULTS	65
5.2.3	RESULTS OBTAINED FROM CALCULATIONS FOR THE S- RISER.	71
5.3	CHALLENGES ENCOUNTERED DURING THE EXPERIMENTS	72
6	CONCLUSION.....	74
7	REFERENCES	76
8	Appendices.....	78

List of Figures

Figure 1 Flow regimes in Vertical pipes, gas-liquid upflow. Source: Two Phase flow in vertical in vertical diameter risers. PHD Thesis. S.F. Ali. Cranfield University.....	13
Figure 2 Flow regimes in horizontal gas-liquid flow. Source: Two Phase flow in vertical in vertical diameter risers. PHD Thesis. S.F. Ali. Cranfield University.....	13
Figure 3 Flow regime map for Vertical Pipes. Source: Ole Jørgen Nydal. Lecture Notes for multiphase flow Handouts 2010.....	14
Figure 4 Flow regime map for Horizontal Pipes. Source: Ole Jørgen Nydal. Lecture Notes for multiphase flow Handouts 2010.....	14
Figure 5 Typical Cross section of flexible pipe. Source: Yong Bai, Qiang Bai Subsea Engineering Handbook.....	19
Figure 6 Main configurations of flexible production risers. Source: Yong Bai, Qiang Bai. Subsea Pipeline and Risers.....	20
Figure 7 Model of a marine riser showing external forces. Image modified from: <i>The Study on Vibration of Marine Riser Under Deep Water</i>	21
Figure 8 Sketch of free hanging riser conveying fluid. Image copied from: Stability of offshore risers conveying fluid. PHD thesis. Guido Kuiper. T.U Delft. January 2008.....	23
Figure 9 Description of severe slugging cycle. Source: Xu, Z. G.: Solutions to Slugging Problems Using Multiphase Simulations. <i>3rd Int. Conf. Multiphase Metering</i> , Aberdeen, United Kingdom (1997).....	27
Figure 10 Aerial view of experiment pool.....	30
Figure 11 Connection from Mobile two-phase flow loop to riser.	32
Figure 12 Position of gas-liquid mixer and pressure sensor.....	34
Figure 13 Method of attachment of accelerometer to flexible hose.....	35
Figure 14 Illustration of sampling direction of accelerometers relative to position of flexible hose.....	35
Figure 15 L-Riser geometry and experimental setup	37
Figure 16 Topside section of experiment setup showing separator and load cell attachment points	38
Figure 17 Close up of attachment point to load cell.	38
Figure 18 Geometry of Section A.....	39
Figure 19 S-Riser geometry and experimental setup	40
Figure 20 Geometry of Section B from S- riser.	41
Figure 21 Direction of acting forces on point of attachment.	43

Figure 22 L-riser geometrical description in OLGA	46
Figure 23 S-riser geometrical description in OLGA.....	47
Figure 24 L-riser inlet Pressure	49
Figure 25 Acceleration curves of a point at the top of the L-riser during cycles.....	49
Figure 26 Acceleration of a point at the middle of the L-riser during the cycles	50
Figure 27 Acceleration of a point at the bottom of the L-riser during the cycles.	50
Figure 28 Force induced by the L-riser on the point of attachment during the cycle in the Z direction.....	51
Figure 29 Force induced by the L-riser on the point of attachment during the cycle in Y direction	51
Figure 30 Resultant Force on point of attachment by displacement cycles of the L-riser.....	52
Figure 31 L-Riser Inlet Pressure (OLGA).....	53
Figure 32 Superficial gas velocity (OLGA)	53
Figure 33 Superficial liquid velocity (OLGA).....	54
Figure 34 Liquid Hold up in L-riser (OLGA).....	54
Figure 36 L-Riser final position (at complete liquid fill-up of column)	56
Figure 35 L-Riser initial position (at end of previous cycle).....	56
Figure 37 Method of calculating displacement of L-Riser at defined points.....	57
Figure 38 S-Riser Inlet Pressure.	61
Figure 39 Acceleration of a point at the top of the S-riser during cycles.....	61
Figure 40 Acceleration of a point at the middle of the S-riser during the cycles.....	61
Figure 41 Acceleration of a point at the bottom of the S-riser during cycles	62
Figure 42 Force induced by the S-riser on the point of attachment during the cycle in Z direction.....	62
Figure 43 Force induced by the S-riser on the point of attachment during the cycle in Y-direction.....	63
Figure 44 Resultant Force on point of attachment by displacement cycles of the S-riser.....	63
Figure 45 S-Riser Inlet Pressure	65
Figure 46 Superficial Velocity of gas (OLGA).....	65
Figure 48 Liquid Hold-up in S- riser (OLGA)	66
Figure 47 Superficial velocity of liquid (OLGA)	66
Figure 49 S-riser initial position (at end of previous cycle)	68

Figure 50 S-riser final position (at complete liquid fill up of column)68
Figure 51 Method of calculating displacement of S-riser at defined points.69

List of Tables

Table 1: Principle of multiphase flow models.....	17
Table 2: Dimensions of experiment pool.....	31
Table 3: Geometry of the flexible hose.	33
Table 4: Properties of Brass rings.	34
Table 5: Properties of liquid supply line from pump to mixing point.....	36
Table 6: Properties of gas supply line from buffer tank to mixing point.....	36
Table 7: Properties of Lead rings.	41
Table 8: Properties of colorant	42
Table 9: Brand, Model, FPS and resolution of video camera	43
Table 10: L-riser FLOWPATH co-ordinates.....	45
Table 11: S-riser FLOWPATH co-ordinates.....	47
Table 12: L- Riser experiment flow rates.	48
Table 13: Displacement of defined points on L-riser.....	58
Table 14: Final Results of L-riser.	59
Table 15: S-riser experiment Flow rates.	60
Table 16: Displacement of defined points on S-riser.....	70
Table 17: Final S-riser results.	71

1 INTRODUCTION

This master thesis is written as part of the final year curriculum in the master program at the Norwegian University of Science and Technology. It represents the largest task during the duration of the master program and accounts for 25 percent of the total required credit units. The experimental work for this thesis was carried out in one of the pools at the MARINTEK (SINTEF) /NTNU hydrodynamic laboratory. The thesis has been supervised primarily by Professor Ole Nydal (Department of Energy and Process Technology, NTNU) in collaboration with Professor Carl Larsen (Department of Marine Technology, NTNU). Assistance was provided by doctorate students Tor Kjeldby (Department of Energy and Process Technology, NTNU) and Arturo Ortega (Department of Marine Technology, NTNU).

1.1 OBJECTIVE

The main objective of this master thesis is to perform small scale experiments on severe slugging in flexible risers to demonstrate the dynamic coupling between the internal flow and flexible riser structure and provide data for numerical simulations. To carry out this objective, subtasks are defined. These subtasks include the construction of a small scale setup of a flexible riser undergoing the severe slugging cycle, installations and qualifications of instrumentation, acquisition of data and if time permits comparison with numerical simulations.

1.2 BACKGROUND

Diminishing hydrocarbon discoveries, economical restraints, improved subsea technology are driving exploration and production of oil and gas in deeper waters (depths greater than 1000feet¹). This has given rise to the frequent use of floating production units for offshore development of oil and gas fields. Floating production units are not bottom supporting structures like conventional concrete or steel leg platforms and their excessive motions generate problems for conventional tensioned steel production risers. To mitigate this problem, flexible production risers (hereafter referred to as “flexible risers”) are used because they can accommodate larger vessel offsets. The configuration of the flexible riser is determined by production requirements, site specific environmental conditions and static analysis.

The internal flow in such a flexible riser can be of different forms (bubble, slug, annular or at the riser base stratified). All these flow regimes will induce different dynamic behaviours in flexible risers and would require individual experiments to investigate. This thesis however, seeks to demonstrate and highlight the dynamic coupling between the flexible riser (marine structure) and the flow phenomenon referred to as “severe or riser based slugging”.

This flow phenomenon is a combination of stratified flow in the upstream region (or lower base section) of the riser and slug flow in the downstream (upper section) region of the riser during blowout. This flow phenomenon has been chosen because of its potential to induce fatigue on the point of attachment of the flexible riser to a topside vessel, due to its cyclic nature. All flexible risers have a similarity. This is the presence of a low point in their geometry where liquid can accumulate and this makes them susceptible to the severe slugging phenomenon.

The department of Marine Technology at the Norwegian University of Science and Technology has experience in modelling the dynamics of flexible risers connecting pipelines at sea bed to floating structures. The research group at the multiphase flow laboratory at the department of Energy and Process Technology at the Norwegian University of Science and Technology have experience with computational methods for the internal two phase flow in risers including non diffusive slug tracking methods. Together they aim to create an interface model which can simulate the interaction between the internal flow conditions present in a flexible riser and the risers’ dynamics.

2 THEORY

2.1 BASIC DEFINITIONS OF MULTIPHASE FLOW PARAMETERS

This section aims to provide the reader with a basic knowledge of multiphase flow parameters and terminologies, so as to understand their application in subsequent chapters of this masters thesis.

Superficial velocity: This is defined as the average instantaneous velocity the phase (liquid or gas) would have, if only it occupied the whole cross sectional area of the pipe.²

$$v_{sg/sl} = \frac{Q_{g/s}}{A} \dots\dots(1)$$

Holdup: is defined as the fraction of an element of pipe which is occupied by liquid at same instant².

$$H = \frac{A_L}{A} \dots\dots(2)$$

Void fraction: Is defined as the fraction of an element of pipe which is occupied by gas at same instant³.

$$\alpha = \frac{A_g}{A} \dots\dots(3)$$

Phase velocity: Is defined as the volumetric flow per phase area. This is the actually flowing velocity of the phase in the pipe at same instant³.

$$v_{g/l} = \frac{Q_{g/l}}{A_{g/l}} \dots\dots(4)$$

Mixture velocity: is defined as the sum total of the volumetric flux in the pipe³.

$$v_m = v_{sg} + v_{sl} \dots\dots(5)$$

Slip: Term used to describe the flow conditions that exist when the phases have different velocities at a cross-section of a conduit. The slip may be quantitatively expressed by the phase velocity difference between the phases⁴. Slip ratio between the phase velocities can be defined as:

$$X = \frac{v_g}{v_l} \quad \dots\dots(6)$$

2.2 MULTIPHASE FLOW

A phase is defined as a class of matter with a defined boundary and a particular dynamic response to the surrounding flow/potential field.⁵

Multiphase flow implies two or more fluids of coexisting matter in motion; it could imply difference in thermodynamic state of the fluids or multiple chemical components like emulsion and slurries. Produced fluids from reservoirs are mostly multiphase in nature, although due to the ratios of phases present, some reservoirs could be considered to be single phase. This implies that what is generally referred to as a gas well have liquid phases present and vice versa in addition to some solid phases.

A number of reservoirs however have relatively high ratios of liquid and gas phases and this is reflected in the production rates of both phases. The produced fluids are described as being in "multiphase conditions". The complexity of multiphase flows means that single phase characteristics are insufficient for describing the nature of these flows. An example of such complexity is the infinite number of possible forms the gas liquid interfacial distribution could assume in a given channel.

The structures of these flows are best described in flow regimes or flow patterns, which are defined as the description of the geometrical distribution of a multiphase fluid moving through a pipe conduit⁶. Flow regimes vary depending on operating conditions, fluid properties, fluid flow rates, and the orientation and geometry of the pipe through which the fluid flows⁷. They are usually determined visually, but other methods such as analysis of the spectral content of the unsteady pressures or the fluctuations in the volume fraction of the phases have also been devised, for situations where visual observation is limited.⁸

A number of investigations have been conducted to determine the dependence of flow regimes on component volume fluxes, on volume fraction and on the fluid properties such as density, viscosity and surface tension. The results are often displayed in the form of flow regime maps that identify the flow patterns occurring in various parts of a parameter space defined by the component flow rates⁹.

2.3 CLASSES AND TYPES OF FLOW REGIMES

There exist two main classes of flow regimes. They include³:

- Mixed flow regimes:

These are flow regimes with strongly coupled (non-separated) phases. They primarily include bubble, slug and churn flows.

- Separated flow regimes:

These are flow regimes with non-coupled (clearly separated) phases. They primarily include stratified and annular flows.

2.4 TYPES OF FLOWS

Bubbly flow: In such flows, gas is dispersed in the continuous liquid phase. This flow can be further classified as dispersed bubbly flow and low liquid input bubbly flow⁸.

- Dispersed bubbly flow: This type of flow is realised over the whole pipe diameter range and inclination. The gas phase is dispersed as small discrete bubbles in a continuous liquid phase⁸.
- Low liquid input bubbly flow: This type of flow is realised due to low liquid superficial velocity and the existence of gas bubbles of approximately same sizes which are evenly distributed in the liquid phase with some occasional coalescence in the core⁸.

Slug flow: This type of flow exists as sequences of Taylor bubbles and liquid slugs. It occurs at moderate velocities of liquid and gas. Taylor bubbles are of equivalent cross section as that of the tube, being separated from the wall by a thin liquid film. The two consecutive Taylor bubbles are separated by a liquid slug that may contain small air bubbles which are being shed from the tail of the leading Taylor bubble^{3,8}.

Churn/ froth flow: As the gas superficial velocity is increased in slug flow regime, the Taylor bubble becomes more distorted at liquid-gas interface. The distorted bubble travels in

churning motion giving rise to irregular shaped portions of gas and liquid. This flow is also referred to as froth slug, dispersed slug, churn-turbulent flow or pulsating annular flow.

Annular flow: Such flow exists with the liquid phase flowing largely as an annular film on the pipe wall with gas flowing as a central core, with some of the liquid entrained as droplets in the gas core⁷. There are two variation of this flow namely;

- Wispy annular flow: Here entrained liquid is present as relatively large drops and liquid film will contain gas bubbles⁸.
- Annular mist flow: Here gas occupies the centre of the core while liquid flows along the periphery. The core gas will contain the liquid entrainment but the drops size is not large⁸.

Stratified flow: This flow consists of two superposed layers of gas and liquid, formed by segregation under the influence of gravity. It may exist as smooth and wavy⁸.

- Stratified smooth flow: Here the liquid-gas interface is smooth⁸.
- Stratified wavy – Here the liquid wave amplitude increases (forming ripples and rolls) as the gas superficial velocity is increased, so that smooth interface transforms into waves⁸.

2.5 FIGURES OF FLOW REGIMES IN VERTICAL AND HORIZONTAL PIPES

Pipe inclination plays a fundamental role in the fluid flow regime. With increasing pipe inclination from horizontal to vertical, stratified flow gradually tends to disappear, and it is possible to identify another regime “churn flow” which exists as irregular slugs of gas moving up the centre of the pipe, carrying droplets of oil or water with them. Unlike slug flow, neither phase in churn flow is continuous. Figure 1 and Figure 2 illustrate the flow regimes in vertical and horizontal pipes.

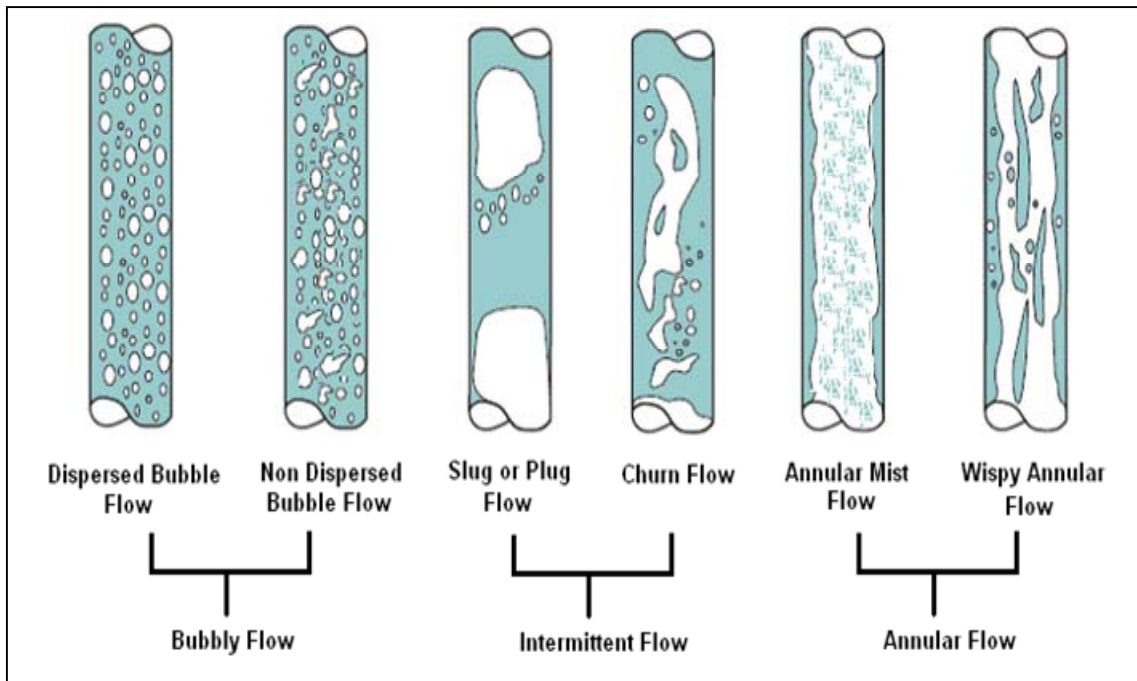


Figure 1 Flow regimes in Vertical pipes, gas-liquid upflow. Source: Two Phase flow in vertical in vertical diameter risers. PHD Thesis. S.F. Ali. Cranfield University

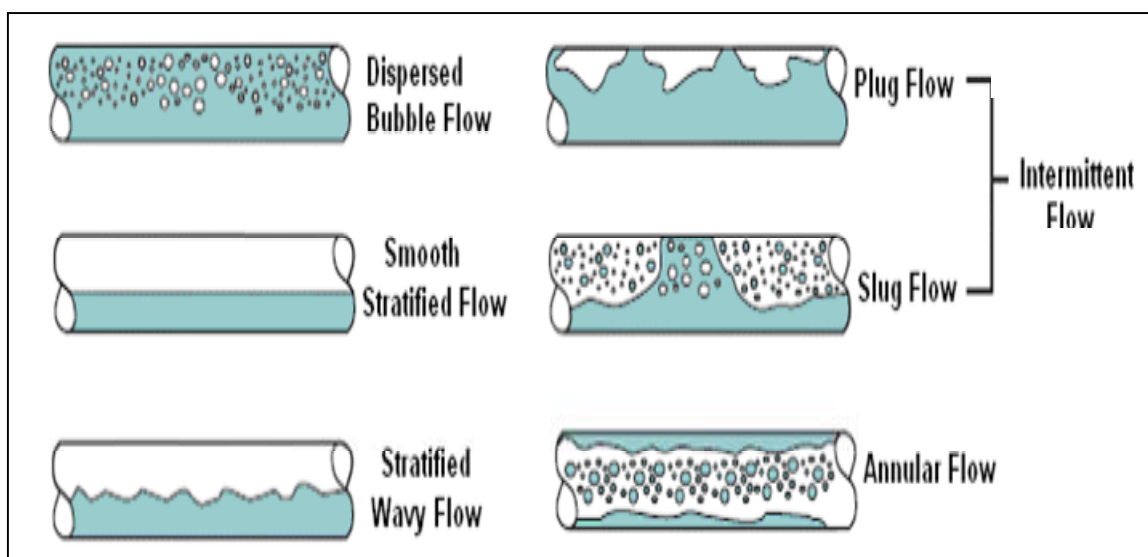


Figure 2 Flow regimes in horizontal gas-liquid flow. Source: Two Phase flow in vertical in vertical diameter risers. PHD Thesis. S.F. Ali. Cranfield University

2.6 FLOW REGIME MAPS

In order to predict the existence of a particular flow regime, flow regime maps are used. There exists numerous types of flow regime maps, due to the difference in boundary conditions like pipe diameter, inclination and empirical correlations used during experiments for the generation of these maps.

Most regime maps are based on the superficial velocities of the phases (i.e. The liquid superficial velocity on the x-axis and the gas superficial velocity on the y- axis), but other maps exists with parameters other than superficial velocities like the Froude number and ratio of the volumetric flow rates of liquid and gas¹⁰. Figures 3 and 4 illustrate the regime maps in vertical and horizontal pipes.

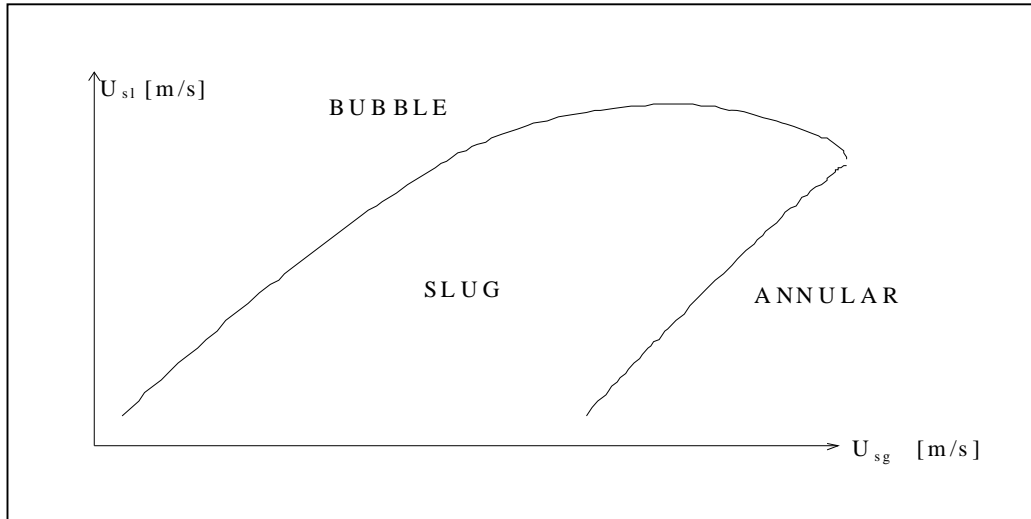


Figure 3 Flow regime map for Vertical Pipes. Source: Ole Jørgen Nydal. Lecture Notes for multiphase flow Handouts 2010

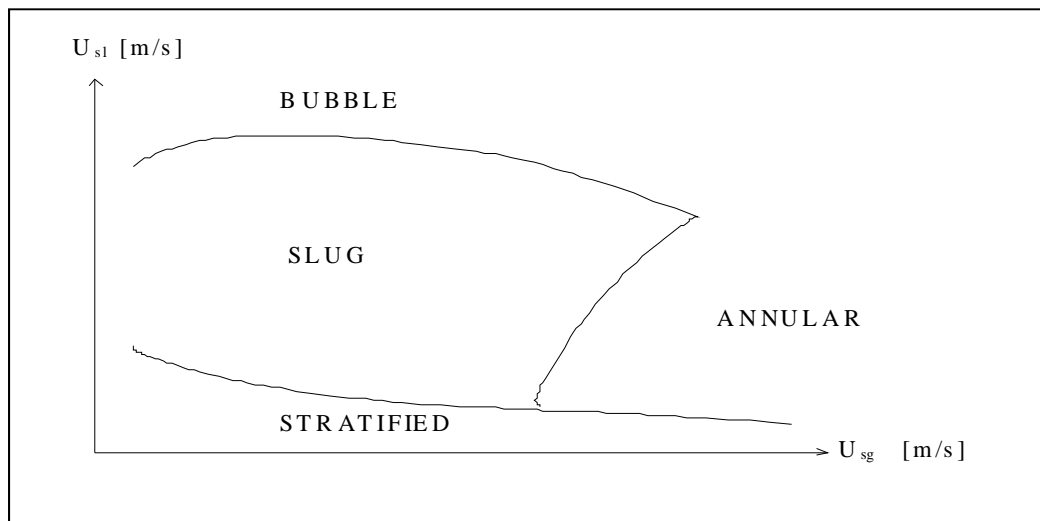


Figure 4 Flow regime map for Horizontal Pipes. Source: Ole Jørgen Nydal. Lecture Notes for multiphase flow Handouts 2010

2.7 COMPUTATIONAL SIMULATION OF MULTIPHASE FLOW

Tools for simulation and computation of multiphase flow are quite available nowadays. Their basic fundamental principles are based on solving the mass, momentum and energy

conservations for the phases present. These simulation tools differ from each other by areas and methods of implementation these equations. The conservation equations stated below are however the basis of the code for the OLGA (Oil and GAs) simulation tool¹¹.

2.7.1 MASS CONSERVATION EQUATIONS

The gas equation is defined by equation 7:

$$\frac{\partial}{\partial t}(V_g \rho_g) = -\frac{1}{A} \frac{\partial}{\partial t}(AV_g \rho_g v_g) + \psi_g + G'_g \quad \text{.....(7)}$$

The bulk liquid equation is defined by equation 8:

$$\frac{\partial}{\partial t}(V_l \rho_l) = -\frac{1}{A} \frac{\partial}{\partial t}(AV_l \rho_l v_l) - \psi_g \frac{V_l}{V_l + V_g} - \psi_e + \psi_d + G'_l \quad \text{.....(8)}$$

The liquid droplets in the gas phase are defined by the equation 9:

$$\frac{\partial}{\partial t}(V_D \rho_l) = -\frac{1}{A} \frac{\partial}{\partial t}(AV_D \rho_l v_D) - \psi_g \frac{V_D}{V_l + V_D} + \psi_e - \psi_d + G'_D \quad \text{.....(9)}$$

2.7.2 MOMENTUM CONSERVATION EQUATION

The momentum equation for the gas phase is defined by equation 10:

$$\begin{aligned} \frac{\partial}{\partial t}(V_g \rho_g v_g) = & -V_g \left(\frac{\partial P}{\partial z} \right) - \frac{1}{A} \frac{\partial}{\partial z} (AV_g \rho_g v_g^2) - \lambda_g \frac{1}{2} \rho_g |v_g| v_g \cdot \frac{S_g}{4A} \\ & + \lambda_l \frac{1}{2} \rho_g |v_r| v_r \cdot \frac{S_i}{4A} + V_g \rho_g \cos \theta + \psi_g v_a - F_D \quad \text{.....(10)} \end{aligned}$$

The momentum equation for the liquid droplets is defined by equation 11:

$$\begin{aligned} \frac{\partial}{\partial t}(V_D \rho_l v_D) = & -V_D \left(\frac{\partial P}{\partial z} \right) - \frac{1}{A} \frac{\partial}{\partial z} (AV_D \rho_l v_D^2) + V_D \rho_l g \cos \theta \\ & - \psi_g \frac{V_D}{V_D + V_l} v_a + \psi_e v_i - \psi_d v_D + F_D \quad \text{.....(11)} \end{aligned}$$

The momentum equation for the liquid film at the wall is defined by equation 12:

$$\begin{aligned}
\frac{\partial}{\partial t}(V_l \rho_l v_l) &= -V_l \left(\frac{\partial P}{\partial z} \right) - \frac{1}{A} \frac{\partial}{\partial z} (AV_l \rho_l v_l^2) - \lambda_l \frac{1}{2} \rho_l |v_l| v_l \cdot \frac{S_l}{4A} \\
&+ \lambda_i \frac{1}{2} \rho_g |v_r| v_r \cdot \frac{S_i}{4A} + V_l \rho_l g \cos \theta - \psi_g \frac{V_l}{V_l + V_D} v_a - \psi_e v_i + \psi_d V_D \\
&- V_l d(\rho_l - \rho_g) g \frac{\partial V_l}{\partial z} \sin \theta \quad \dots\dots(12)
\end{aligned}$$

Combining equations 10 and 11 eliminates the gas droplet drag term and thus the new equation becomes:

$$\begin{aligned}
\frac{\partial}{\partial t}(V_g \rho_g v_g + V_D \rho_l v_D) &= -(V_l + V_D) \left(\frac{\partial P}{\partial z} \right) - \frac{1}{A} \frac{\partial}{\partial z} (AV_g \rho_g v_g^2 + AV_D \rho_l v_D^2) \\
&- \lambda_g \frac{1}{2} \rho_g |v_g| v_g \cdot \frac{S_g}{4A} - \lambda_i \frac{1}{2} \rho_g |v_r| v_r \cdot \frac{S_i}{4A} + (V_g \rho_g + V_D \rho_l) g \cos \theta \\
&+ \psi_g \frac{V_D}{V_l + V_D} v_a + \psi_e v_i - \psi_d V_D \quad \dots\dots(13)
\end{aligned}$$

2.7.3 ENERGY CONSERVATION EQUATION

$$\begin{aligned}
\frac{\partial}{\partial t} \left[m_g \left(E_g + \frac{1}{2} v_g^2 + gh \right) + m_l \left(E_l + \frac{1}{2} v_l^2 + gh \right) + m_D \left(E_D + \frac{1}{2} v_D^2 + gh \right) \right] &= \\
- \frac{\partial}{\partial z} \left[m_g v_g \left(H_g + \frac{1}{2} v_g^2 + gh \right) + m_l v_l \left(H_l + \frac{1}{2} v_l^2 + gh \right) \right] &+ H_s + U \quad \dots\dots(14) \\
+ m_D v_D \left(H_D + \frac{1}{2} v_D^2 + gh \right) &
\end{aligned}$$

Modelling of Separated flows is achieved by implementation of a two fluid model which has separate momentum equations for the gas/droplet field and the liquid bulk field.

Modelling of Mixed flows is achieved by the use of a mixture (or drift flux) model which combines two dynamic momentum equations (liquid and gas). It reduces the total number of field and constitutive equations required in formulation in comparison with the two fluid model.

The two fluid and mixture (drift flux) models are explained in Table 1.

Table 1: Principle of multiphase flow models

MODEL	EQUATIONS	CLOSURES EQUATIONS
Two fluid model	5 mass conservation equations <ul style="list-style-type: none"> • Gas • Oil film • Oil droplets • Water film • Water droplets 2 Momentum conservation equations <ul style="list-style-type: none"> • Gas + droplets • Liquid bulk 	<ul style="list-style-type: none"> • Interface Friction • Liquid Wall friction • Gas Wall friction • Bubble velocity • Entrainment • Depositions
Drift flux model	5 mass conservation equations <ul style="list-style-type: none"> • Gas • Oil film • Oil droplets • Water film • Water droplets 1 momentum conservation. equation <ul style="list-style-type: none"> • Mixture momentum equation 	<ul style="list-style-type: none"> • Mixture friction • Slip relation (Holdup equation) • Bubble velocity • Gas void fraction

Another example of a different multiphase simulation tool is the SLUGGIT tool, which is a non-commercial tool for multiphase flow simulations at the department of Energy and Process Technology at NTNU. It incorporates a lagrangian slug tracking method for dynamic gas-liquid slug flow using an object-oriented approach, whereby slugs and bubbles are treated as discrete computational objects, and organised in linked lists. This tool will be

used in combination with a structural simulation tool to simulate the dynamic coupling between internal flow and riser dynamics.

2.8 OFFSHORE MARINE STRUCTURES

These are defined as structures which exist in a marine environment for the production of oil and gas. They range from large structures like bottom supporting platforms, semi submersibles to small structures like jetty's and groynes.

Marine structures are complex and must take into account a number of external and internal parameters to accurately predict their behaviour in both static and dynamic modes. Examples of such parameters include waves and currents. This is important because of the need to accurately ascertain the optimal operation window in which the loads exerted on the structure by all parameters both external and internal do not exceed the design strength of the structure.

The marine structure in focus is the production riser, which are essentially conductor pipes that connect a floater to well heads on the sea bed¹². This differs completely from a drilling riser in function and design. There exists primarily two types of production risers; these are rigid and flexible risers. In these report, the flexible riser is the production riser in focus.

A flexible riser is defined as a flexible pipe transporting fluids or gas between a sub-sea pipeline and the process plant on a platform or FPSO, it can be supported both laterally and vertically in the topside structure and transmit actions from thermal effects, wave action, gravity and variations in fluid flow to the topside structure¹³. They are complex in design and are mainly composed of polymers and steel, in addition to other materials.

2.8.1 STRUCTURE OF A FLEXIBLE MARINE RISER

The structure of a riser comprises the following elements ¹⁴:

- a) Carcass: Spirally wound interlocking structure manufactured from a metallic strip. The carcass prevents collapse of the inner liner.
- b) Inner liner: This is an extruded polymer layer that confines the internal fluid integrity.
- c) Pressure armour: Consist of a number of structural layers comprised of helically wound C-shaped metallic wires. This armour layers provide resistance to radial loads
- d) Tensile armour: This layer provides resistance to axial tension loads. This is made up of a number of structural layers consisting of helically wound flat wires.
- e) Outer sheath: The outer sheath is an extrusive polymer layer. Its function is to shield the pipes structural elements from the outer environment and to give mechanical protection.

Figure 5 shows the arrangement of these elements in a typical flexible riser.

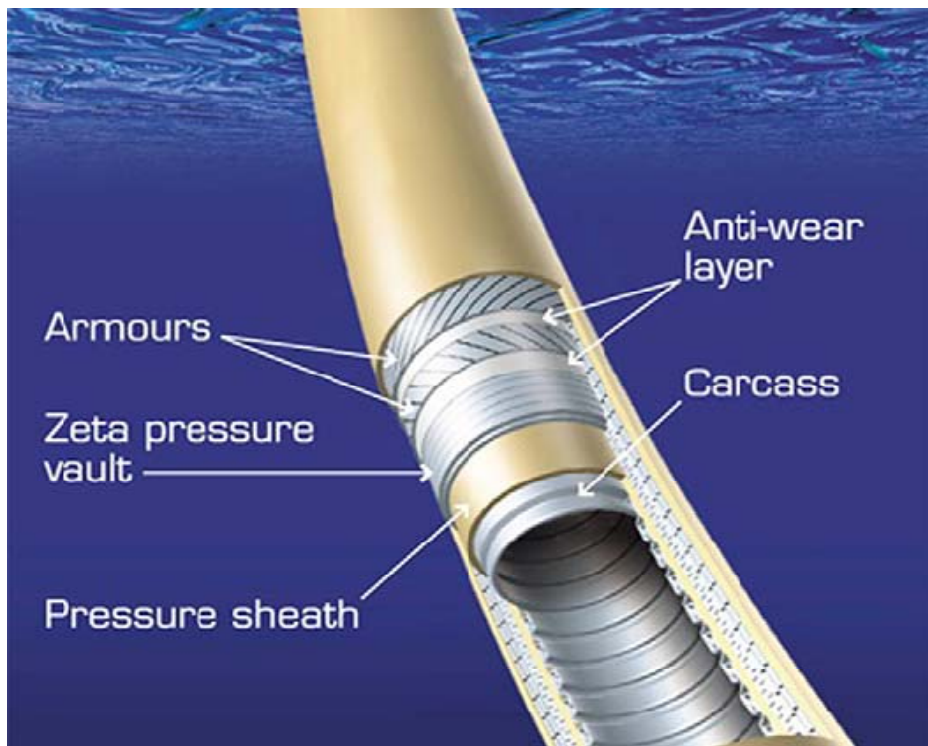


Figure 5 Typical Cross section of flexible pipe. Source: Yong Bai, Qiang Bai Subsea Engineering Handbook

2.8.2 TYPES OF FLEXIBLE MARINE RISER

There exist six main configurations of flexible production risers¹⁰.

- Free Hanging catenary or L-riser.
- Lazy wave
- Steep wave
- Lazy S
- Steep S
- Pliant wave

These different flexible riser configurations are shown in Figure6.

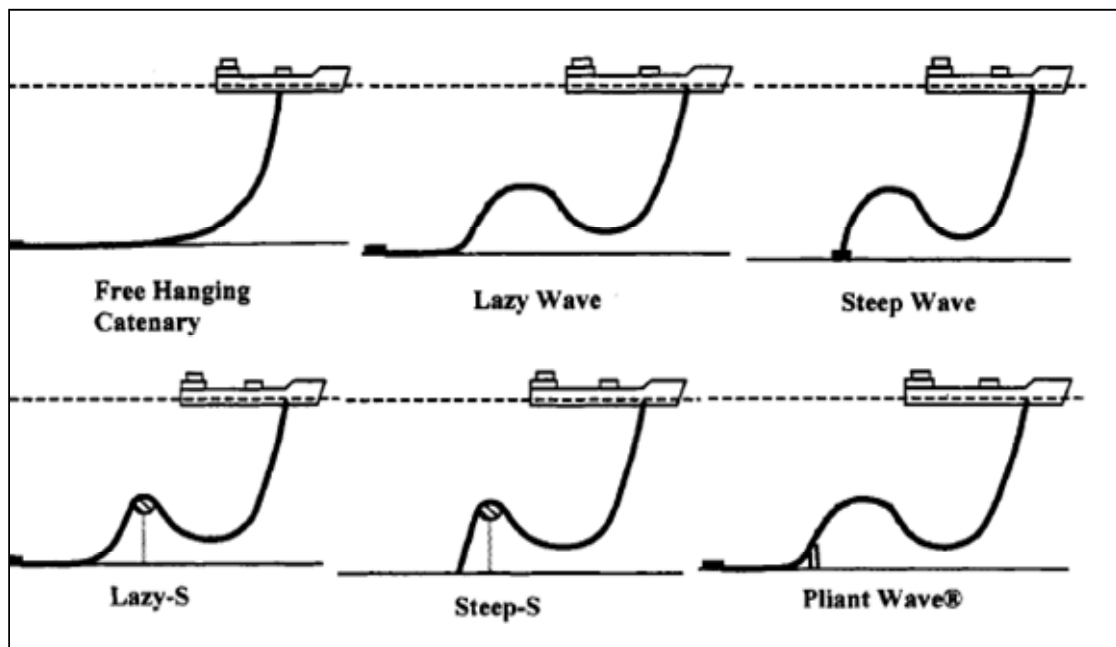


Figure 6 Main configurations of flexible production risers. Source: Yong Bai, Qiang Bai. Subsea Pipeline and Risers

The choice of configuration is driven by production parameters such as environmental data, water depth, host vessel motion characteristics and access; hang off location, field layout (number and type of risers) and mooring layout.

A flexible riser is subject to different sorts of complex forces, both external and internal. These forces play a major role in its excitation, fatigue and probable failure. Some of the forces like gravitation, buoyancy, tension, bend stress, wave force and current forces are illustrated in Figure 7.

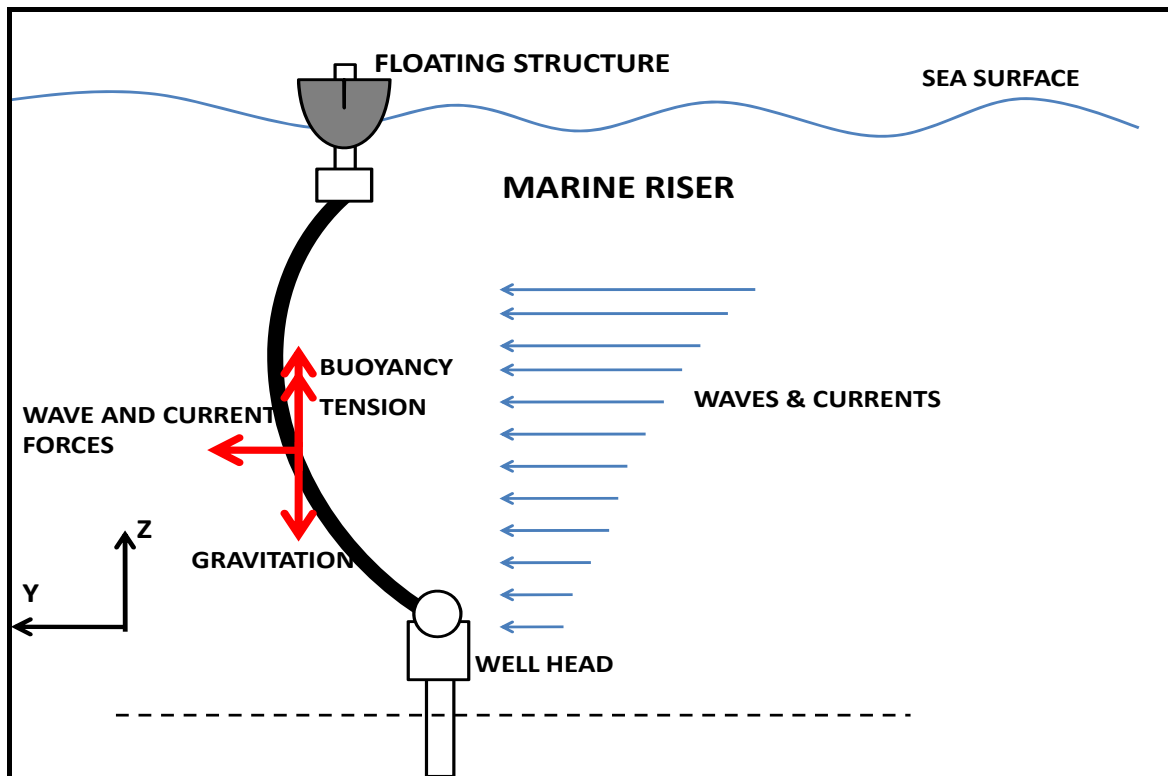


Figure 7 Model of a marine riser showing external forces. Image modified from: *The Study on Vibration of Marine Riser Under Deep Water.*

Chunjie Han and Tie Yan.

The reliability of results from computational simulations of flexible risers are continuously being improved to save costs and increase the life span of installed risers. Current models in use provide reasonable results but in comparison with each other, there have been found to exist a certain degree of scatter¹⁵, which may cast doubt on the accuracy of the results provided by a specific model. One way of improving the reliability of results obtained during such simulations is to take into account more of the external and internal influences on the riser. Such influences include the effect of the unsteady internal flows in the riser and this is part of the basis for this thesis

2.8.3 COMPUTATIONAL SIMULATION OF FLEXIBLE RISERS.

The main stages in the design procedure of flexible risers comprise of static and dynamic analysis. The main design parameters include:

- Choice of configuration
- Length of the riser
- Overall system geometry
- Sizing of the buoyancy modules and subsurface buoy or arch

Using these parameters as input the required riser properties are computed.

The first stage in the design of a flexible riser system is based on static analysis and involves a parametric study to assess the effect of changing the design parameters on the static curvature and tension of the riser¹⁶.

The second stage in the design procedure is based on dynamic analysis and involves the use of a series of dynamic load cases which combine different wave and current conditions, vessel positions and riser contents to prove an overall assessment of the riser suitability in operational and survival conditions¹⁶.

There exists a number of computational tools for computational simulation of flexible risers. Some of these tools include REFLEX, RIFLEX, MOBDEX, FENRIS, MOBDEX, AQWAFLEX, ORCAFLEX, SEAPIPE, RISER, FENRIS etc¹⁵. Data from this thesis will be primarily compared with simulation results from RIFLEX, which is a non-linear finite element code for 3-D global analysis of riser static and dynamic analysis, frequency and time domain analysis, and assessment of test parameters.

The equation of motion of a marine riser is an important part of computational simulations of flexible risers. These are illustrated in subsequent sections.

2.8.4 EQUATION OF RISER HORIZONTAL MOTION¹⁷

Figure 8 illustrates a straight, tubular and fully submerged riser that conveys fluid up to a floating barge. It is connected by a flex-joint connection that fixes the translational motion of the riser top to that of the barge and provides a linear elastic reaction against a relative angular motion of the barge and the riser top (free hanging).

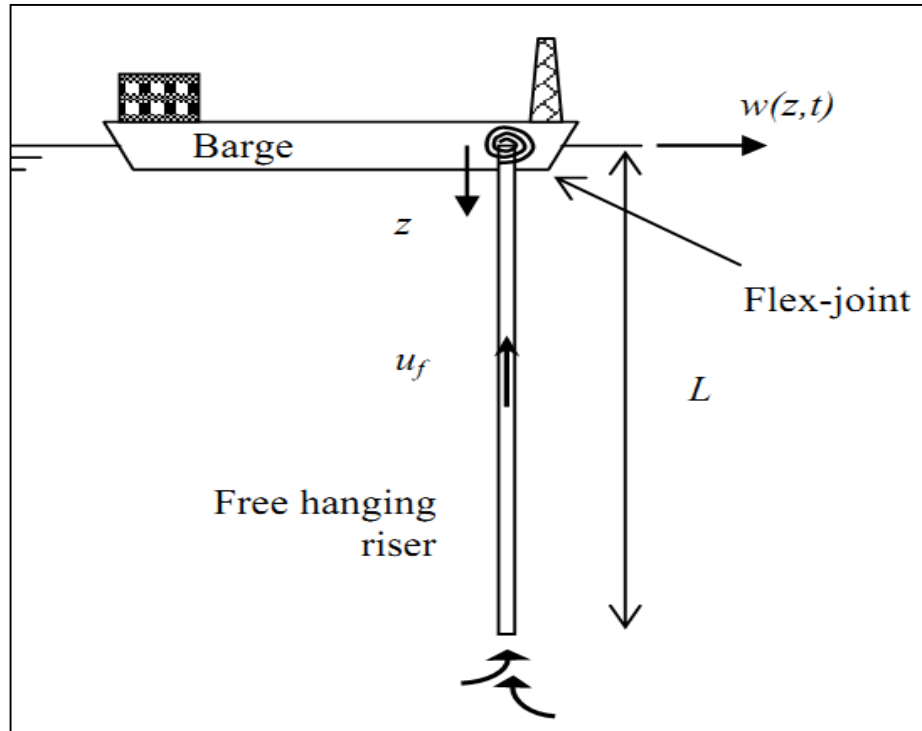


Figure 8 Sketch of free hanging riser conveying fluid. Image copied from: Stability of offshore risers conveying fluid. PHD thesis. Guido Kuiper. T.U Delft. January 2008

The equation that governs the horizontal motion of the differential element of the riser can be written as shown in equation 15:

$$EI \frac{\partial^4 w}{\partial z^4} - \frac{\partial}{\partial z} \left(T_r(z) \frac{\partial w}{\partial z} \right) + \rho_f A_i \left(u_f^2 \frac{\partial^2 w}{\partial z^2} - 2u_f \frac{\partial^2 w}{\partial z \partial t} + \frac{\partial^2 w}{\partial t^2} \right) - \frac{\partial}{\partial z} \left((A_e p_e(z) - A_i p_i(z)) \frac{\partial w}{\partial z} \right) + \rho_r A_r \frac{\partial^2 w}{\partial t^2} = f(z,t), \quad \dots(15)$$

Where $w(z,t)$ is the horizontal riser displacement, z is the co-ordinate along the riser (directed downward), t is the time, EI is the bending stiffness of the riser, T_r is the axial

tension of the riser, ρ_r and ρ_f are the mass density of the riser and the fluid respectively, A_r and A_e are the internal and external cross sectional areas of the riser respectively, $A_r = A_e - A_i$ is the cross sectional area of the pipe wall, $p_i(z)$ and $p_e(z)$ are the water pressure inside and outside the risers respectively, U_f is the velocity of the flow through the riser (directed upwards) and $f(z,t)$ is the normal dynamic reaction of the surrounding water on the riser element.

- The first and last term on the left hand side of equation 15, form the bending motion of a beam according to the Euler Bernoulli theory.
- The second term in equation 15:

$$\frac{\partial}{\partial z} \left(T_r(z) \frac{\partial w}{\partial z} \right) \dots\dots(16)$$

Is due to the longitudinal tension in the riser that is caused by gravity and internal fluid resistance. This tension reads:

$$T_r(z) = \rho_r A_r g(L - z) - \rho_f A_r gL - \rho_f A_i \frac{f_{DW}}{D_i} \frac{u_f^2}{2} (L - z) \dots\dots(17)$$

Where g is the gravity acceleration, L is the length of the riser (Figure 8) D_i is the inner diameter of the pipe and f_{DW} is the resistance coefficient of Darcy Weisbach. The origin of the reference system is fixed to the riser top. At the free end of the riser i.e at $z=L$, only the second term on the right hand of the above equation remains. This term represents the static buoyancy force.

- The third term on the left hand side of equation 15 is the transverse loading per unit length exerted by the internal flow on the pipe.
- The fourth term of equation 15 is due to the pressure on the pipe wall and is represented by equation 18:

$$\frac{\partial}{\partial z} \left((A_e p_e(z) - A_i p_i(z)) \frac{\partial w}{\partial z} \right) \dots\dots(18)$$

The external hydrostatic pressure $p_e(z)$ neglecting the temperature effects and compressibility may be assumed to vary linearly with z , so that

$$p_e(z) = \rho_f g z \dots\dots(19)$$

The dynamic reaction of the surrounding water on the riser, $f(z,t)$ is assumed to be a superposition of an inertia force $f_{in}(z,t)$ and a drag force $f_d(z,t)$. The inertia force depends on the acceleration of the riser and of the surrounding water as:

$$f_{in}(z,t) = \rho_f A_e (C_a + 1) \frac{\partial u}{\partial t} - \rho_f A_e C_a \frac{\partial^2 w}{\partial t^2} : \dots\dots(20)$$

Where $u(z,t)$ is the horizontal component located in the plane (w,z) of the surrounding water velocity and C_a is the added mass coefficient. The drag force depends on the relative motion of the riser and of the surrounding water non-linearly.

2.9 SEVERE OR TERRAIN INDUCED SLUGGING

This is an unsteady flow phenomenon which leads to long duration, large amplitude instabilities in pipeline-riser systems and can damage topside equipments. These instabilities are due to competition between restoring forces due to gravity and lift forces due to gas flow¹⁸.

Severe slugging is characterised by extremely long slugs (50-1000 pipeline diameters) that are generated by pipeline-riser geometry due to hilly terrain rather than because of the Kelvin-Helmholtz instability (slug formation criteria). Typical situations are severe slugging in pipeline-riser configurations which typically resemble U-tube (or catenary) geometries. The slug lengths and the amplitude of pressure and velocity variations become larger the longer and steeper the pipelines¹⁹.

For severe slugging to occur in a pipeline-riser system, certain conditions must be fulfilled.

- The pipeline must be sloped upstream, to allow stratification of the flow in the upstream section and to allow the formation of liquid blockage (due to accumulation) in the lowest point of the pipeline-riser system.
- There must be sufficient upstream compressibility of the gas
- When the liquid has blocked the lowest point, the hydrostatic pressure by the liquid in the downstream rising section of the pipeline (or riser column) must increase faster than the gas compression pressure build up in the pipeline in order to keep the gas locked.

2.9.1 SEVERE SLUGGING MECHANISM

- It begins with the accumulation of liquid in the low point of the system illustrated in part A of Figure 9, due to the fact that because of the low flow rates, the gas is unable to push/lift the liquid upwards.
- Due to the accumulation of the liquid, the gas flow path becomes blocked, Figure 9(B) and this result in the compression of the gas upstream of the low point of the system (Slug generation). When the upstream pressure has increased such that it exceeds the hydrostatic pressure of the fluid column in the downstream section of the system, the liquid slug begins to move forward and be produced (slug production).
- As the liquid slug is produced, the gas penetrates into the downstream section Figure 9(C), the hydrostatic pressure in the column is reduced and the gas expands, accelerating both gas and liquid rapidly up the downstream section (bubble penetration) resulting in a high flow followed by a gas stream (blowout) Figure 9(D).
- At the end of the blowout, some liquid falls back, due to the fact that as the gas produced at the riser bottom reaches the top, the pressure becomes minimal and the liquid is no longer gas-lifted, thus the liquid begins to fall back (gas blow down) and accumulate in the low point of the system causing the cycle to repeat itself.

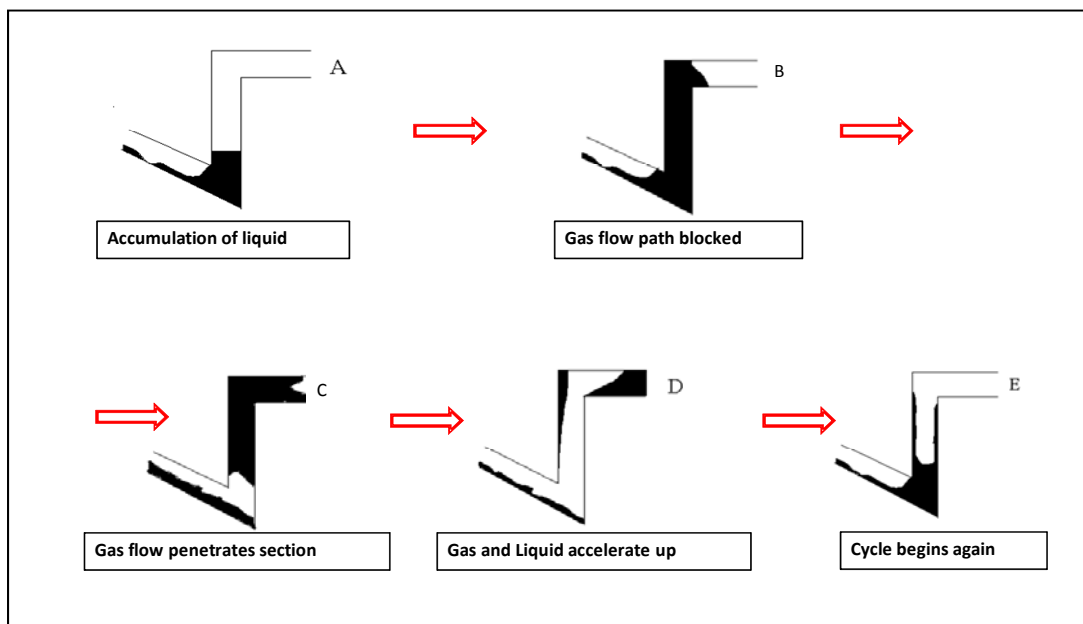


Figure 9 Description of severe slugging cycle. Source: Xu, Z. G.: Solutions to Slugging Problems Using Multiphase Simulations. *3rd Int. Conf. Multiphase Metering*, Aberdeen, United Kingdom (1997).

2.9.2 PREDICTING ONSET OF SEVERE SLUGGING.

Prediction of severe slugging can help in the design process of a pipeline-riser system by efficiently designing processing and control system.

Pots et al developed a model for predicting the onset of severe slugging in pipeline – riser systems²⁰ and this is illustrated in equation 21.

$$\Pi_{ss} = \frac{Q_g ZRT}{Q_l M_g g L (1 - H_l)} \leq 1 \quad \text{.....(21)}$$

2.9.3 EFFECTS OF SEVERE SLUGGING:

Slugs generated during the severe slugging cycle can be several hundred metres long and could fill the entire riser column. Inlet separators downstream cannot handle such volumes at once and these may cause overflowing and trip the production. Also the severe slugging cycle can cause intense flow and pressure oscillations. These highly affect downstream topside equipments like separator vessels and compressors which are not designed to handle intense transients.

It is important to note that severe slugging can also affect the mechanical integrity of equipments. Generally, slugs may travel at relatively high velocities (values in excess of 16m/s have been recorded)²¹. When coupled with a high liquid holdup, which can occur at high velocity if water cuts are high, long slugs can have considerable momentum. A 150 metre long slug with liquid holdup of 0.8 in a 24 inch line has a mass of about 30 tonnes²¹.

3 EXPERIMENT

The main purpose of these experiments is to highlight the dynamic coupling between the internal flow inside a flexible riser and the dynamics of the riser. In addition it will generate data for comparison with numerical simulations. This is done to be able to take into account the effects of unsteady internal multiphase flow on flexible risers.

Particular areas of interest are:

- The displacement experienced by the riser during the severe slugging cycle.
- The load exerted on the point of attachment of the riser to the topside vessel during the severe slugging cycle.

A rig has been set up to carry out small scale experiments on severe slugging in flexible risers. The riser is simulated using a flexible plastic, transparent hose.

3.1 MODIFICATIONS FROM PRECEEDING PROJECTS.

This thesis work is a continuation of the work carried out in the autumn semester project work by the author, where the aim of that work was to identify a proper coupling and interaction between the flexible marine riser and the internal multiphase flow moving in it. The results obtained and documented revealed a convincing case for this coupling and made recommendations for further work which have now been implemented as modification to the present thesis work. The modifications implemented include:

- The depth of the pool has been increased from 1,5 metres to 5 metres in a bid to intensify the magnitude of the blowouts and capture visually the whole riser frame during the cycle.
- The flexible hose diameter has been increased, so as to intensify the magnitude of the blowouts, ease visualization of the flow regimes in the pipes at a particular point and obtain a larger model for easy scaling with a real prototype.

- Brass and lead rings are used on the hose to easily submerge the hose and force it to maintain a catenary or s-configuration even when empty. This is to eliminate the buoyancy tendencies of the hose which are minimal in real marine risers due to their corrugated structures which give them a density higher than that of the surrounding water
- A larger buffer tank has been used in an effort to increase the upstream compressible volume of the gas; this is also in a bid to increase the magnitude of the blowout of the slugs in the severe slugging cycle.

The general configurations of the riser in the project work and thesis have remained the same in one case (L shaped riser) but an additional configuration (S- shaped riser) has also been investigated.

3.2 EXPERIMENT SET UP

As part of this work, a small scale riser set up was to be constructed. The new setup differed from the setup in previous experiments by the modifications explained in section 3.1.

3.2.1 GEOMETRY AND DIMENSIONS OF THE EXPERIMENT POOL

Figure 10 illustrates the size of the experiment pool and arrangement of equipments.

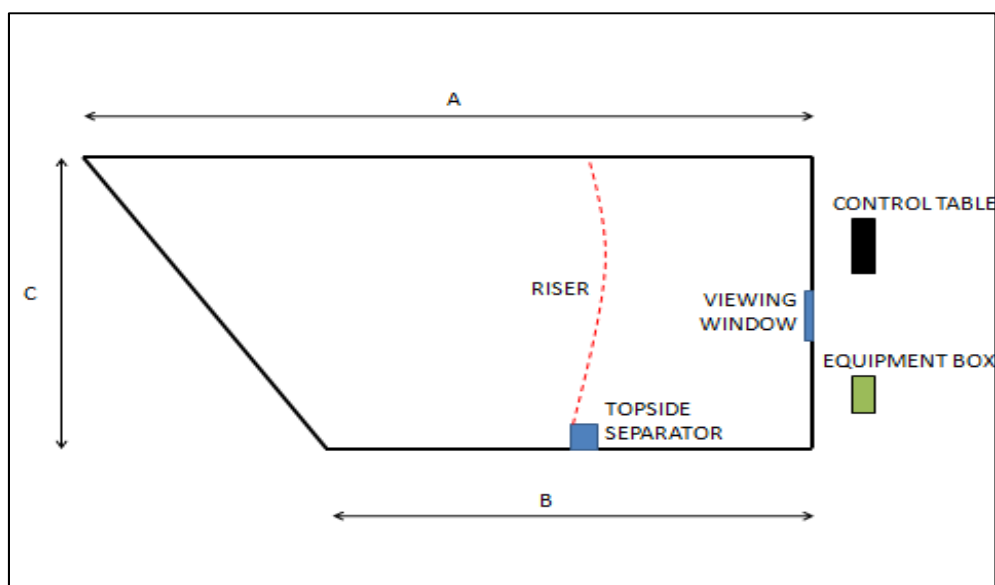


Figure 10 Aerial view of experiment pool

3.2.2 DIMENSIONS OF THE POOL

Table 2 illustrates the dimensions of the experiment pool.

Table 2: Dimensions of experiment pool.

A	9 metres
B	5.5metres
C	4,25 metres
Depth	5 metres
Depth of viewing window from surface	3 metres

3.2.3 EQUIPMENTS AND INSTRUMENTATION.

- A flexible plastic transparent hose to serve as the flexible riser
- A topside separator vessel of total volume 0.03 m³
- Load cells for sensing the loads exerted by the riser on the point of attachment during severe slugging cycles.
- Air compressor (Maximum working pressure = 4 bar)
- Centrifugal Water Pump (Maximum flow=14m³/hr; Maximum head = 13 m)
- Buffer tanks to sustain upstream compressibility of gas.
- Air and water flow meters
- Three accelerometers for measuring the acceleration of the riser at defined points.
- Brass rings for submerging the flexible hoses.
- Computer data acquisition (DAQ) system
- Casio compact video camera
- Ten metres flexible light emitting diodes (LED) stripes.
- Lead rings for submerging the flexible hoses.

3.2.4 MOBILE TWO-PHASE FLOW LOOP

The mobile two phase flow loop measures approximately 0.72m*0.56m*0.40m ($L*B*H$). It contains the following equipments which are all connected together:

Air compressor, Buffer tank 1, Water pump, control valves, water storage tank and pressure gauges.

The connection schematic from the two phase loop (represented by the area enclosed by the dotted red line) to the flexible riser is shown in Figure 11.

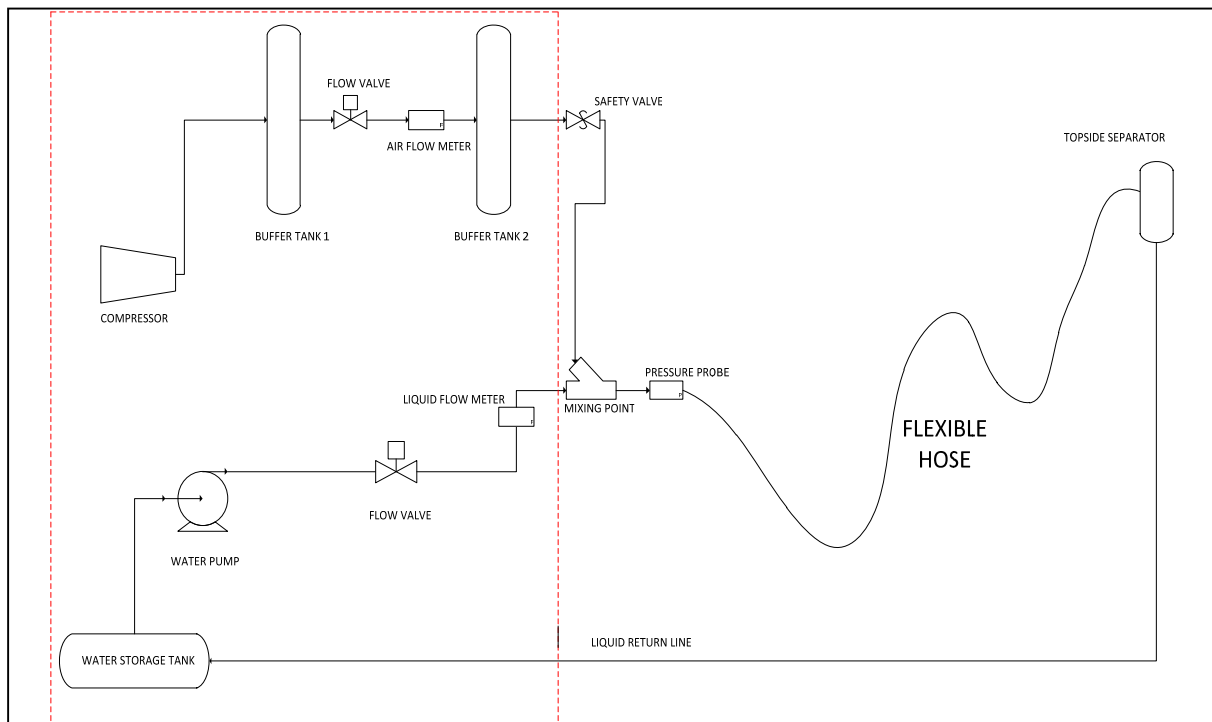


Figure 11 Connection from Mobile two-phase flow loop to riser.

3.2.5 DATA ACQUISITION SYSTEM.

Catman program is used in the data acquisition process during the experiment.

A Hottinger MGC plus amplifier is used to amplify the signal in addition to butter-worth filters. Six channels are used in the data acquisition process. The principle of operation of the catman program and the graphic user interface (GUI) is illustrated in Appendix B.

3.2.6 GEOMETRY AND PROPERTIES OF THE FLEXIBLE HOSE.

Table 3 illustrates the geometry of the flexible hose.

Table 3: Geometry of the flexible hose.

DESCRIPTION	DIMENSIONS
Total Length (upstream and downstream sections)	12.35 metres
External diameter	0.02075 metres
Internal diameter	0.016 metres
Nominal weight	0.24 kilograms per metre
Maximum working pressure	4 bar

The flexible, plastic transparent hose was scaled accordingly:

- Assuming an average water depth of 1000 meters.
- Pool depth of 6 meters.
- Assume a prototype flexible riser of Length of 900 metres and internal diameter of 0.2032 metres.

We could assume the following geometrical scaling:

- Length scale factor= $1000/6= 166.66$
- Therefore length of model = $900/166.66= 5.40$ metres.

Since there exists no direct relationship between the diameter and length, as even if the length increases the diameter remains constant through the whole pipe sections.

We can assume a geometrical scaling in terms of the actual relationships between the diameter of the model and the diameter of the prototype.

- Diameter of model = 0,016 metres
- Diameter of prototype = 0,2032 metres
- Diameter scale factor = $0,2032/0,016 = 12,7$.

These scale factors can be used to relate the production rates and volumes of the model to a real life scenario.

3.3 EXPERIMENT PROCEDURE

For the first configuration (Free hanging catenary or L-riser):

- The riser is connected to the mixer as shown in Figure 12.

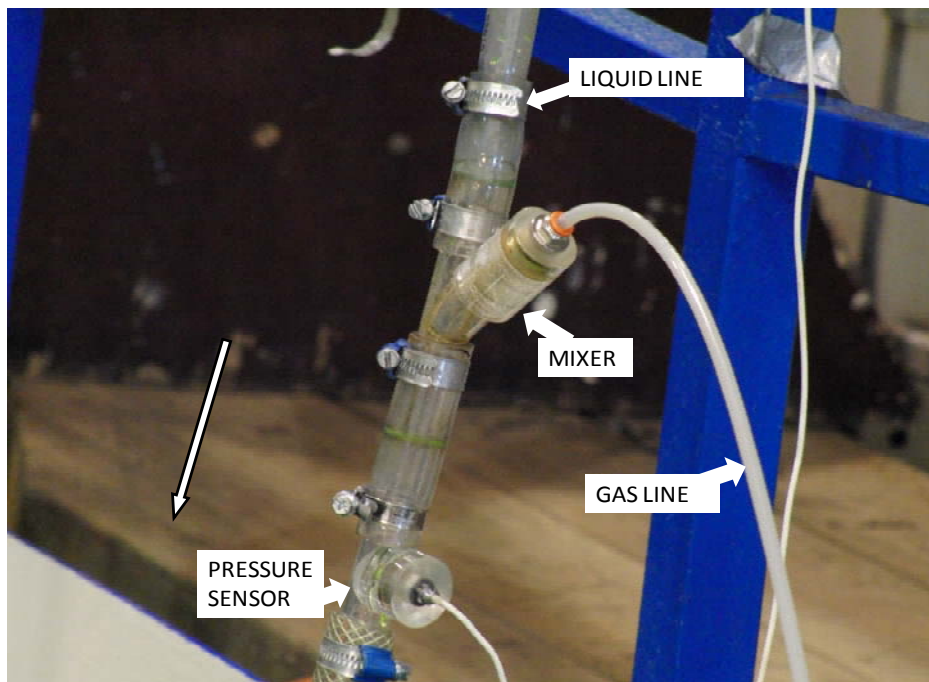


Figure 12 Position of gas-liquid mixer and pressure sensor.

- 43 Brass rings are attached on the flexible riser, at a distance of 573 centimetres from the attachment point of the riser to the load cell to submerge it. The properties of the brass rings are illustrated in Table 4

Table 4: Properties of Brass rings.

BRASS RINGS	DIMENSIONS
Length	3.5 centimetres
External Diameter	2.8 centimetres
Weight per ring	0.035 Kilograms
Total Weight of rings (43 pieces)	1.505 Kilograms

- Three accelerometers are attached to the riser as shown in Figure 13 at distance 179 centimetres, 311 centimetres and 441 centimetres from the load cell along the riser.

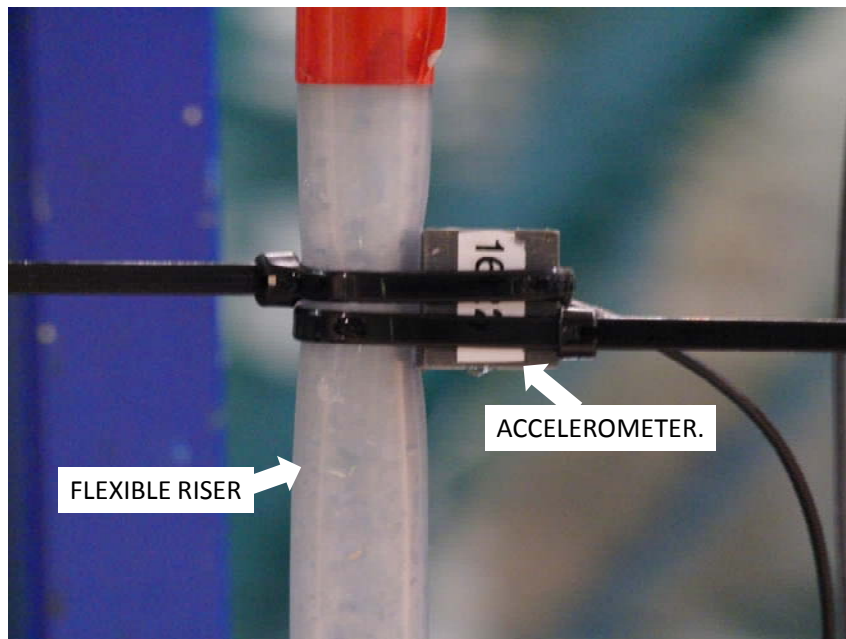


Figure 13 Method of attachment of accelerometer to flexible hose

3.3.1 SAMPLING DIRECTION OF ACCELEROMETERS

Figure 14 shows the sampling direction of the accelerometers relative to its position.

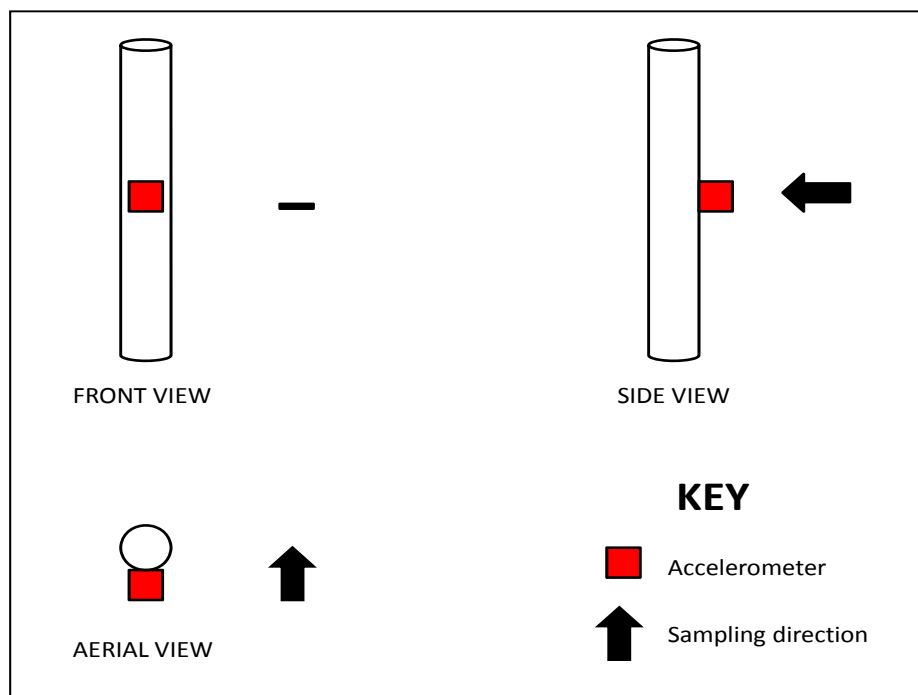


Figure 14 Illustration of sampling direction of accelerometers relative to position of flexible hose

3.3.2 RISER CONFIGURATIONS

As explained in section 2.8.2, flexible risers have different configurations. The investigated configurations in these experiments where:

- The free hanging catenary or L- riser
- Lazy S risers.

These configurations were chosen because of their wide applications in the offshore oil and gas industry.

The Properties of the Liquid line which runs from the liquid pump to the mixing point has been illustrated in Table 5.

Table 5: Properties of liquid supply line from pump to mixing point

Length	10.250 metres
External diameter	0.016 metres
Internal diameter	0.012 metres
Nominal weight	0.108 kilograms/metre

The properties of the gas line which runs from the buffer tank to the mixing point is been illustrated in Table 6.

Table 6: Properties of gas supply line from buffer tank to mixing point.

Length	6 metres
External diameter	0.005 metres
Internal diameter	0.003 metres

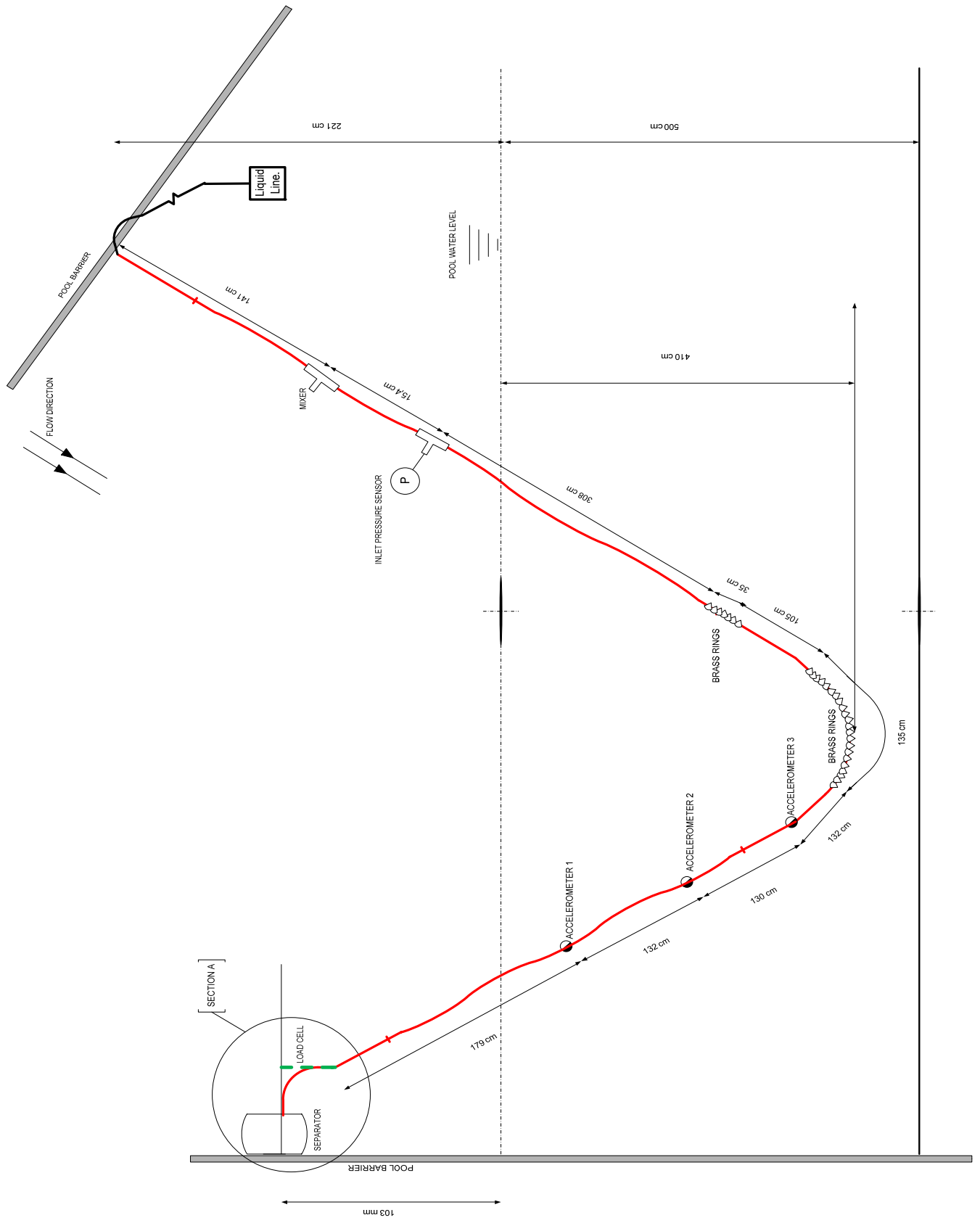


Figure 15 L-Riser geometry and experimental setup

Figure 16 and 17 illustrate the topside of the experimental set-up.

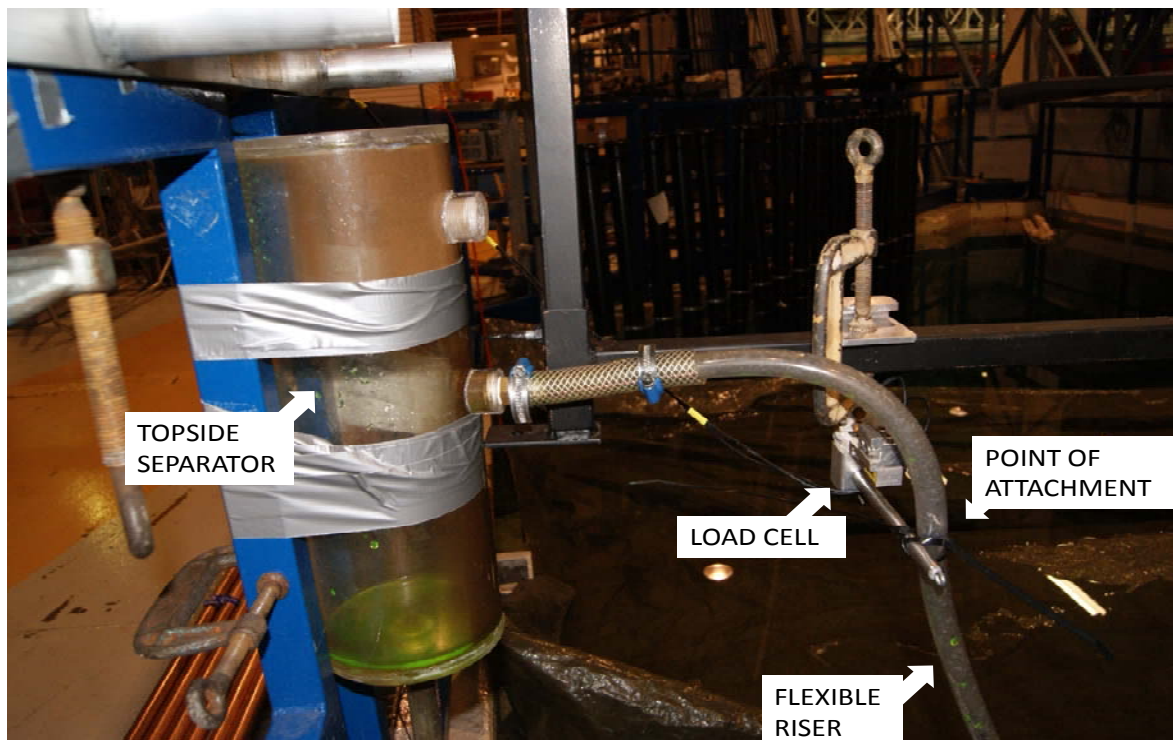


Figure 16 Topside section of experiment setup showing separator and load cell attachment points

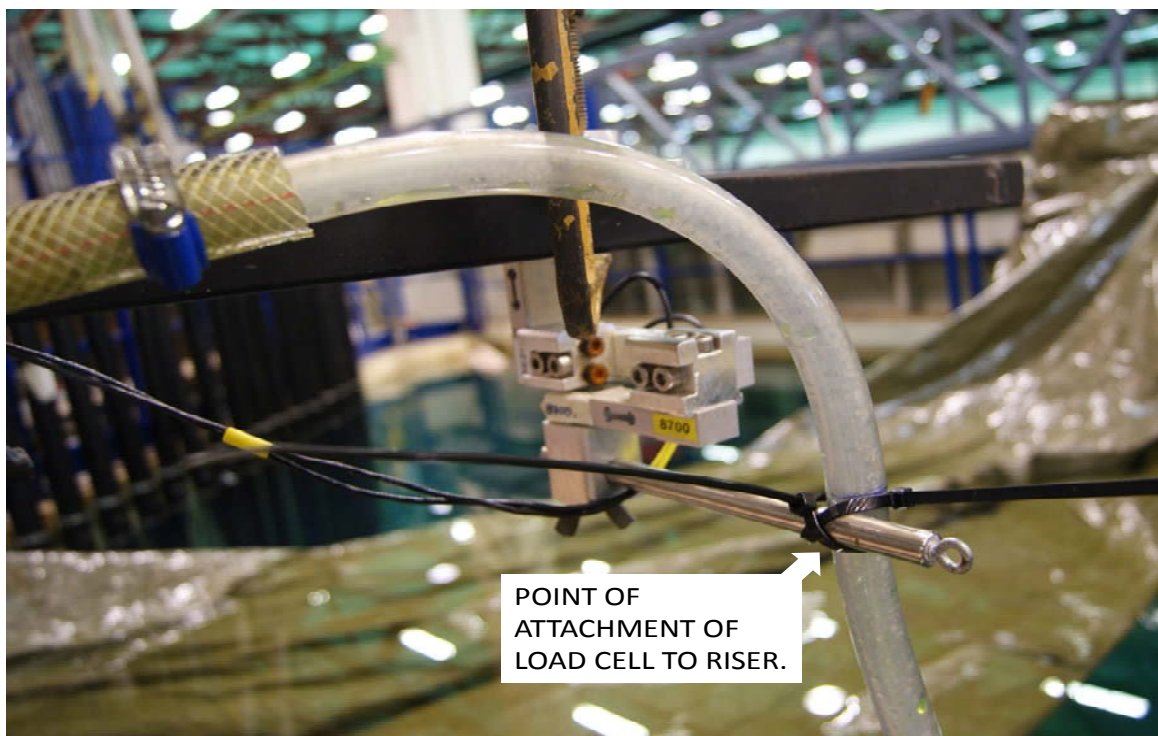


Figure 17 Close up of attachment point to load cell.

3.3.3 SECTION A DIMENSIONS

Section A represents the topside of the experiment setup. Its geometry and configuration is illustrated in Figure 18

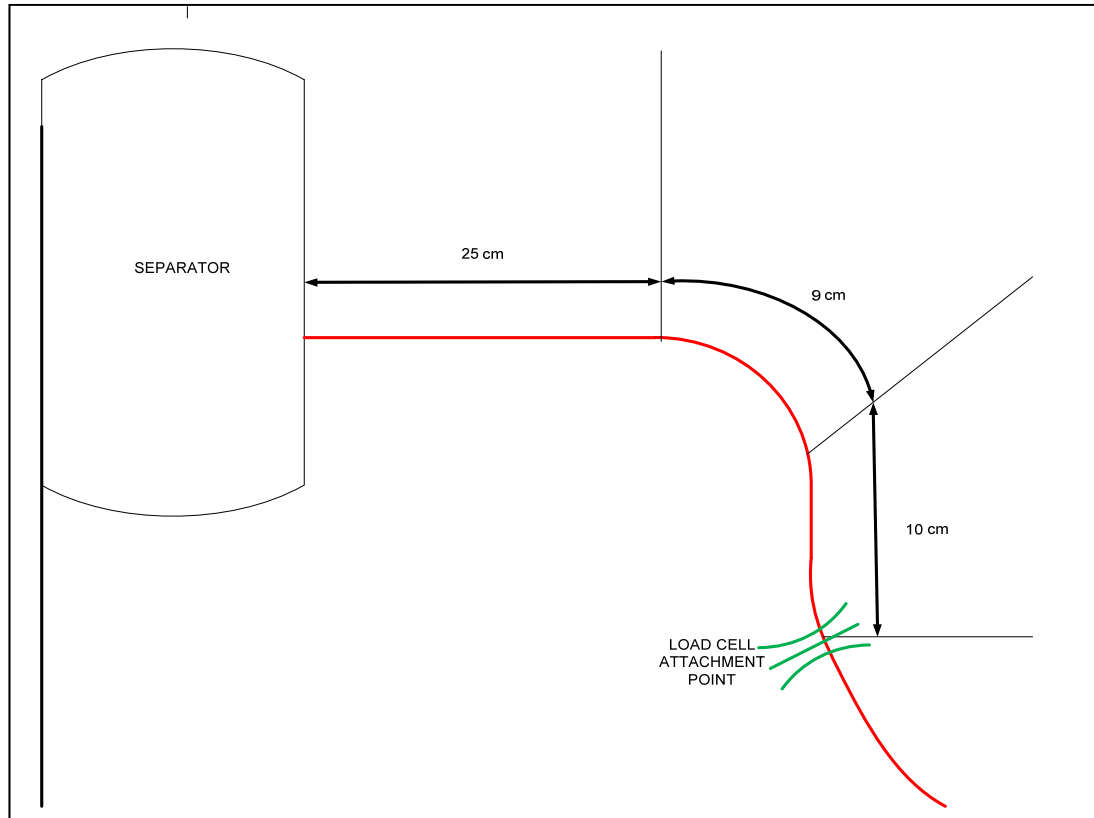


Figure 18 Geometry of Section A.

For the second configuration (Lazy S configuration):

- Buoyancy elements constructed from 15 pieces of divynycell foam of total weight 0.065 kilograms are attached to the riser from defined positions and spaced 15 cm apart. This is shown in Appendix C
- In addition to the brass rings already attached on the riser, additional lead rings are also attached at length 200.5 centimetres from the load cell along the flexible riser.

This is done to achieve the double dip (catenary) form of the lazy s riser. This illustrated in Figure 19.

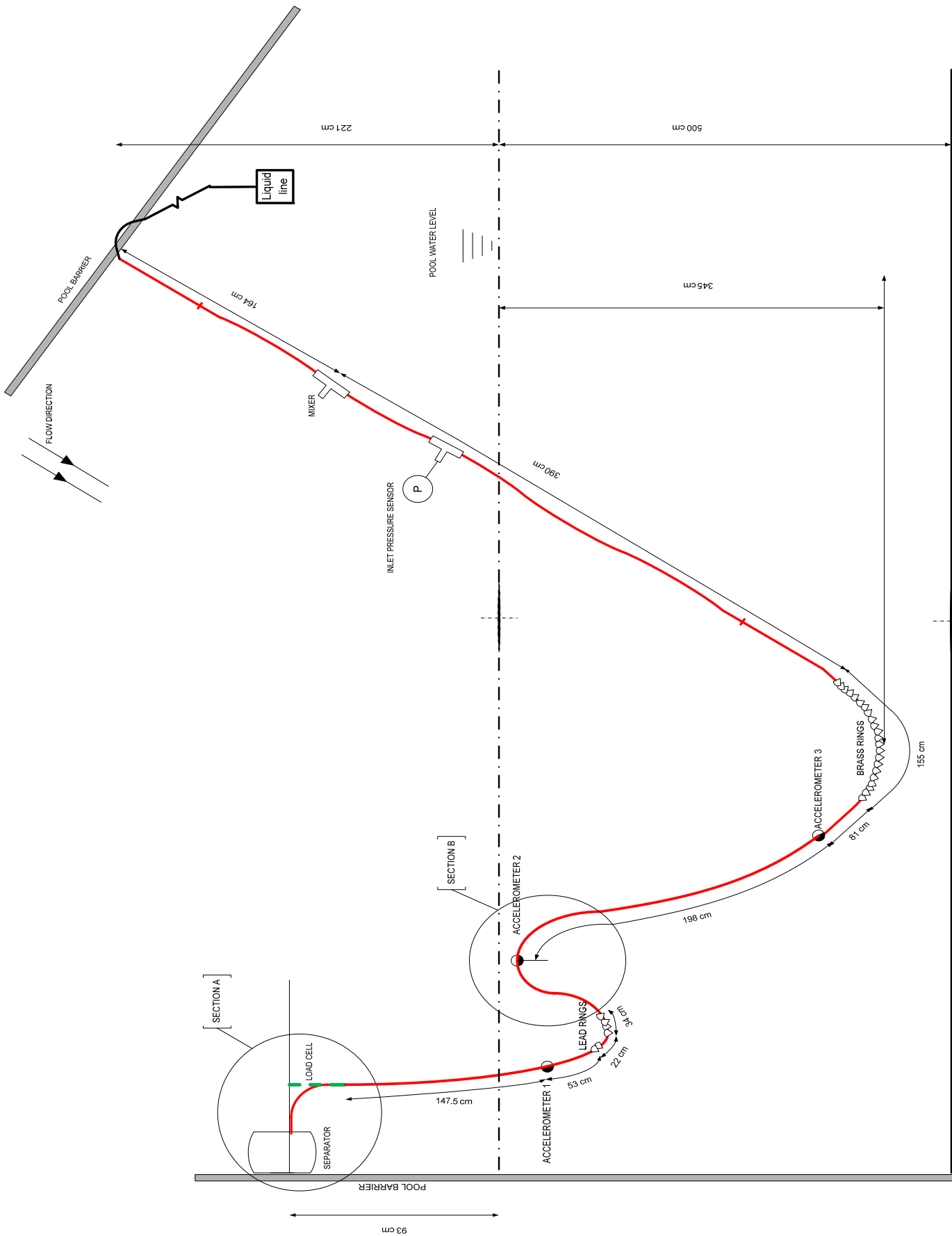


Figure 19 S-Riser geometry and experimental setup

3.3.4 S-CASE SECTION B DIMENSIONS

Section B represents the curved (arc shaped) portion of the S-riser. Its geometry and configuration is illustrated in Figure 20

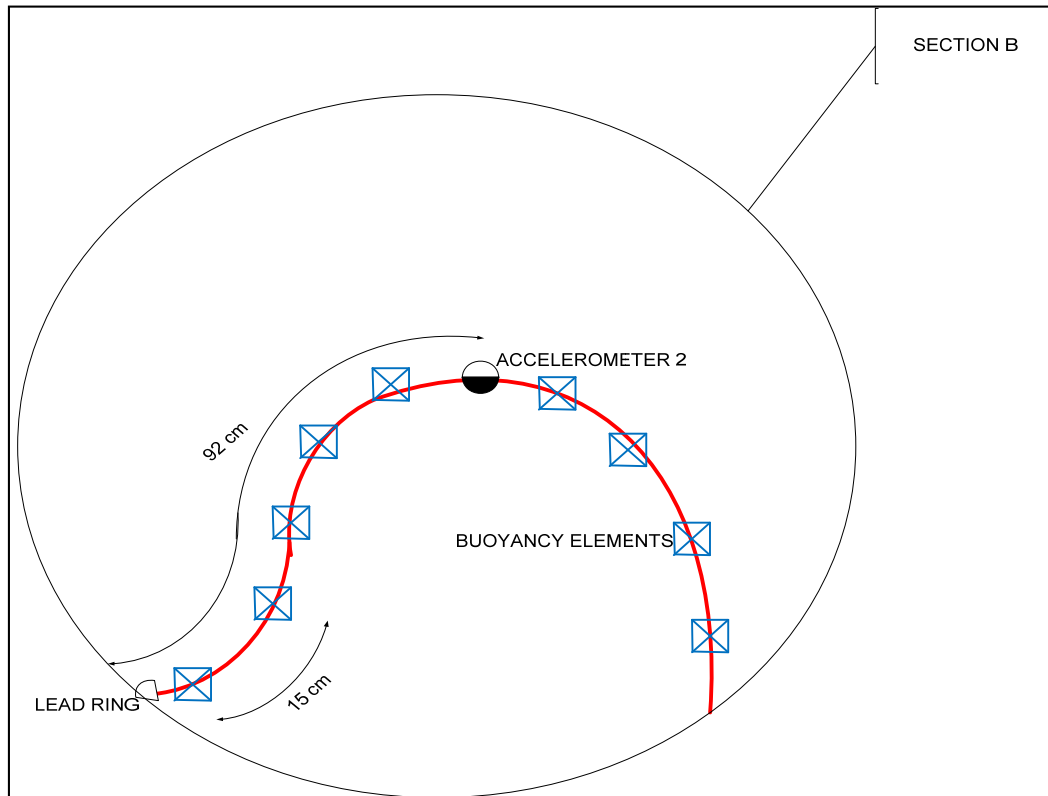


Figure 20 Geometry of Section B from S- riser.

The Properties of the additional lead rings used to submerge the S-riser is shown in Table 7

Table 7: Properties of Lead rings.

LEAD RINGS	DIMENSIONS
Length	10.0 centimetres
External Diameter	2.8 centimetres
Average weight per ring	0.22875 Kilo grams
Total weight of rings (4 pieces)	0.915 Kilograms

When the flexible risers are setup as shown in Figure 15 and Figure 19, the air compressor and water pump are turned on, with both control valves in a completely closed position.

Gradually the control valve for the gas line is opened before the control valve for the liquid line to avoid flooding the gas line with liquid. The control valve on the liquid supply line is also gradually opened and both flow rates are manually tuned until the severe slugging cycle is obtained.

At the start of each experimental case, a 'decay' test is carried out, to ascertain the values obtained due to noise and vibrations. After this the real data is logged for each experiment case.

When the severe slugging cycle is obtained, the data acquisition system is turned on to acquire data for the Load cell, accelerometers and inlet pressure.

Corresponding flow rates for the gas and liquid supply are read off both the digital gas meters and the analogue liquid flow meter.

The experiment is repeated for different flow rates, data is acquired and logged. The configuration of the riser is changed from L to S and the experiment procedure is repeated again.

VIDEO

To capture with the motions of the riser, the flow regimes and phenomenon inside the riser the liquid is illuminated with a colorant. The property of the colorant is shown in Table 8.

A waterproof light emitting diode (LED) strip is attached to the riser to illuminate the fluid inside and the riser itself, after this the motions of the riser are captured with a compact camera from the viewing window of the pool. The properties of the camera is shown in Table 9.

Table 8: Properties of colorant

Brand	Name	Chemicals	Colour
Merck	Flourescent Natrium	$C_{20}H_{10}Na_2O_5$	Fluorescent Green

Table 9: Brand, Model, FPS and resolution of video camera

Brand	Model	FPS	Resolution
Casio	EX-F1	30	1280 x 720

3.3.5 PRINCIPLE OF RESOLUTION OF FORCES ACTING ON POINT OF ATTACHMENT OF MARINE RISER TO TOPSIDE VESSEL.

To determine the force acting on the attachment, Forces in the Z and Y direction as shown in Figure 21 are logged.

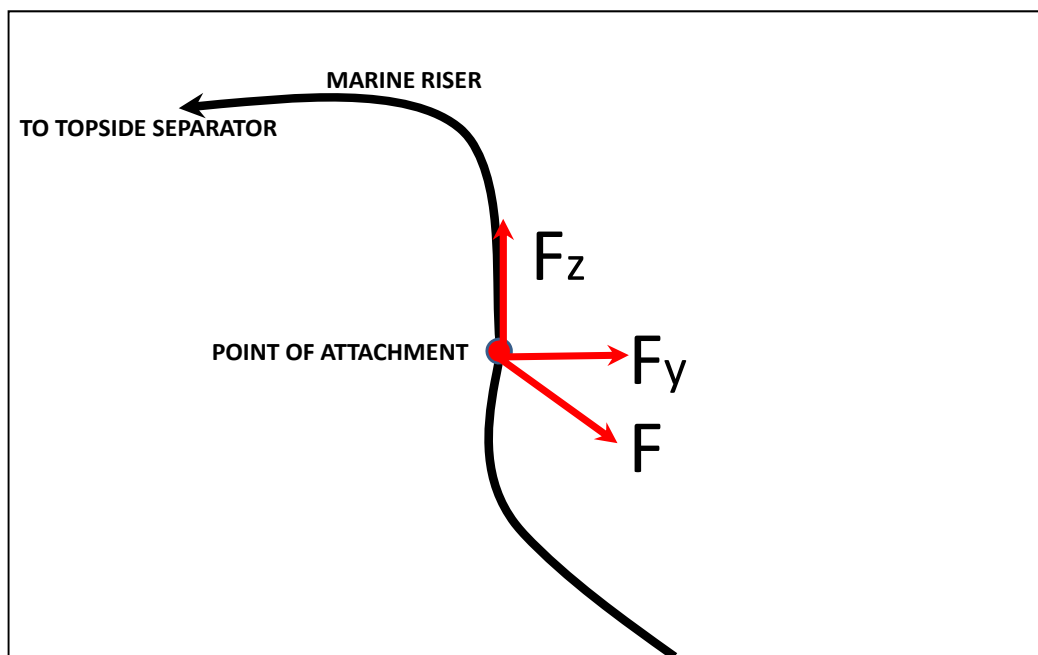


Figure 21 Direction of acting forces on point of attachment.

The resolved force F induced by the motions of the riser on the point of attachment is derived by use of the cosine rule.

4 OLGA VERIFICATION

A part of the scope of this thesis was the generation of experimental data for comparisons with numerical simulations. The interface model which was to be used for the numerical simulations, at the time of completion of the experimental work was still being developed and hence data from the experiment could not be compared with that model. Alternatively it was proposed that the measured data from the experiments be compared with the multiphase simulator OLGA, to verify the data measured and obtain additional information which was not measured in the course of the experiment.

To verify the experimental data, an OLGA model was built. The model was simplified so as to capture the most important aspects of the experiments. Verification was mainly performed to emphasize the accuracy of the following parameters:

- Riser Inlet Pressure.
- Liquid mass flow rate
- Gas mass flow rate
- Period of severe slugging cycle.

4.1 OLGA CASE DESCRIPTION

The Initial and boundary conditions were simplified and used as follows:

- Riser (pipe) diameter = 0.016 metres
- Outlet Pressure = Atmospheric pressure = 1 atmosphere.

The presence of a buffer tank in the experiment is represented by a pipeline section:

- Volume of section = 0.025 m³
- Assumed diameter of section = 0.20 m
- Length of pipe section = 1.4 m

Pressure Velocity Temperature (PVT) tables are normally used in OLGA simulations. This is due to the fact that when simulating multiphase flow, single phase correlations are not applicable.

PVT tables are generated using a program called PVTsim developed by *Calsep*. This program calculates the fluid properties for multiphase flows containing hydrocarbons and process fluids. The PVT file used in this simulation was supplied by doctorate student Tor Kjeldby and was generated for an air-water mixture at 15°C.

Simulation ENDTIME was set at 1000 seconds with MAXDT and MINDT set at 10 and 3.24e-005 seconds respectively.

On OPTIONS, the TEMPERATURE option is turned off as the simulation is performed as an adiabatic simulation. This simplifies the simulation and removes the need to supply pipeline wall parameters for heat transfer and temperature profile calculations.

4.1.1 OLGA L-RISER NUMERICAL SIMULATION

The Free hanging catenary (L- riser) configuration was modelled in the FLOWPATH with the X-Y coordinates shown in Table 10.

Table 10: L-riser FLOWPATH co-ordinates.

PIPE	X (metres)	Y (metres)	LENGTH (metres)	#SECTIONS	DIAMETER (metres)	ROUGHNESS (metres)
1	0.989949	-0.98995	1.4	50	0.20	1e -005
2	2.08	-7.194	6.29908	100	0.016	1e -005
3	2.2532	-7.493	0.345542	5	0.016	1e -005
4	2.9104	-7.493	0.6572	20	0.016	1e -005
5	3.0836	-7.1931	0.346321	10	0.016	1e -005
6	4.12549	-1.2843	5.9999	100	0.016	1e -005
7	4.12549	-1.09425	0.19005	4	0.016	1e -005
8	4.32549	-1.09425	0	4	0.016	1e -005

The values in Table 10 correspond to a simplified geometry as shown in Figure 22.

Curvatures of the flexible riser in the experimental model were simplified in the computational model and were represented by sections of small pies lying at angles to each other.



Figure 22 L-riser geometrical description in OLGA

Simplifications and Limitations:

- Pipe 1 represents the buffer tank and is simulated as a pipe section.
- Pipe 1 is given an angle of inclination to avoid gas flowing in a reverse direction. This angle is assumed to be 45° .
- Pipe 2, 3 and 4 are designed as a 3 side part section of an octagon to capture the curved nature of the bottom of the riser.
- The angle of curvature between pipe 6 and 7 is replaced by a simpler 90° degree angle.

4.1.2 OLGA S RISER NUMERICAL SIMULATION.

Table 11: S-riser FLOWPATH co-ordinates

PIPE	X (metres)	Y (metres)	LENGTH	DIAMETER (metres)	ROUGHNESS
1	0.989949	-0.98994	1.4	0.2	1e -005
2	1.9866	-6.6429	5.740	0.016	1e -005
3	2.18035	-6.978	0.387	0.016	1e -005
4	2.95535	-6.978	0.775	0.016	1e -005
5	3.1491	-6.6424	0.387	0.016	1e -005
6	3.5085	-4.604	2.07	0.016	1e -005
7	3.7385	-4.2056	0.460	0.016	1e -005
8	4.1985	-4.2056	0.46	0.016	1e -005
9	4.6585	-5	0.918	0.016	1e -005
10	4.7285	-5.1212	0.140	0.016	1e -005
11	5.0085	-5.1212	0.28	0.016	1e -005
12	5.0785	-5	0.140	0.016	1e -005
13	5.4266	-3.0254	2.005	0.016	1e -005
14	5.4266	-2.8354	0.19	0.016	1e -005
15	5.6266	-2.8354	0.20	0.016	1e -005

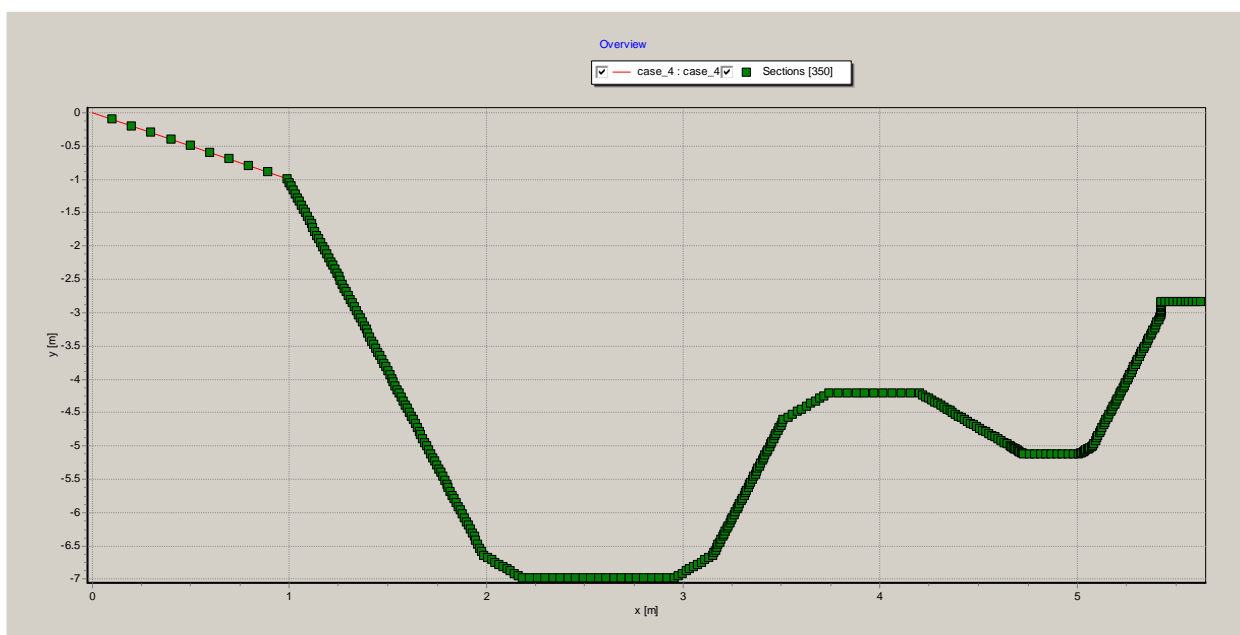


Figure 23 S-riser geometrical description in OLGA

5 RESULTS AND DISCUSSIONS

5.1 L-RISER RESULTS

Table 12: L- Riser experiment flow rates.

TEST CASE	GAS MASS FLOW RATE (kg/s)	LIQUID MASS FLOW RATE (Kg/s)
1. Decay	-	-
2. Zero Settings	-	-
3. Alpha 02	0.0001319	0.079
4. Alpha 03	0.0001315	0.082
5. Alpha 04 (MOST ACCURATE)	0.00013175	0.08
6. Alpha 05	0.00013175	0,08

- The Liquid density is assumed to be 1000 kg/m^3
- The Air density is assumed to be 1.2 kg/m^3

Alpha 04 data was chosen to be used as the simulation flow rates due to its closeness to the computed average mean flow rates.

It was observed during the course of the experiments, that for a particular pipeline-riser system (configuration, diameter and length), the flow rates that could induce severe slugging phenomenon lay in a small range and when this range was exceeded, the flow phenomenon completely stopped. A steady flow regime would then be generated depending on which phases volumetric flow rate was increased. When the liquid flow rate was increased, bubble flow was observed and when gas flow rate was increased annular flow was observed.

The reported results in the subsequent sections are for Test case 5 (Alpha 04).

5.1.1 SEVERE SLUGGING IN L-RISER EXPERIMENTAL RESULTS

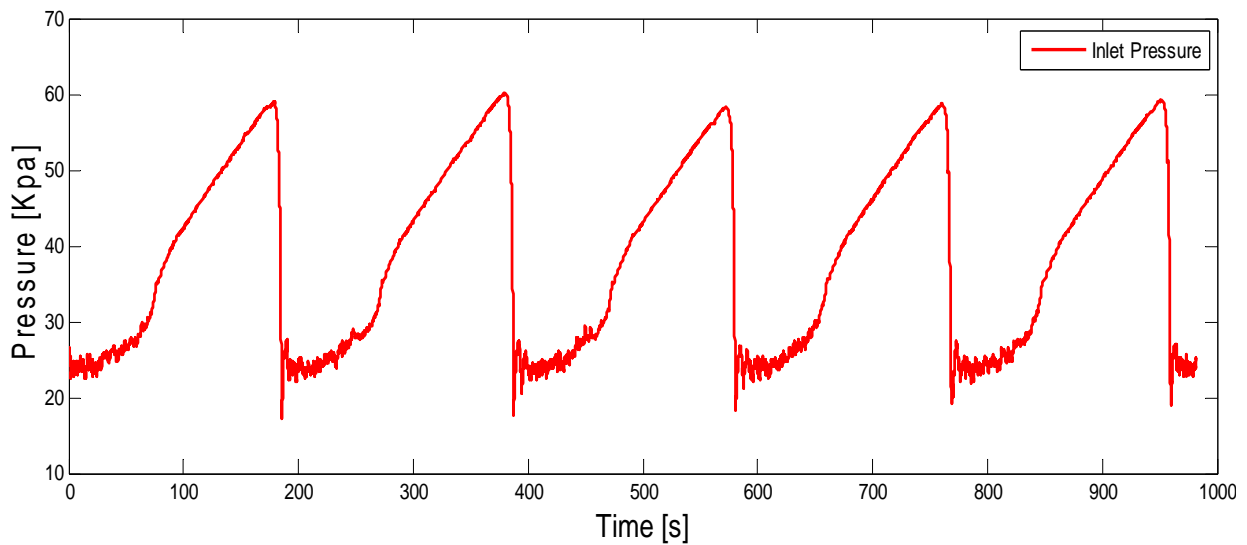


Figure 24 L-riser inlet Pressure

Figure 24 above illustrates the inlet pressure to the L-riser. The values correspond with the expected numerical hydrostatic head of the liquid in the riser column. From the graph it is possible to deduce that the period for one severe slugging cycle is approximately 200 seconds. The pressure recorded is the gauge pressure in Kilo Pascal.

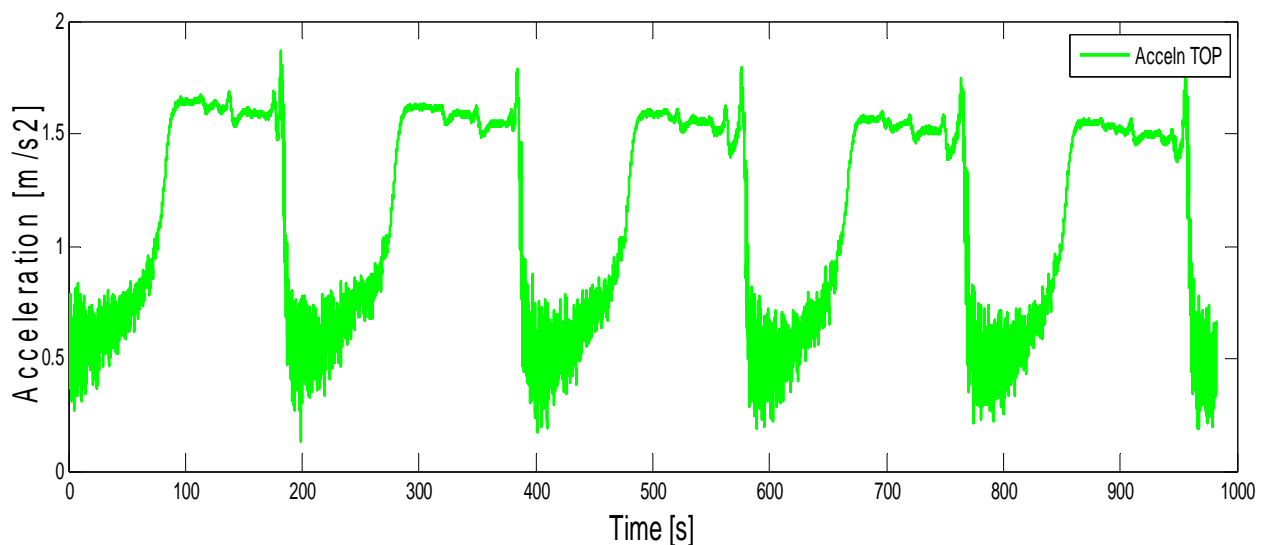


Figure 25 Acceleration curves of a point at the top of the L-riser during cycles.

Figure 25 represents the acceleration of a point (defined in Figure 15) at the top of the flexible riser during the cycle. The trend shows that as the riser column is being filled with liquid, the riser accelerates from its initial position, in a positive direction, when it is completely filled with liquid, the riser remains in a stationary position. As the bubble

penetrates the liquid in the column for blowout to occur, the riser accelerates in a negative direction back to its initial position. This negative direction does not correspond to deceleration, because it doesn't mean that the riser from its position when completely filled with liquid is still accelerating or has a constant acceleration, but at this position, the riser is stationary. The riser during blowout just accelerates in the opposite direction back to its initial position. This principle applies to the subsequent acceleration curves.

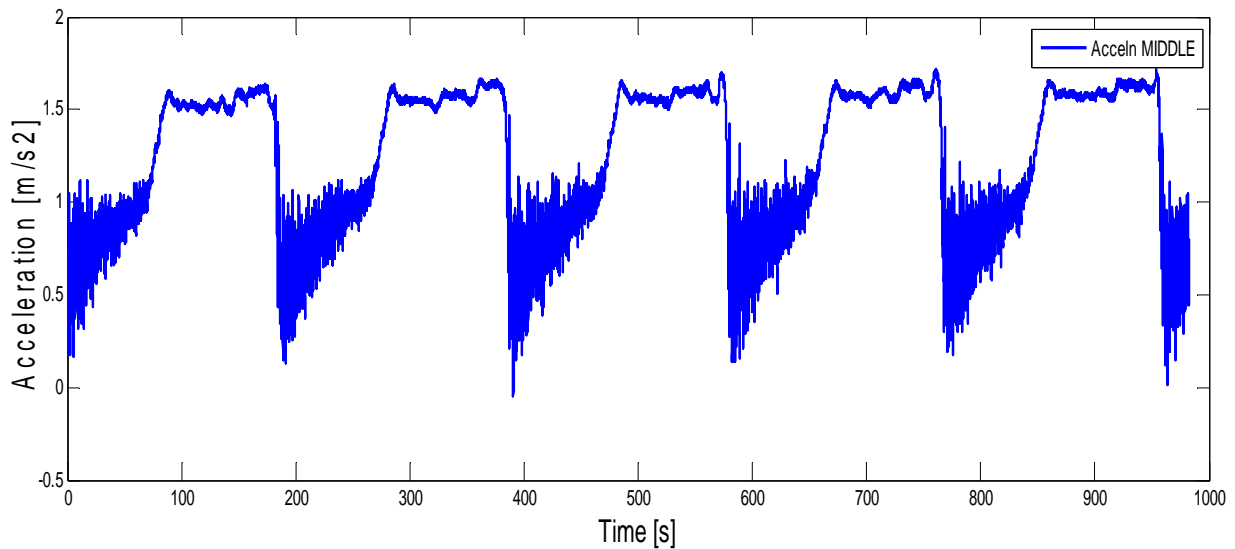


Figure 26 Acceleration of a point at the middle of the L-riser during the cycles

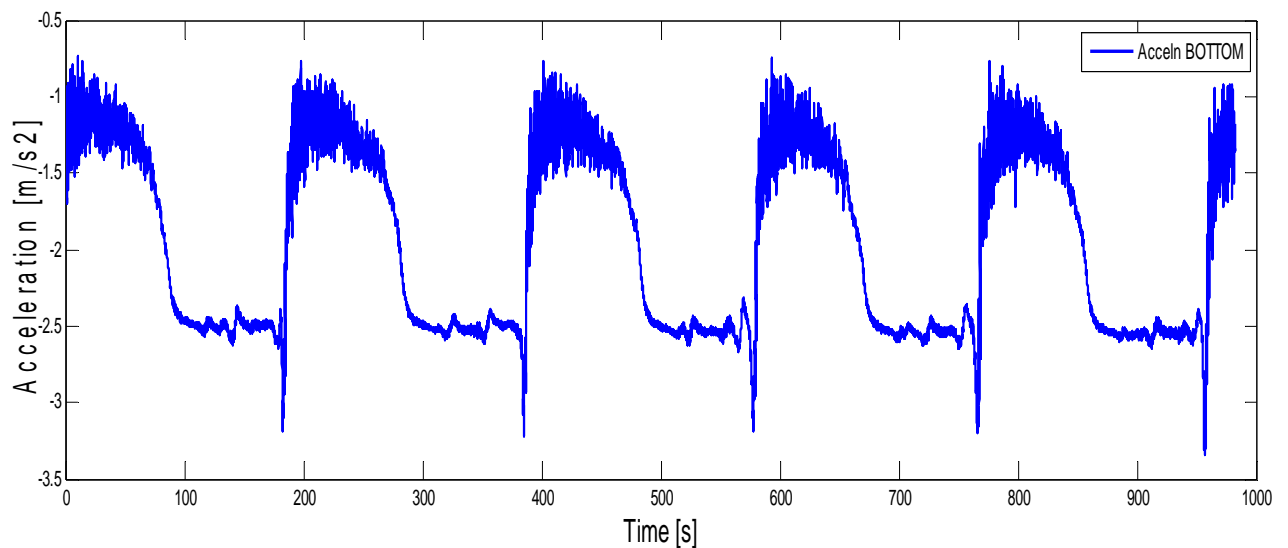


Figure 27 Acceleration of a point at the bottom of the L-riser during the cycles.

Figures 25, 26 and 27 above illustrate the acceleration of the L-riser at the top middle and bottom positions. The exact positions of these accelerometers on the riser are discussed in

section 3.3 .The readings from the accelerometer at the “bottom” illustrated in Figure 27, are of the negative value due to the residual curvature of the riser (inability to lie perfectly straight) thus the accelerometers orientation in space on the riser is reversed and thus it results are reversed, but the magnitude remains the same. The plots do not bottom out at zero due to residual currents and waves in the experiment pool. The equation of the curves above has been generated in appendix A. This defines the acceleration of a single point on the riser with time.

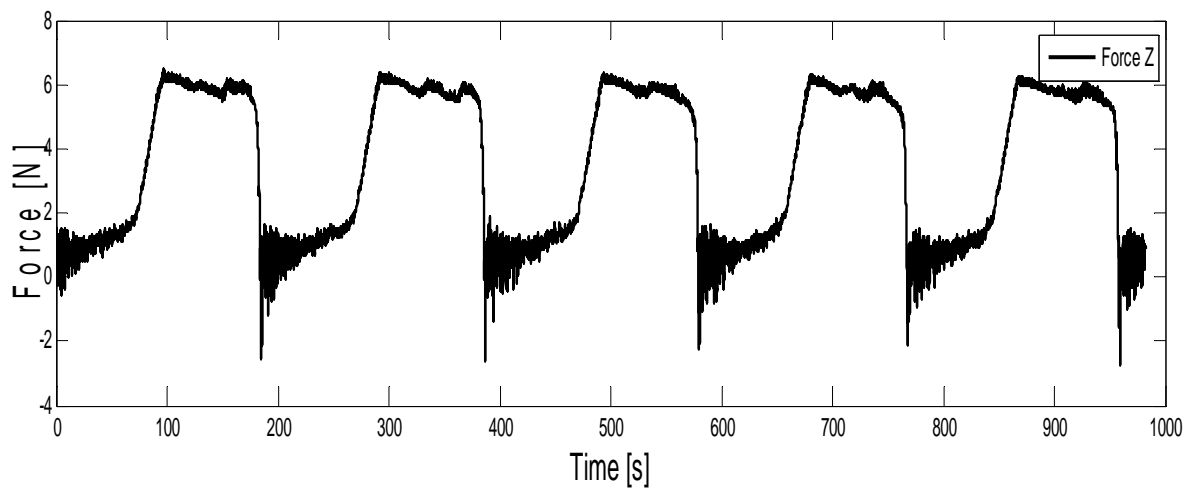


Figure 28 Force induced by the L-riser on the point of attachment during the cycle in the Z direction.

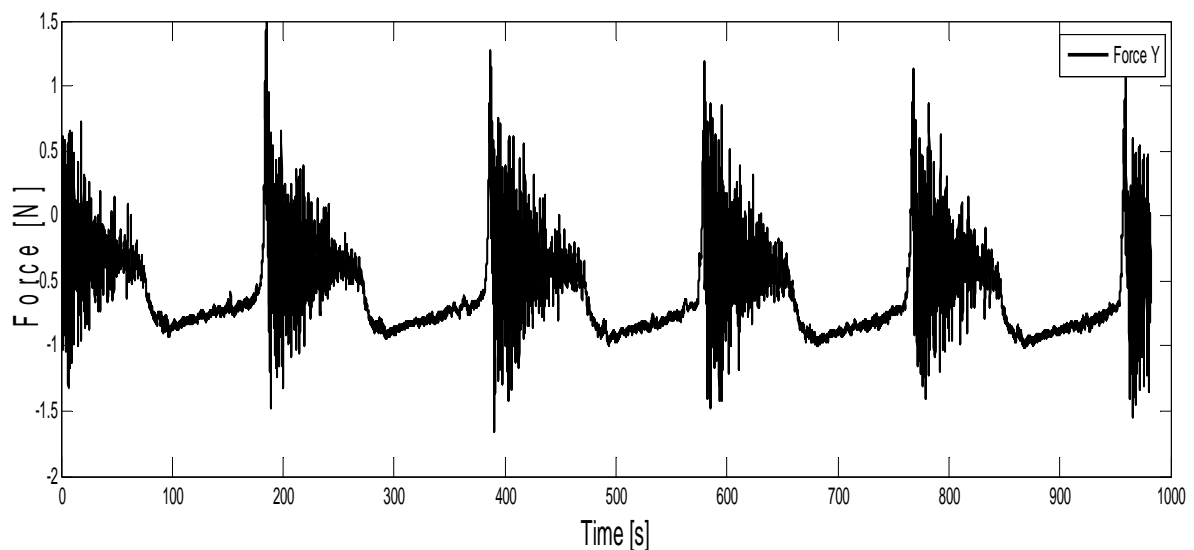


Figure 29 Force induced by the L-riser on the point of attachment during the cycle in Y direction

Figures 28 and 29 illustrate the magnitude of the forces in Newton exerted on the load cell due to the displacement of the L-riser during the severe slugging cycle. This helps to compute the force that will be exerted at the point of attachment of the L-riser to a topside vessel as was illustrated in section 3.3.5.

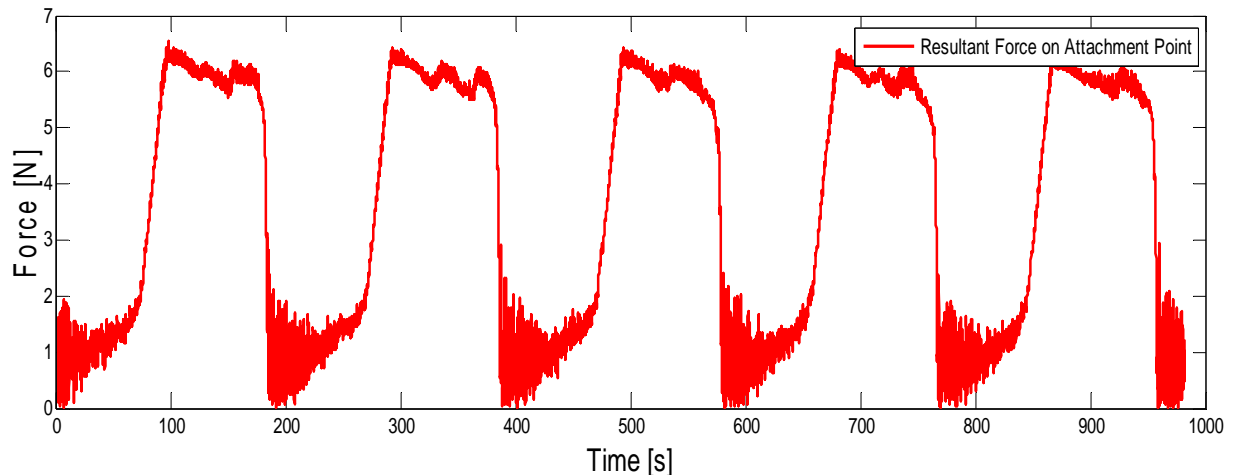


Figure 30 Resultant Force on point of attachment by displacement cycles of the L-riser.

Figure 30 illustrates the magnitude of the force on the point of attachment of the riser to a topside vessel. It ranges from 6.4 Newtons to 0.4 Newton.

The trend for this curve shows that when the riser column is being filled with liquid, the load on the attachment point increases, when the column is completely filled with liquid, the attachment point experiences the maximum load of 6.4 Newton for approximately 100 seconds which is about 50 % of the cycle period. As the gas bubble penetrates the liquid column in the riser, the weight of the column gradually reduces and when the blowout occurs with the production of little (hydrodynamic) slugs, the load on the attachment point is at its minimum level of 0.4 Newton. This cycle is repeated over again.

The cyclic nature of this resultant force is what induces fatigue at the point of attachment of the riser to the topside vessel.

5.1.2 SEVERE SLUGGING IN L-RISER OLGA SIMULATION RESULTS

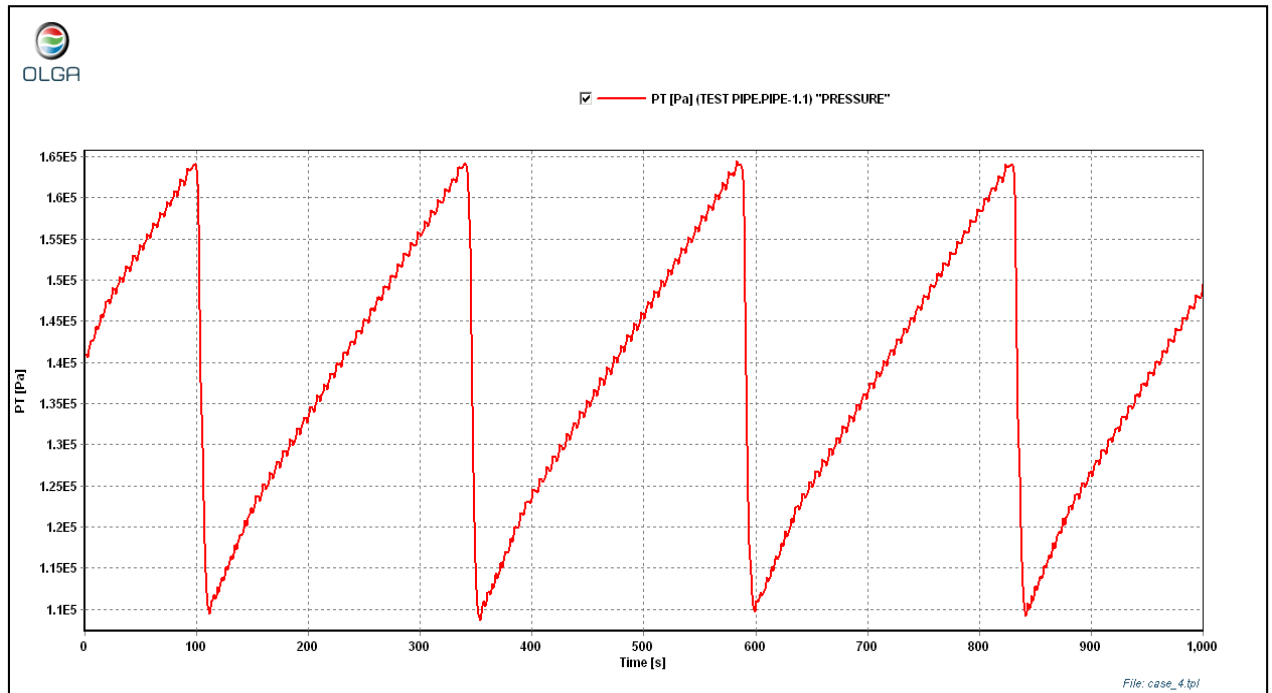


Figure 31 L-Riser Inlet Pressure (OLGA)

Figure 31 illustrates the simulated L-Riser inlet pressure . This shows a good match with the experimentally obtained results. The measured pressure is of the absolute format in Pascals.

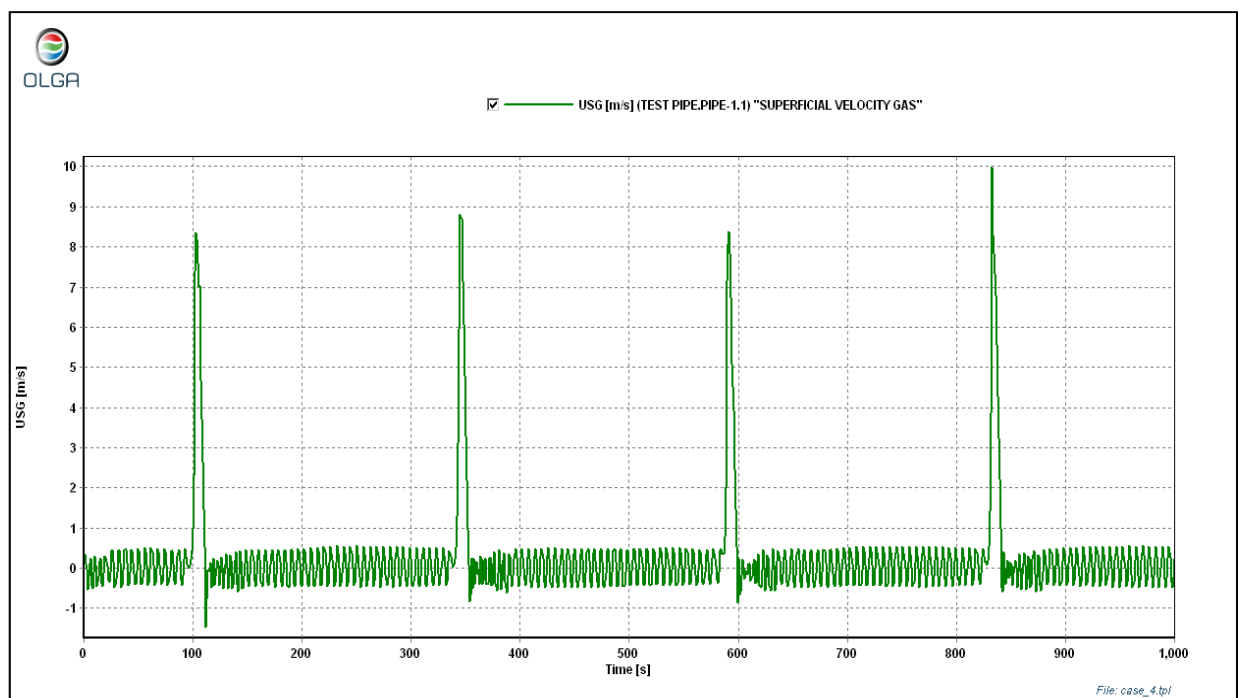


Figure 32 Superficial gas velocity (OLGA)

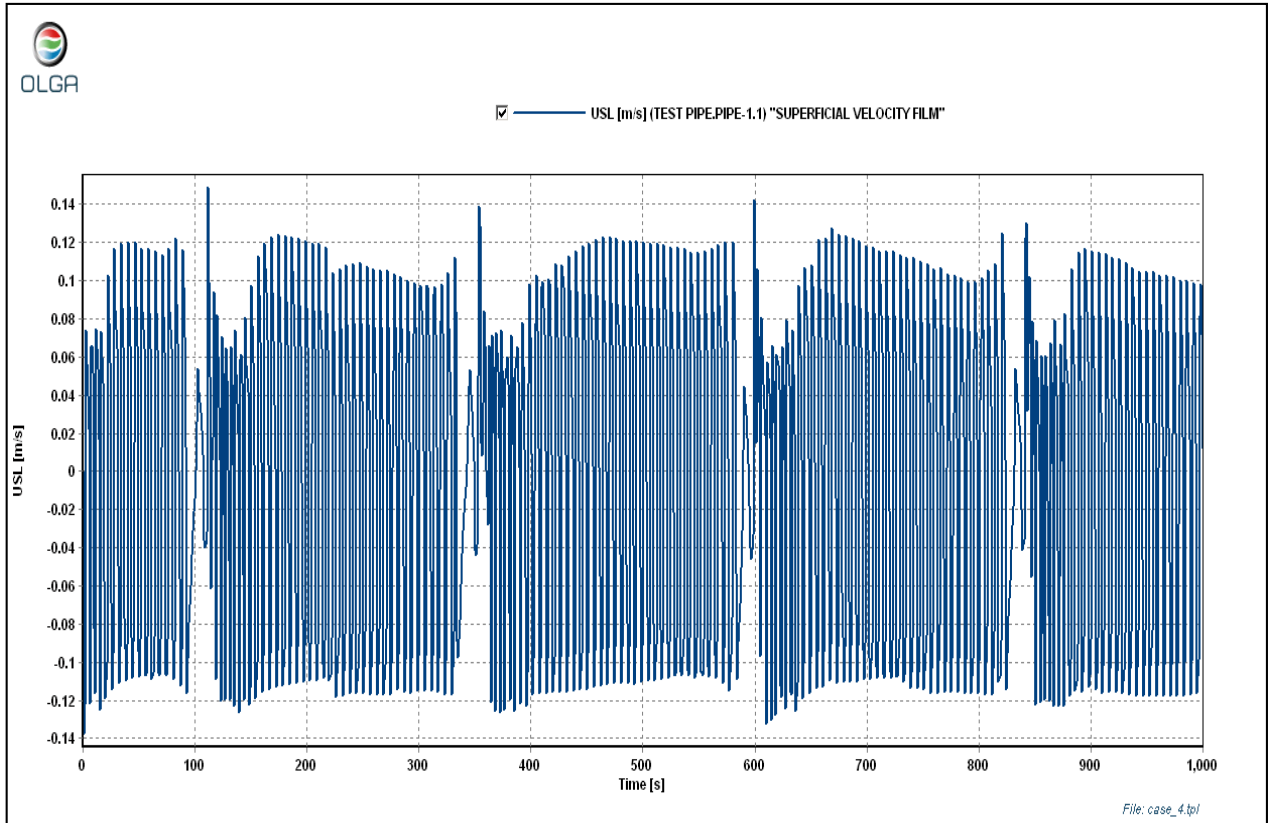


Figure 33 Superficial liquid velocity (OLGA)

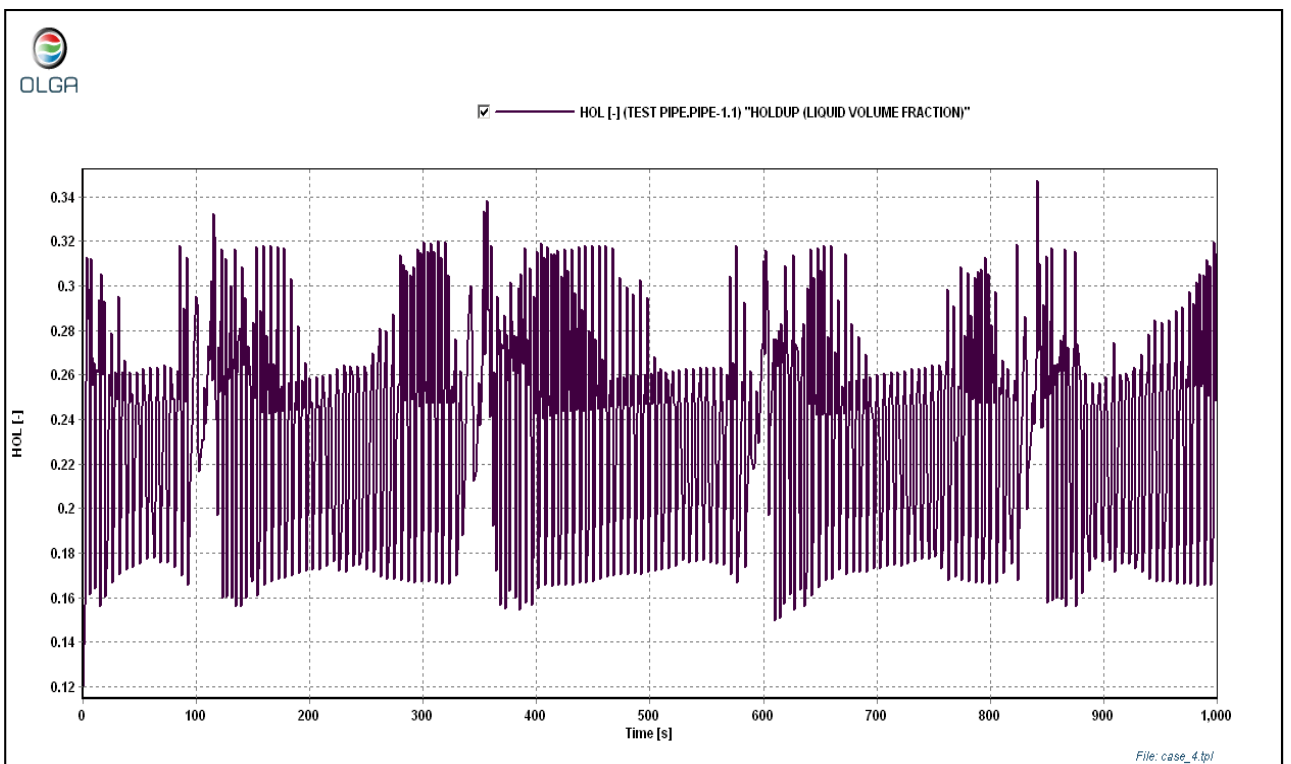


Figure 34 Liquid Hold up in L-riser (OLGA)

Figure 32 and Figure 33 illustrate the trend of superficial velocities of the gas and the liquid during the cycle. These values are important during computations due to the varying phase area of liquid and gas along the pipeline –riser system. Figure 34 illustrates the hold up in the riser during the cycle and its fluctuations conform to the expected trend.

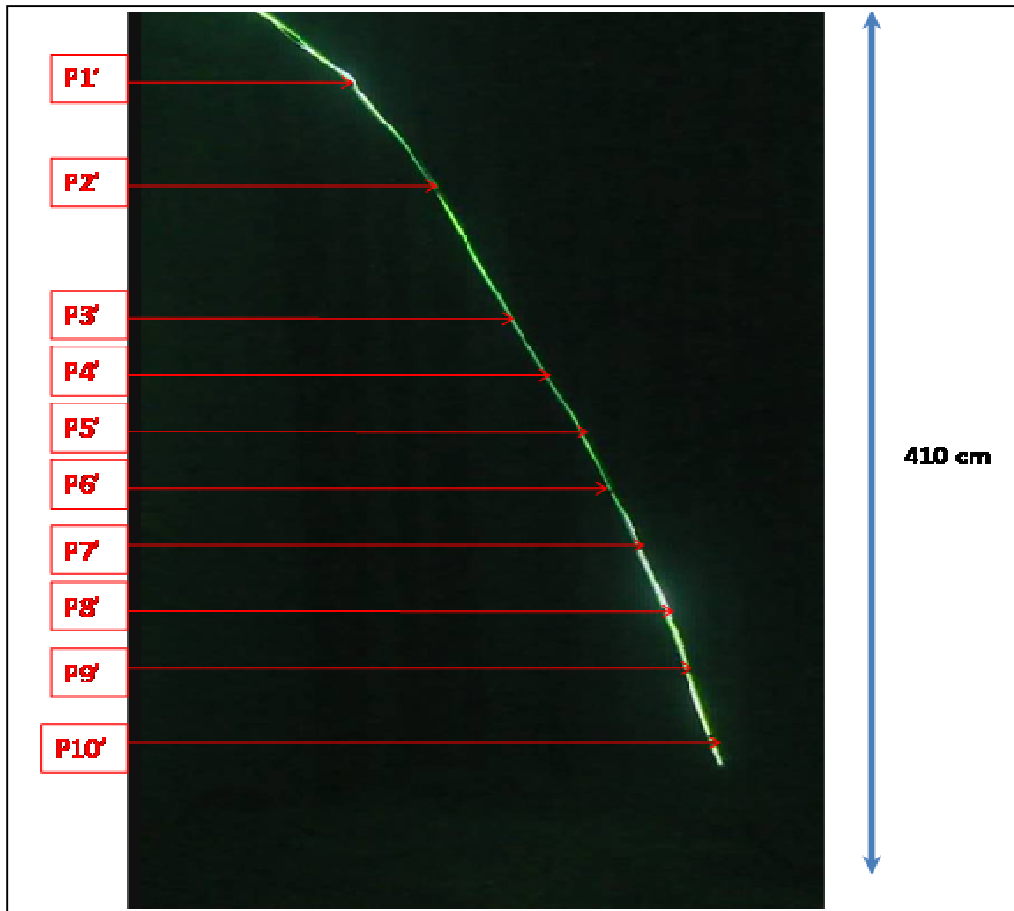


Figure 36 L-Riser initial position (at end of previous cycle)

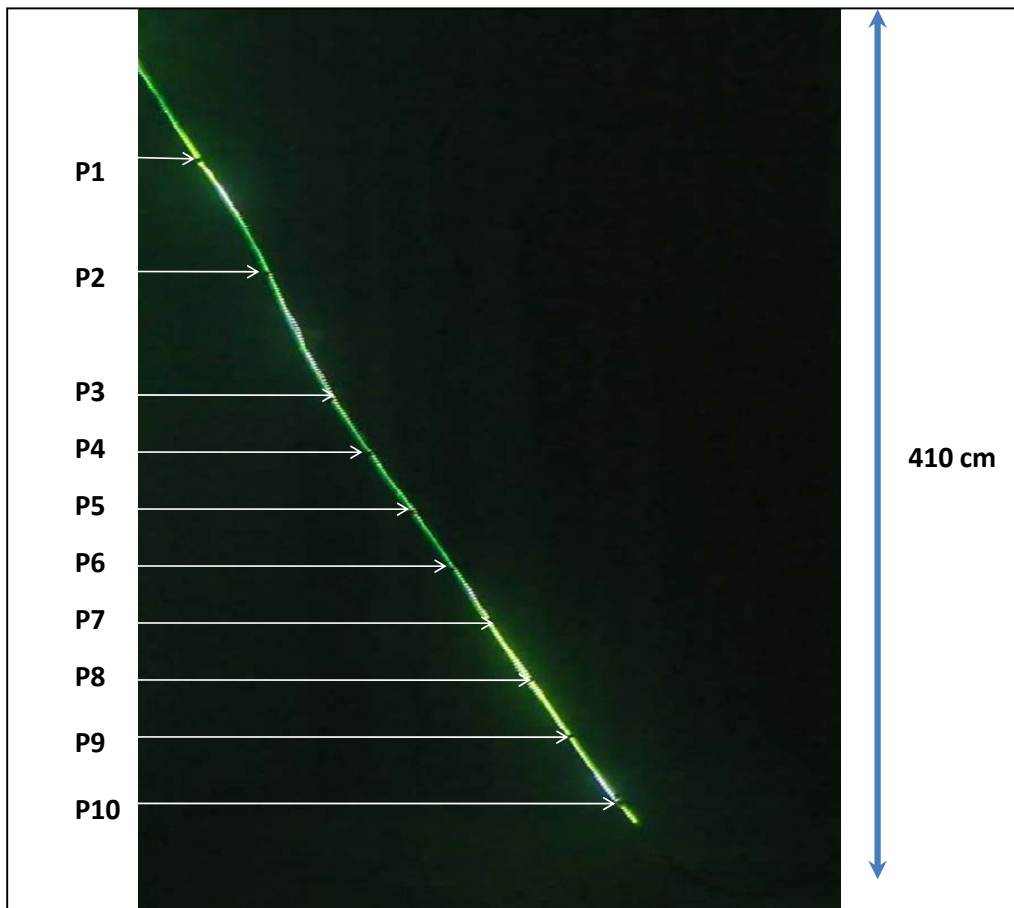


Figure 35 L-Riser final position (at complete liquid fill-up of column)

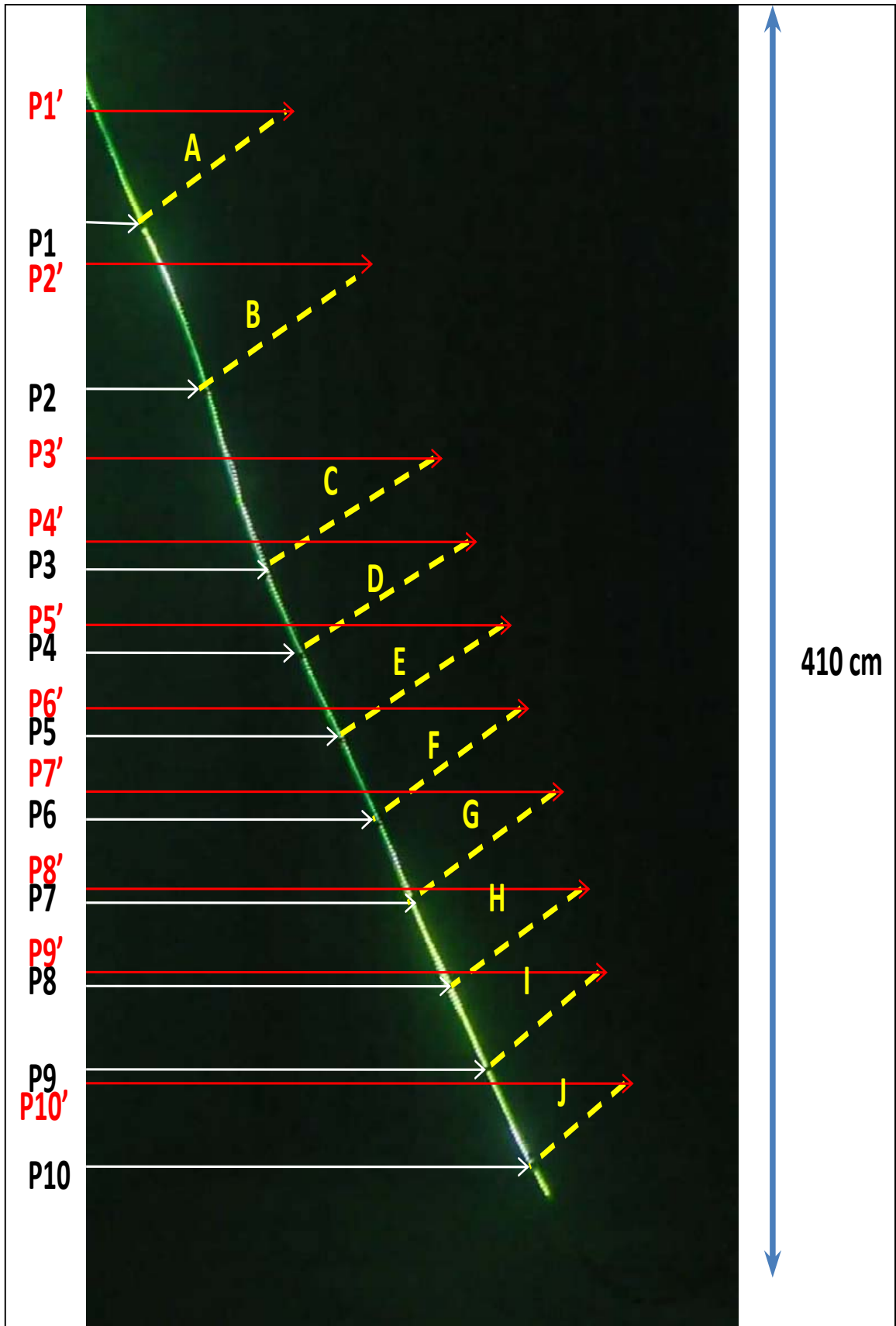


Figure 37 Method of calculating displacement of L-Riser at defined points

Figure 35 illustrates the initial position of the L-riser and this is assumed to be at the end of

a previous severe slugging cycle, right after the blowout. Figure 36 illustrates the L-riser final position which is at complete liquid fill up of the riser column. Figure 37 illustrates the method of calculating the displacement of the riser which is the difference between the initial and final position and this is shown in Table 13.

Table 13: Displacement of defined points on L-riser.

POINT	INTERVAL	DISTANCE FROM LOAD CELL POINT (metres)	DISPLACEMENT (metres)
A	P1'-P1	0,77192	0,8588
B	P2'-P2	1.6308	0,9369
C	P3'-P3	2.5218	0,9369
D	P4'-P4	2.9192	0,9760
E	P5'-P5	3.3486	0,9760
F	P6'-P6	3.7781	0,8588
G	P7'-P7	4.1684	0,8588
H	P8'-P8	4.6369	0,7808
I	P9'-P9	5.0273	0,7027
J	P10'-P10	5.5346	0,5856

5.1.3 RESULTS OBTAINED FROM CALCULATIONS FOR THE L- RISER.

Table 14: Final Results of L-riser.

PARAMETERS	RESULTS
Riser displacement (TOP) Position A	0.8588 metres
Riser displacement (MIDDLE) Position E	0.9760 metres
Riser displacement (BOTTOM) Position J	0.5856 metres
Force at attachment Point (min)	0.1 Newtons
Force at attachment point (max)	6.4 Newtons

5.2 LAZY S RISER RESULTS:

Table 15: S-riser experiment Flow rates.

TEST CASE	GAS MASS FLOW RATE (Kg/s)	LIQUID MASS FLOW RATE (Kg/s)
1. Decay	-	-
2. Zero Settings	-	-
3. S-case real test 01	0.001299	0.058899
4. S-case real test 02	0.000135	0.05749
5. S-case real test 03 (MOST ACCURATE)	0.000135	0.05675
6. S-case real test 04	0.000135	0.05675
7. S-case real test 05	0.000133	0.059495

- The Liquid density is assumed to be 1000 kg/m^3
- The Air density is assumed to be 1.2 kg/m^3

S-case real test 03 data was chosen to be used as the simulation flow rates due to its closeness to the computed average mean flow rates.

It was also observed during the course of the experiments, that for a particular pipeline-riser system (configuration, diameter and length), the flow rates that could induce severe slugging phenomenon lay in a small range and when this range was exceeded, the flow phenomenon completely stopped. A steady flow regime would then be generated depending on which phases volumetric flow rate was increased. When the liquid flow rate was increased-bubble flow was observed and when gas flow rate was increased-annular flow was observed.

The reported results in the subsequent sections are for Test case 5 (S-case real test 03).

5.2.1 SEVERE SLUGGING IN S-RISER EXPERIMENTAL RESULT

Figure 38 S-Riser Inlet Pressure.

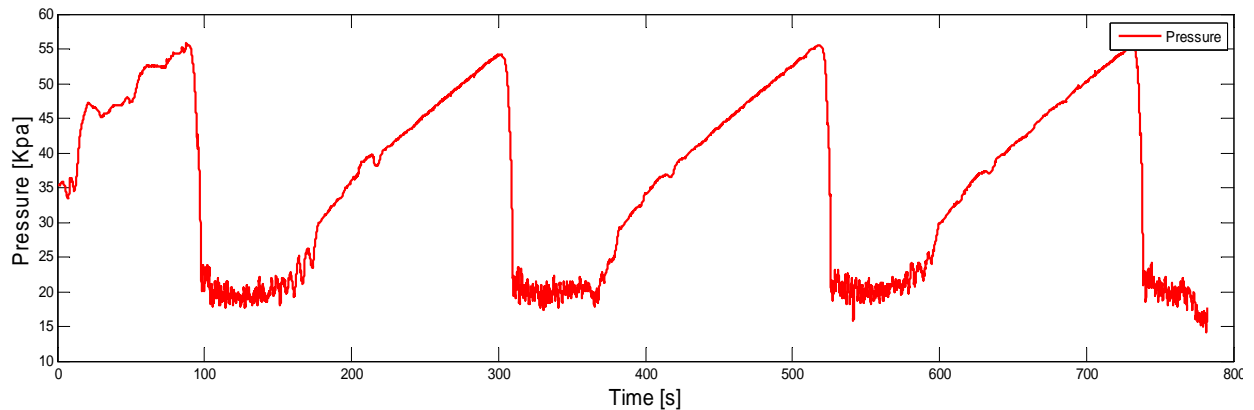


Figure 38 above illustrates the inlet pressure to the S-riser. The values correspond with the expected numerical hydrostatic head of the liquid in the riser columns. From the graph it is possible to deduce that the period for one severe slugging cycle is approximately 200 seconds. The pressure recorded is the gauge pressure in Kilo Pascal

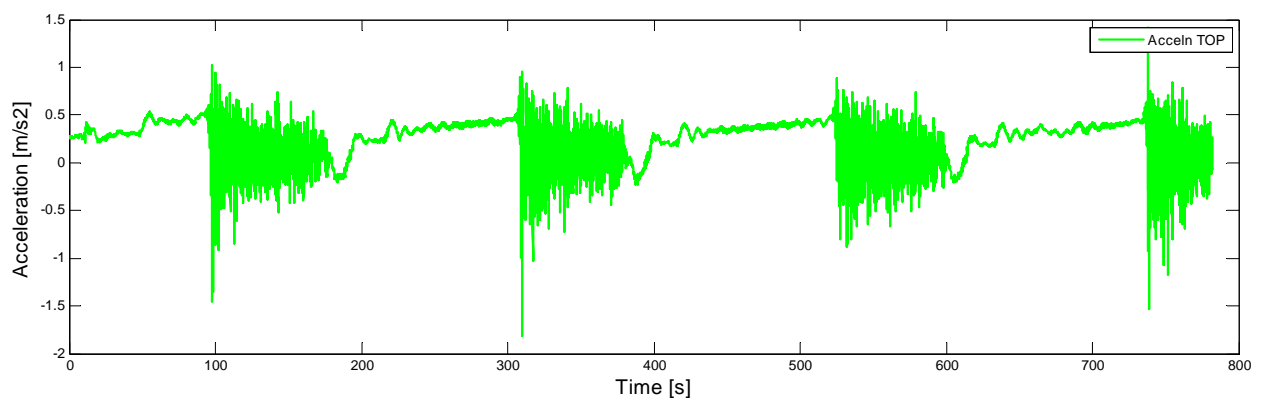


Figure 39 Acceleration of a point at the top of the S-riser during cycles

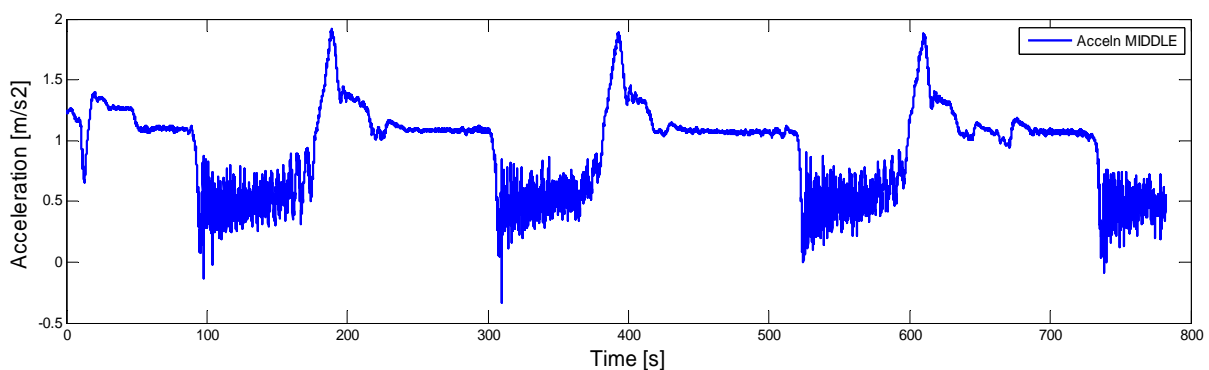


Figure 40 Acceleration of a point at the middle of the S-riser during the cycles

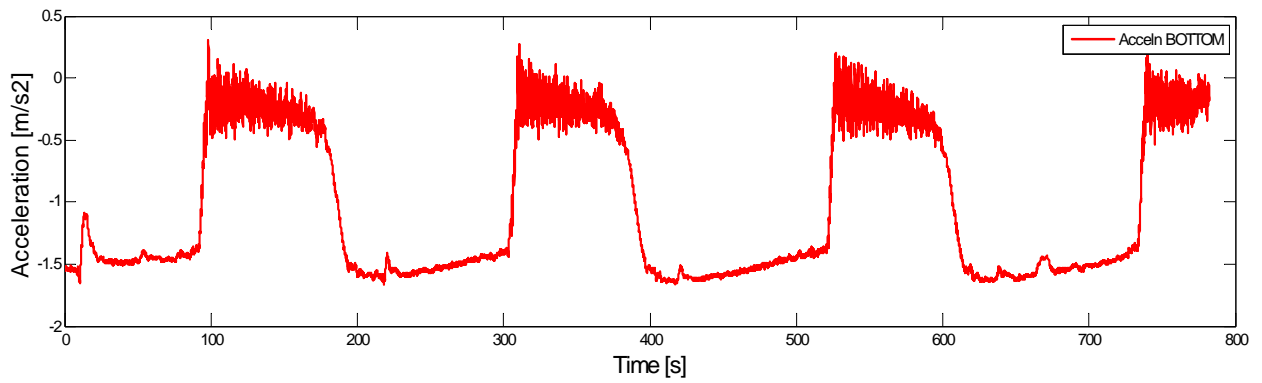


Figure 41 Acceleration of a point at the bottom of the S-riser during cycles

Figures 39, 40 and 41 above illustrate the acceleration of points on the S-riser at the top middle and bottom positions. The exact positions of these accelerometers on the S-riser are illustrated in Figure 19 .The readings from the accelerometer at the “bottom” illustrated in Figure 41, are of the negative value due to the residual curvature of the riser (inability to lie perfectly straight) thus the accelerometers orientation in space on the riser is reversed and thus it results are reversed, but the magnitude remains the same. The plots do not bottom out at zero due to residual currents and waves in the experiment pool.

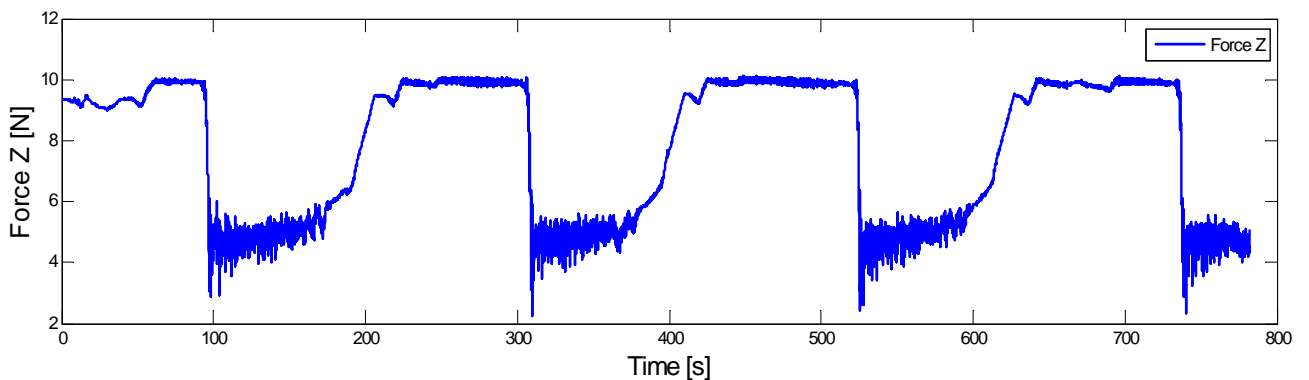


Figure 42 Force induced by the S-riser on the point of attachment during the cycle in Z direction.

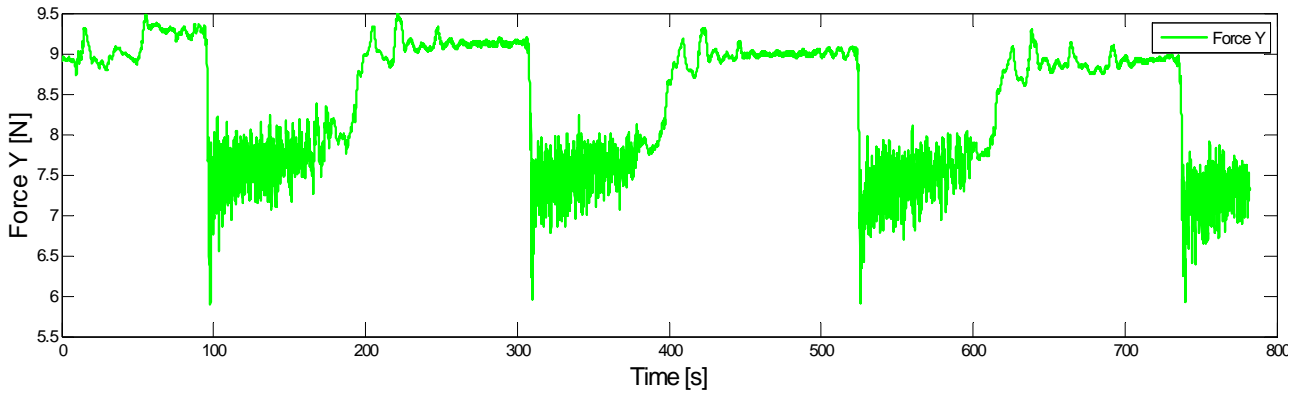


Figure 43 Force induced by the S-riser on the point of attachment during the cycle in Y-direction.

Figures 42 and Figure 43 illustrate the magnitude of the forces in Newton exerted on the load cell due to the displacement of the S-riser during the severe slugging cycle. This helps to compute the resultant force that will be exerted at the point of attachment of the S-riser to a topside vessel as was illustrated section 3.3.5.

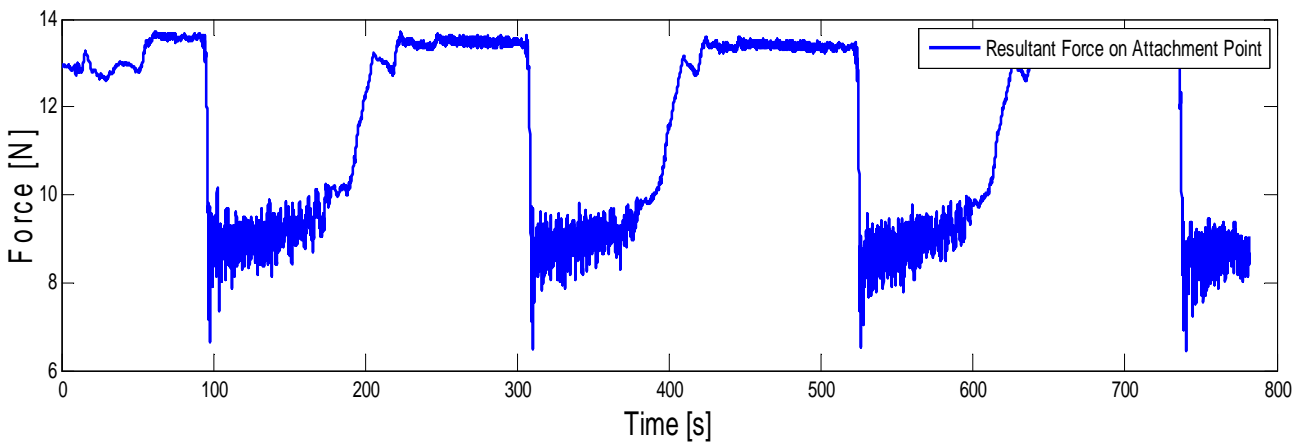


Figure 44 Resultant Force on point of attachment by displacement cycles of the S-riser.

Figure 44 illustrates the magnitude of the force on the point of attachment of the riser to a topside vessel. It ranges from 13.6 Newton to 8.0 Newton.

The trend for this curve is as the trend for the L-riser. It shows that when the riser column is being filled with liquid, the load on the attachment point increases, when the column is completely filled with liquid, the attachment point experiences the maximum load of approximately 13.6 Newton for approximately 100 seconds which is about 50 % of the cycle

period. As the gas bubble penetrates the liquid column in the riser, the weight of the column gradually reduces and when the blowout occurs with the production of little (hydrodynamic) slugs, the load on the attachment point is at its minimum level of approximately 8.0 Newton. This cycle is repeated over again.

The cyclic nature of this resultant force is what induces fatigue at the point of attachment of the S-riser to the topside vessel.

5.2.2 SEVERE SLUGGING IN LAZY S-RISER OLGA SIMULATION RESULTS

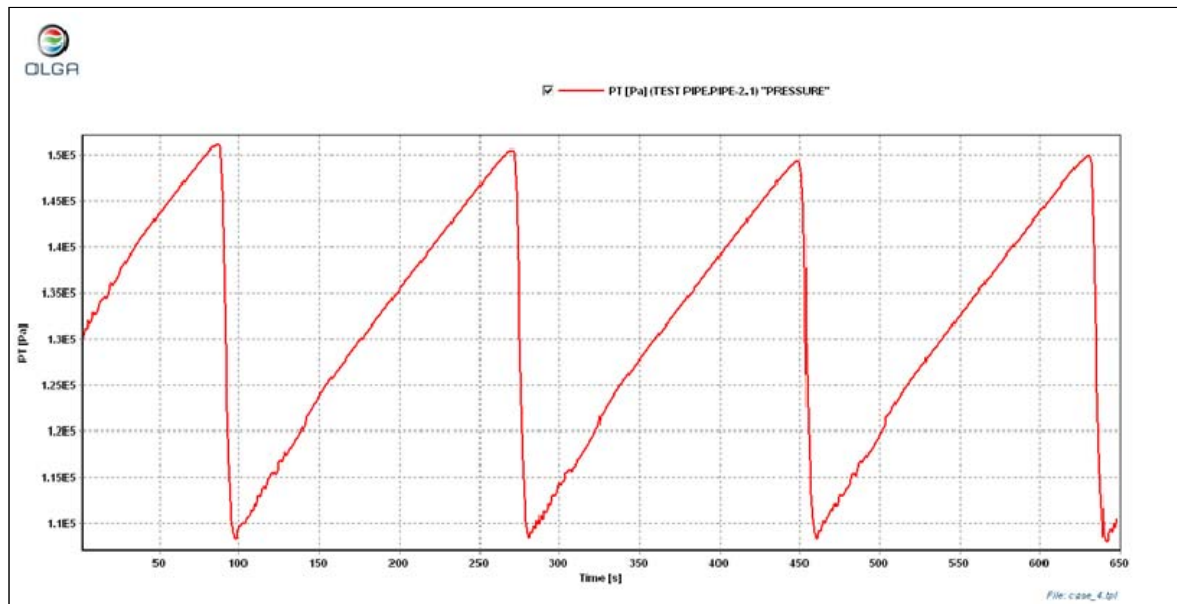


Figure 45 S-Riser Inlet Pressure

Figure 45 illustrates the simulated S-Riser inlet pressure. This shows a good match with the experimentally obtained results. The measured pressure is of the absolute format in Pascals.

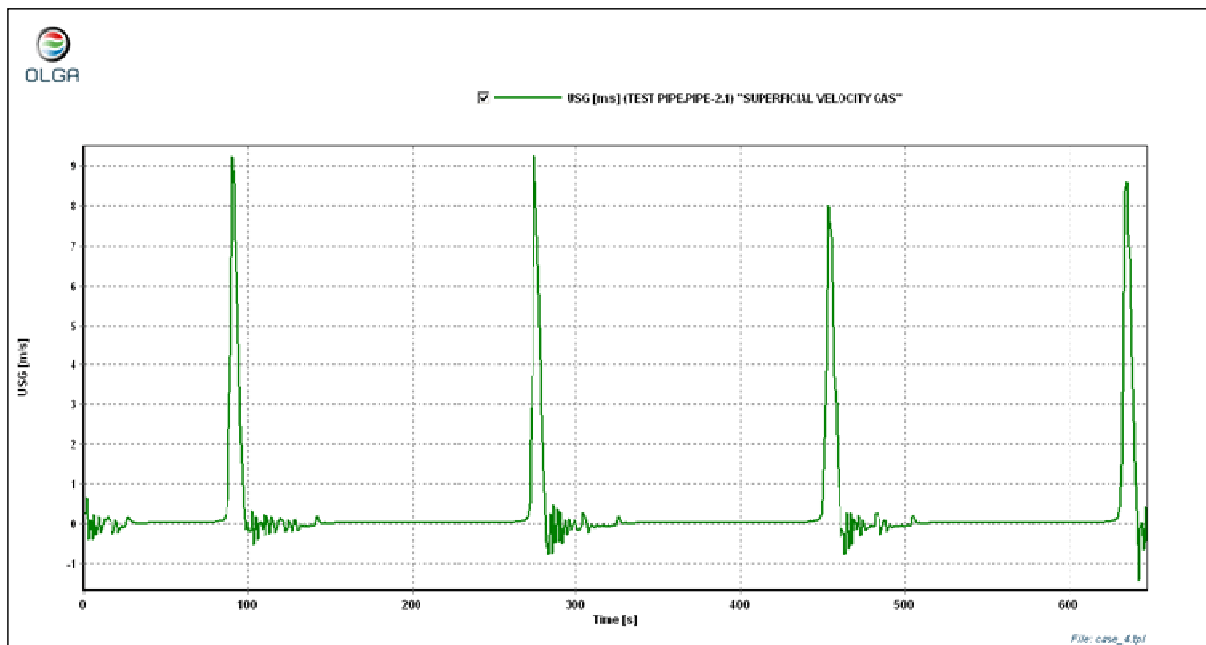


Figure 46 Superficial Velocity of gas (OLGA)

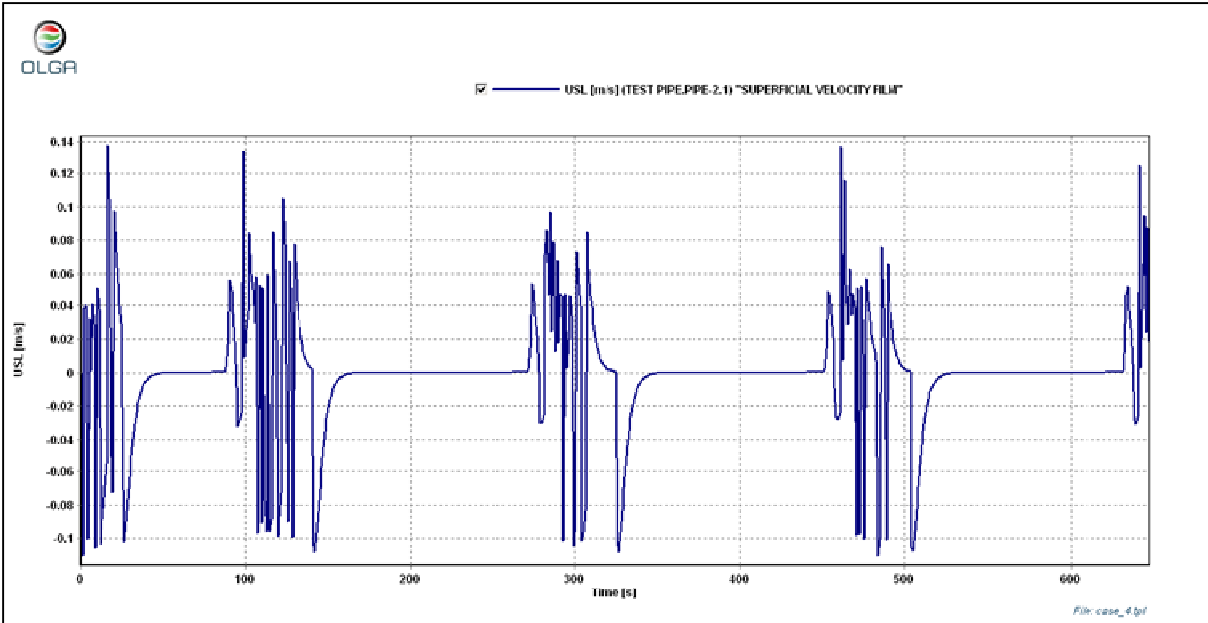


Figure 47 Superficial velocity of liquid (OLGA)

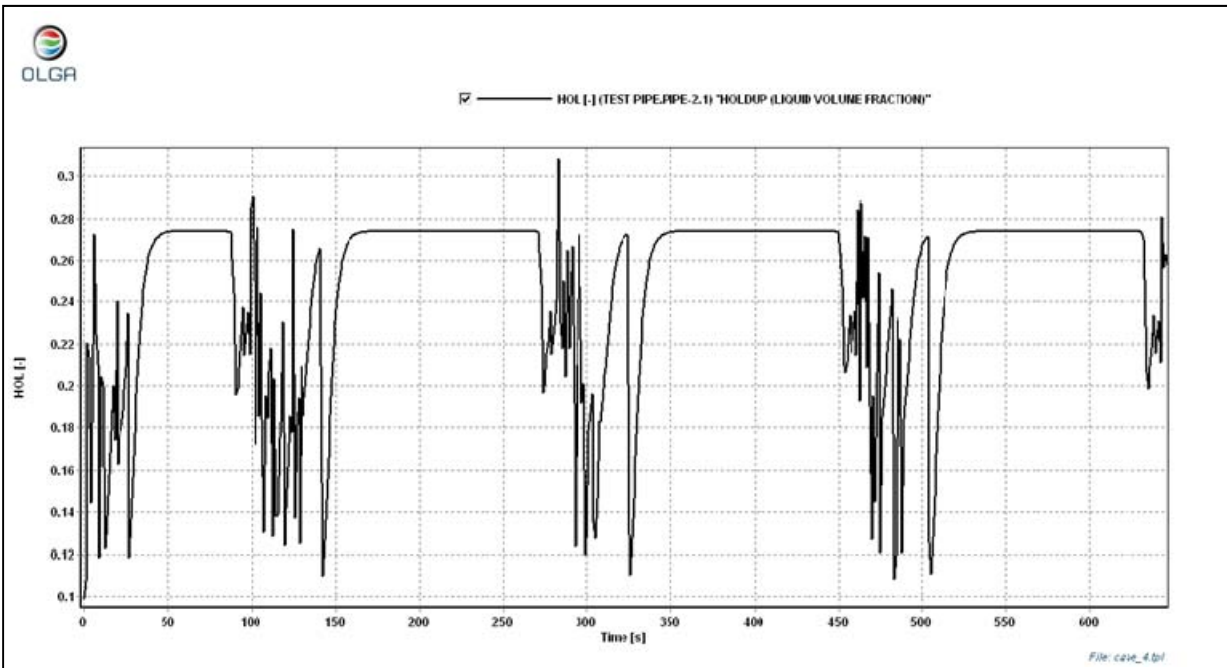


Figure 48 Liquid Hold-up in S- riser (OLGA)

Figure 46 and Figure 46 illustrate the trend of the superficial velocities of the gas and the liquid during the cycles. These values are important during computations due to the varying phase area of liquid and gas along the pipeline –riser system. Figure 48 illustrates the hold up in the riser during the cycle and its fluctuations conform to the expected trend

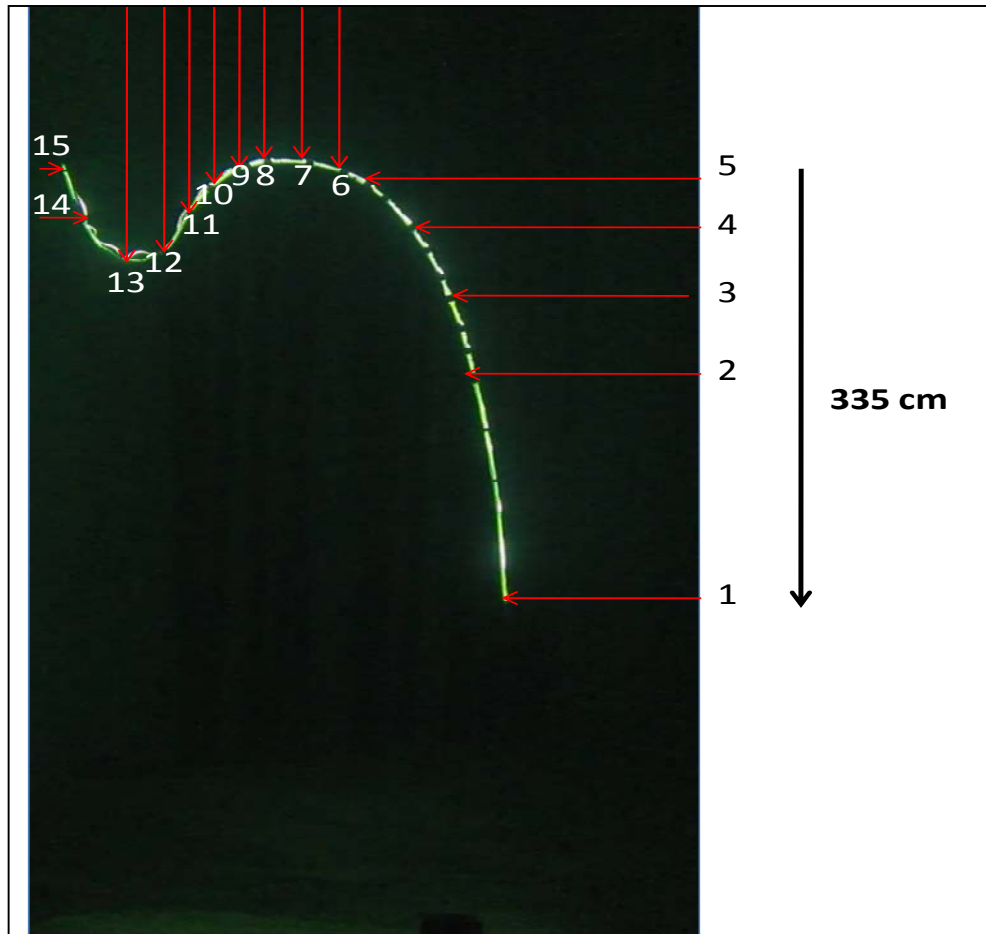


Figure 49 S-riser initial position (at end of previous cycle)

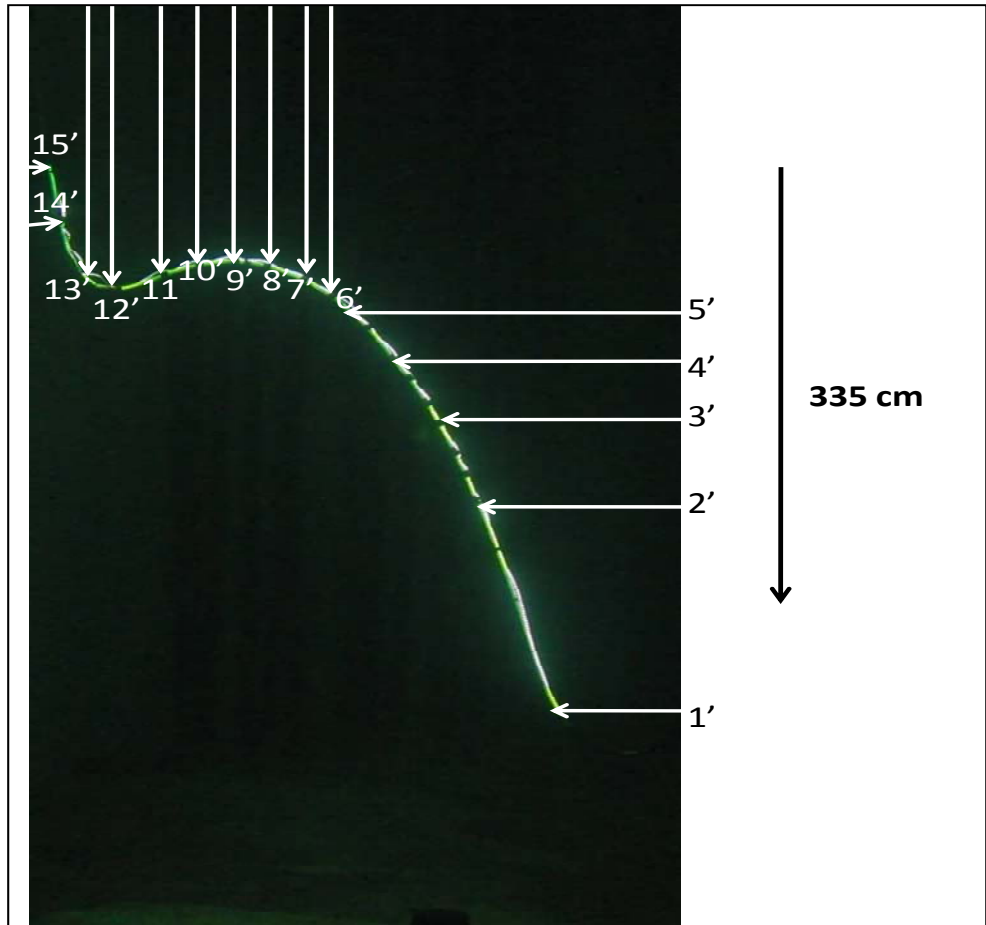


Figure 50 S-riser final position (at complete liquid fill up of column)

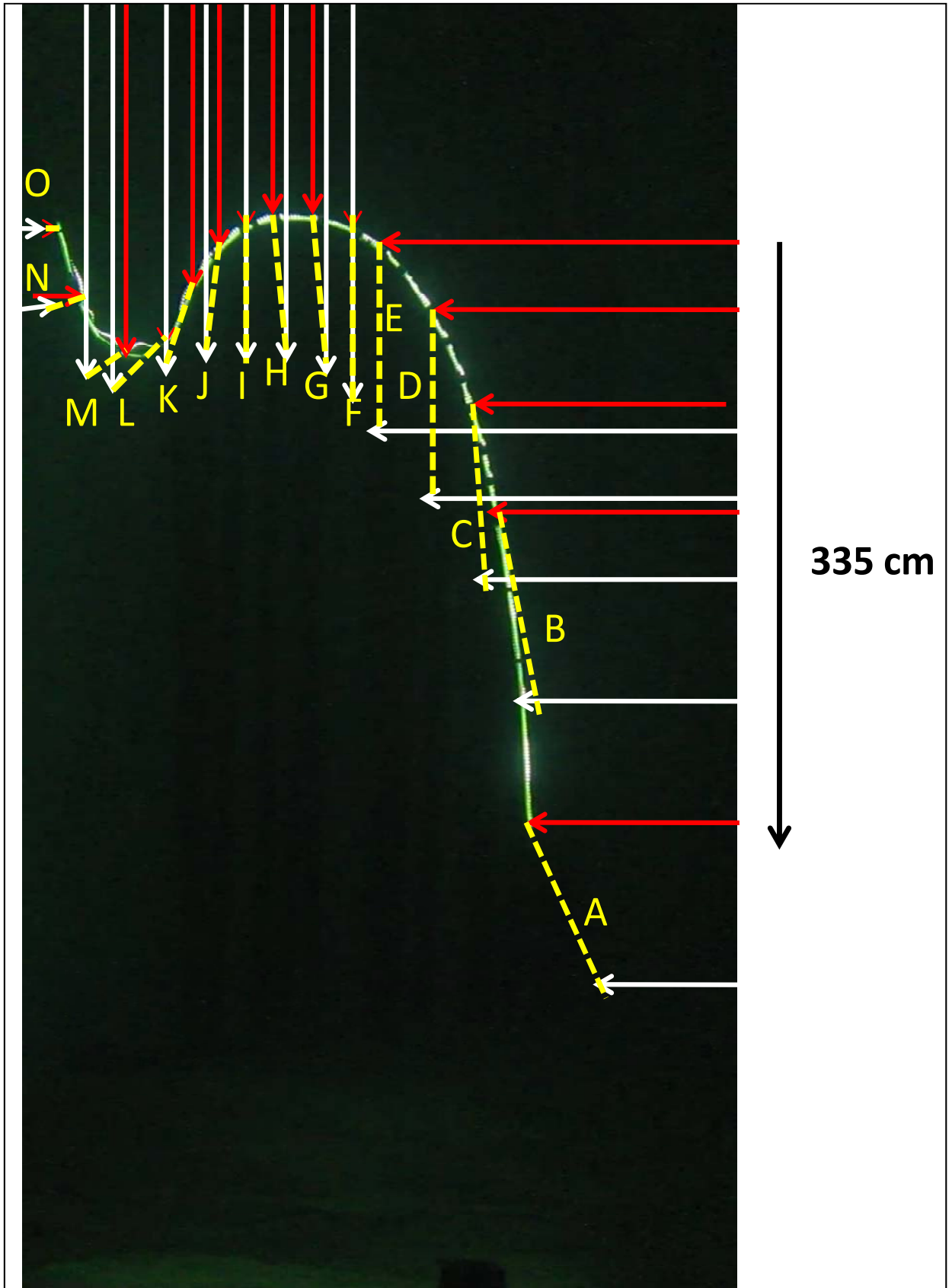


Figure 51 Method of calculating displacement of S-riser at defined points.

Figure 49 illustrates the initial position of the s-riser and this is assumed to be at the end of a

previous severe slugging cycle, right after the blowout. Figure 50 illustrates the S-riser final position which is at complete liquid fill up of the riser column. Figure 51 illustrates the method of calculating the displacement of the S-riser which is the difference between the initial and final position and this is shown in Table 16.

Table 16: Displacement of defined points on S-riser.

POINT	INTERVAL	DISTANCE FROM BRASS RING SET BELOW (ALONG RISER) metres	DISPLACEMENT metres
A	1-1'	0.08	0,957
B	2-2'	1.723	1,005
C	3-3'	2.39298	0,957
D	4-4'	3.06296	1,005
E	5-5'	3.58939	1,005
F	6-6'	3.80479	0,957
G	7-7'	4.04409	0,909
H	8-8'	4.28339	0,766
I	9-9'	4.47479	0,766
J	10-10'	4.71409	0,574
K	11-11'	5.09689	0,4786
L	12-12'	5.47969	0,4786
M	13-13'	5.81469	0,239
N	14-14'	6.38899	0,239
O	15-15'	6.81969	0,112

5.2.3 RESULTS OBTAINED FROM CALCULATIONS FOR THE S- RISER.

Table 17: Final S-riser results.

PARAMETERS	RESULTS
Riser displacement (TOP) Position O	0.112 metres
Riser displacement (MIDDLE) Position H	0.776 metres
Riser displacement (BOTTOM) Position A	0.957 metres
Force at attachment Point (min)	8.0 Newton
Force at attachment point (max)	13.6 Newton

5.3 CHALLENGES ENCOUNTERED DURING THE EXPERIMENTS

During the course of the experiment, the following challenges were encountered:

1. Access to bottom of the pool: The pool could only be accessed from the top and this led to difficulty in setting up the experiments as everything had to be done from the surface of the pool (approximately 6 metres from the bottom of the pool). The difficulties were in submerging the risers, attaching the accelerometers and LED strips, as when they were attached to the riser on the surface and submerged, their orientation in the pool changed, and the riser had to be extracted again to change their positions. This procedure had to be repeated until the orientations of the elements on the riser, when inside the pool were correct.
2. Flow meters: The initial flow meters which were available were not in the range of the flow rates being measured. For the initial analogue gas meter, its range was from 6 to 50 litres per minute, but it showed some inaccuracy when measuring rates so close to its minimum values. This was solved by replacing the initial meter with a more accurate digital gas meter which eliminated this problem. For the liquid flow meter, the indication needle oscillated between values frequently during the experiments. To solve this, a stopwatch and measuring cylinder was used to verify the liquid flow rate. The obtained flow rates were later verified and confirmed in the OLGA simulation.
3. Liquid pump: The initial pump which was present in the mobile two phase flow loop was not powerful enough to overcome the backpressure exerted by the two phase flow in the riser. Therefore, at initial stages of the experiment, a reversal of liquid in the liquid line was observed. This was solved by replacing the initial pump with a much stronger one of Head 13 metres.
4. Lighting and Video: This was a major challenge during the experiment. The challenge was to illuminate the riser as well as possible so as to be captured by an underwater camera. The initial underwater lamps used, illuminated the pool quite well but also illuminated the particles suspended in the pool and this resulted in a "dusty like"

resolution. Subsequent attempts to change the position of the underwater lamps did not improve the quality of the video obtained.

It was then proposed to use a flexible light emitting diode (LED) strip, which would be attached along the riser while in the pool. The next challenge was in obtaining a submersible, waterproof LED strip in the time window of access to the MARINTEK laboratory. After approximately Two weeks of searching, the LED strips were found and bought from "SEATRONIC båtutstyr" in Moss, Norway.

When the strips arrived, they were strapped on the riser, but the underwater camera was still picking up the reflections of the particles suspended in the water due to the way the LED strip was attached to the riser. Finally, it was decided to try a different ordinary compact camera from the viewing window, this gave excellent video quality, it eliminated the reflections from the suspended particles and the illuminated flow inside the riser could be seen and captured.

5. Interface model: At the time of conclusion of this experimental work, the interface model which would couple the structural model to the multiphase model is still been developed by the doctorate student and thus the author is unable to use it to compare the experimental data obtained.

6 CONCLUSION

A small scale experimental setup with a flexible marine riser has been constructed in the MARINTEK/SINTEF- NTNU hydrodynamic laboratory to carry out experiments on severe slugging (unsteady multiphase flow) in flexible risers. It was possible to induce the severe slugging phenomenon in the riser and the experiments were performed repeatedly for different flexible riser configurations (L and S). The experiment setup had three important modifications from previous experiments performed by the author on the same case. First the water depth was increased from 1.5 metres to 5 metres, this increase ensured that it was possible to observe the behaviour of the whole flexible riser at one instance and it also helped in intensifying the slug blowout. Second, the size of the buffer tank was increased. This increased the upstream compressible volume of the gas and helped to intensify the slug blowout. Third, the flexible riser diameter was increased from internal diameter of 0.012 to 0.016 metres. This enhanced visualization of the fluid behaviour and patterns inside the flexible riser and was critical in obtaining good video analysis.

A load cell was used to capture the loads acting on the point of attachment of the riser to a top side vessel during the severe slugging cycle. This showed a cyclic loading on this attachment point with the maximum load occurring when the riser column was completely filled with liquid and the minimum during normal slug production from the riser. The cyclic nature of these loads is a concern because of its potential to induce fatigue and this has been illustrated.

Video recordings were performed with a compact camera. This is a high definition camera with a frame rate of 30 frames per second, and was sufficient for the experiments. It was used to capture the displacements of the flexible riser during the severe slugging cycle. The initial position of the riser was considered to be the position of the riser at the end of a previous severe slugging cycle. From this position, the maximum displacement from the initial position was recorded and this was when the riser column was completely filled with liquid before the blowout. From the video recording, video analysis was performed to obtain 'snapshots' of the riser at its initial and final positions during the cycle. This snapshots in combination with a scale derived from the relationship between the true size of the riser and the size of the image captured, the displacement of the flexible riser at numerous

points was calculated. To obtain more data points, the pixels in the video can be analysed using computer programs.

A model of the experiments has also been simulated in OLGA; this was done to verify the flow rates and inlet pressure results obtained during the experiments. The results obtained in OLGA supported the experimental results and also provides other information which could not be obtained experimentally for example the liquid hold up in the risers.

Finally, the experiments were successful in highlighting the dynamic coupling between internal flows in a riser and the dynamics of a flexible riser. The generated results can be used in the future to compare with the developed interface model.

7 REFERENCES

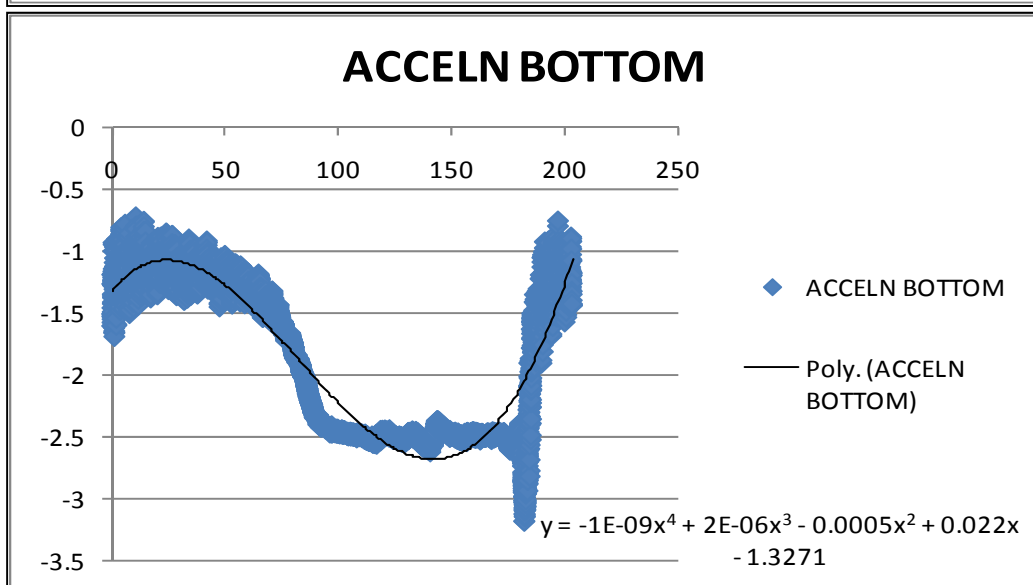
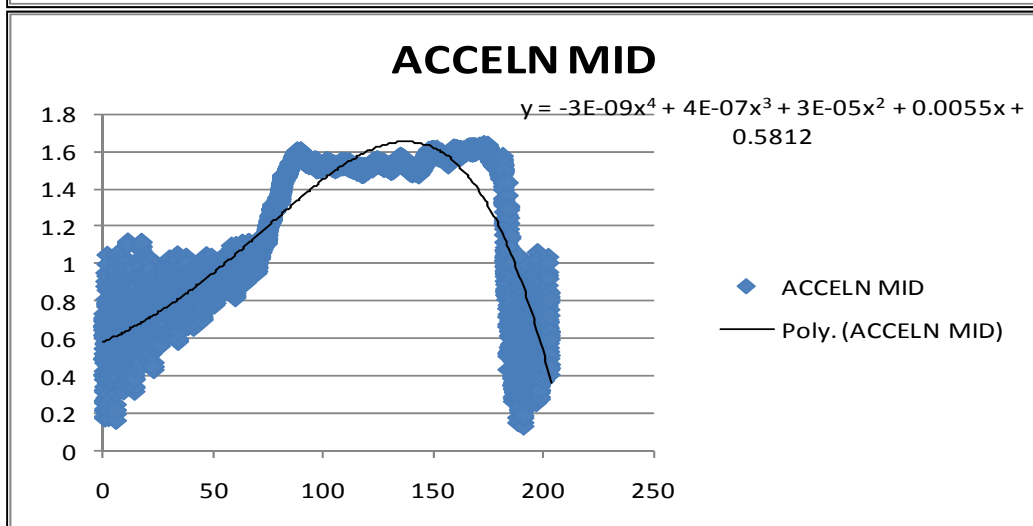
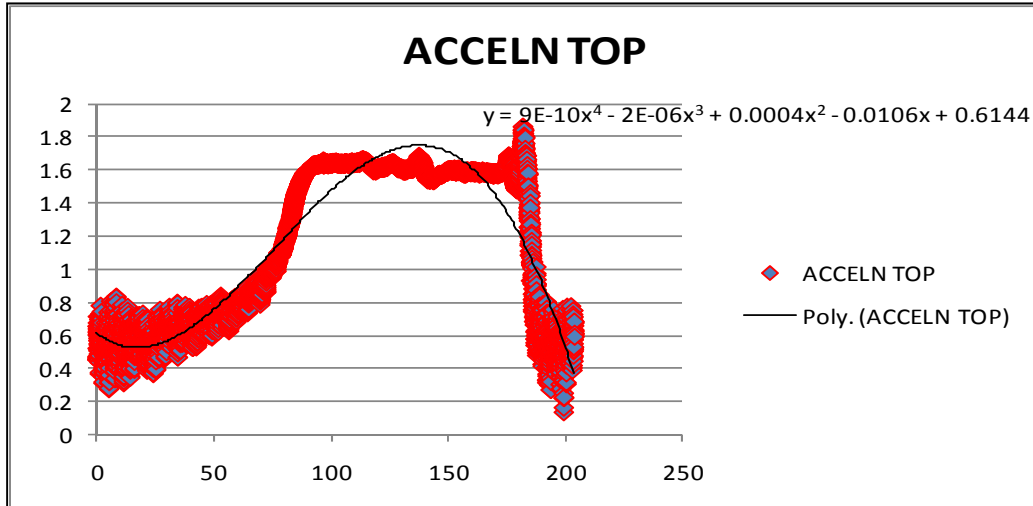
- 1) PFC Energy white paper. *Importance of the Deepwater gulf of Mexico*. February 2011.
- 2) Ove Bartland, Multiphase flow assurance, Pipe Flow 2.
- 3) Ole Jørgen Nydal, Lecture Notes for multiphase flow Handouts 2010.
- 4) Henri Cholet. *Well Production practical Handbook. New Edition*. Institut Francais Du Petrole.
- 5) Gergerly Kristof. Lecture slides on Multiphase flow modelling. Handouts 2010.
- 6) Schlumberger Online Oilfield glossary.
<http://www.glossary.oilfield.slb.com/Display.cfm?Term=flow%20regime>
- 7) Saeid Mokhatab et al. *Handbook of natural gas transmission and processing*. Gulf Professional publishing.
- 8) S.F. Ali. Two Phase Flow in Large diameter Vertical riser. PHD thesis Cranfield University.
- 9) Christopher Brennen. *Fundamentals of Multiphase Flows* Cambridge University Press.
- 10) Spedding, P. L. and Nguyen, T. Van. (1980) "Regimes for air-water two phase flow". Chemical Engineering Science, Volume 35 (4), pp. 779-793.
- 11) K. Bendiksen, D. Malnes, R. Moe, S. Nuland .*The Dynamic Two fluid model OLGA. Theory and Application* Institute for Energy Technology. SPE Production Engineering. May 1991
- 12) Yong Bai, Qiang Bai. *Subsea Pipeline and risers*. Elsevier 2005.
- 13) Petroleum and Natural gas International standardization (PNGIS) Online glossary.
http://www.pngis.net/glossary/default.asp?txtLang=English&txtSearch=riser&field_name=Term&Button=Search
- 14) Yong Bai, Qiang Bai Subsea Engineering Handbook, Elsevier 2010
- 15) C.M Larsen. Flexible riser analysis — comparison of results from computer programs. Norwegian Institute of Technology. University of Trondheim. 1992
- 16) D.Hoffman , N.M Ismail, R. Nielsen, R Chandwani .*The design of flexible marine risers in deep and shallow water*. OTC Houston May 6-9 1991
- 17) Guido Kuiper. Stability of offshore risers conveying fluid. PHD thesis. T.U Delft. January 2008

- 18) Fabre, Jean, Peresson, Lucien L., Odello, Robert *Severe Slugging in Pipeline/Riser Systems* SPE 1987.
- 19) University of Stavanger Lecture Handouts.
- 20) Boyun Guo , Shanhong song, Jacob Chacko, Ali Ghalambor. *Offshore pipelines* Gulf professional publishing. Elsevier.2005.
- 21) T. J. Hill and D.G Wood '*Slug flow occurrence, consequence and prediction*' SPE 1994.

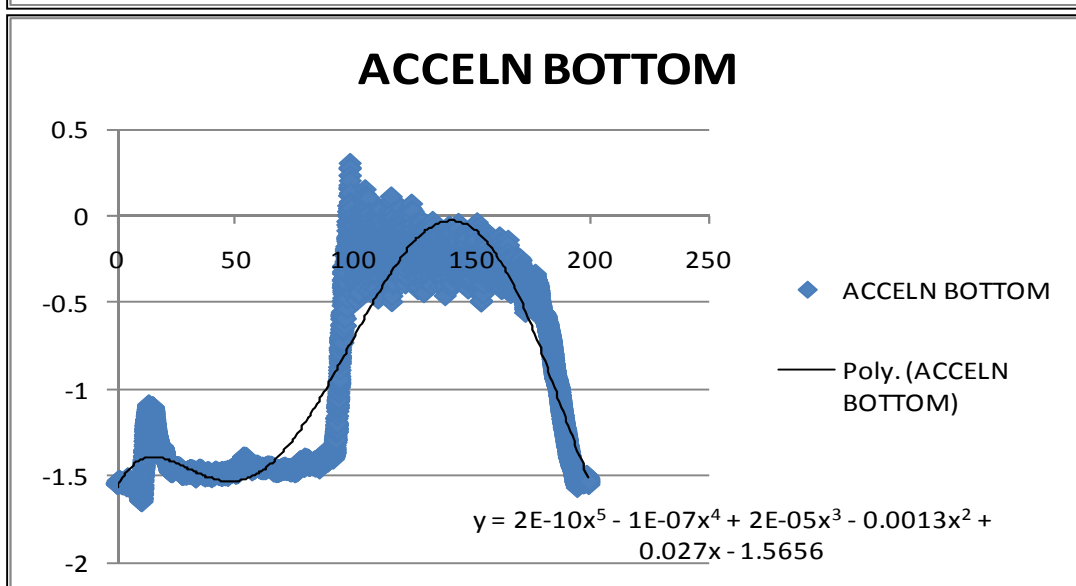
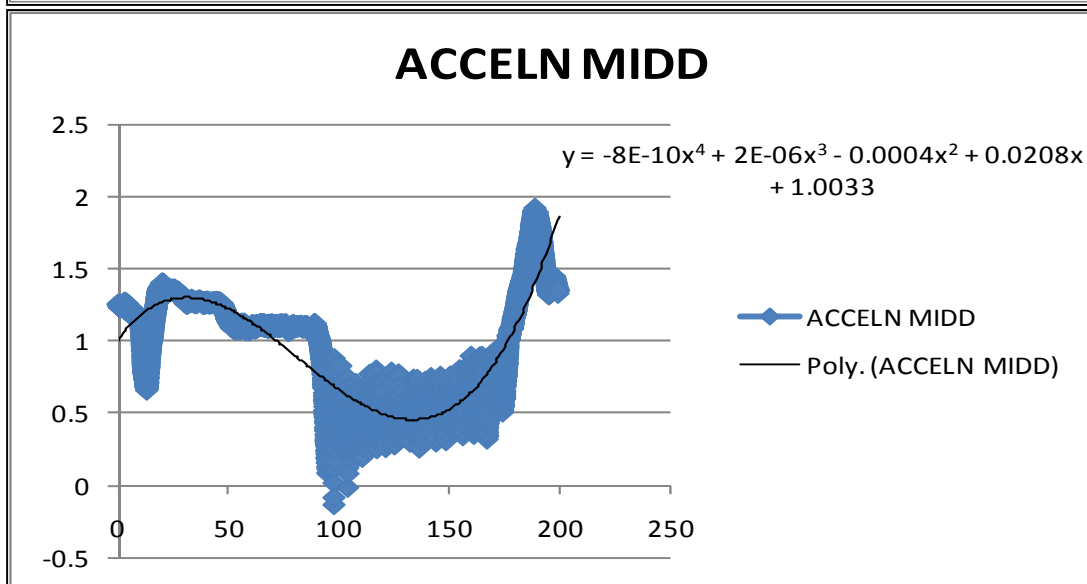
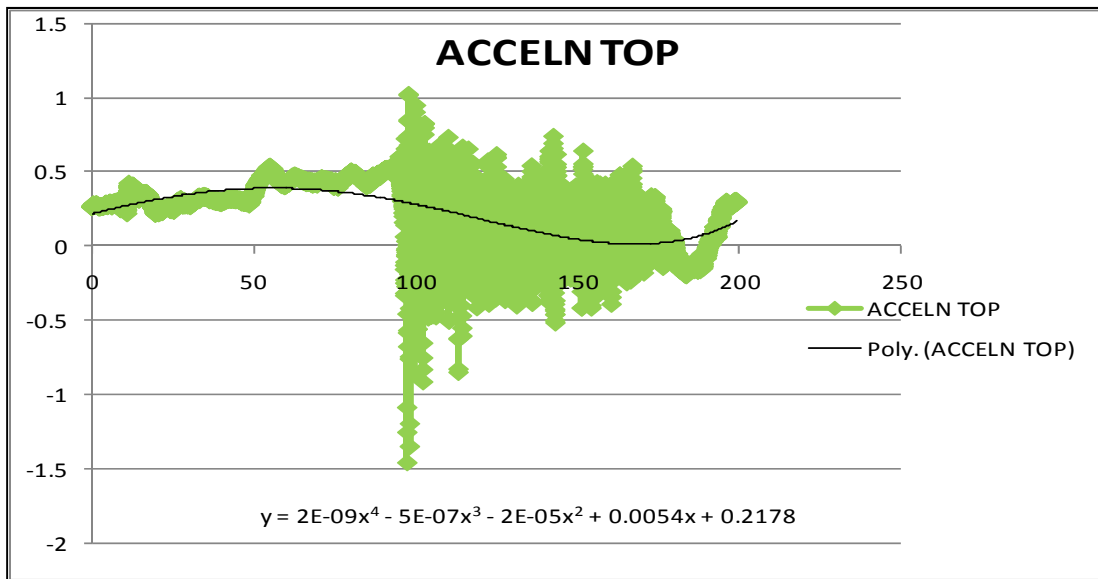
8 Appendices

APPENDIX A

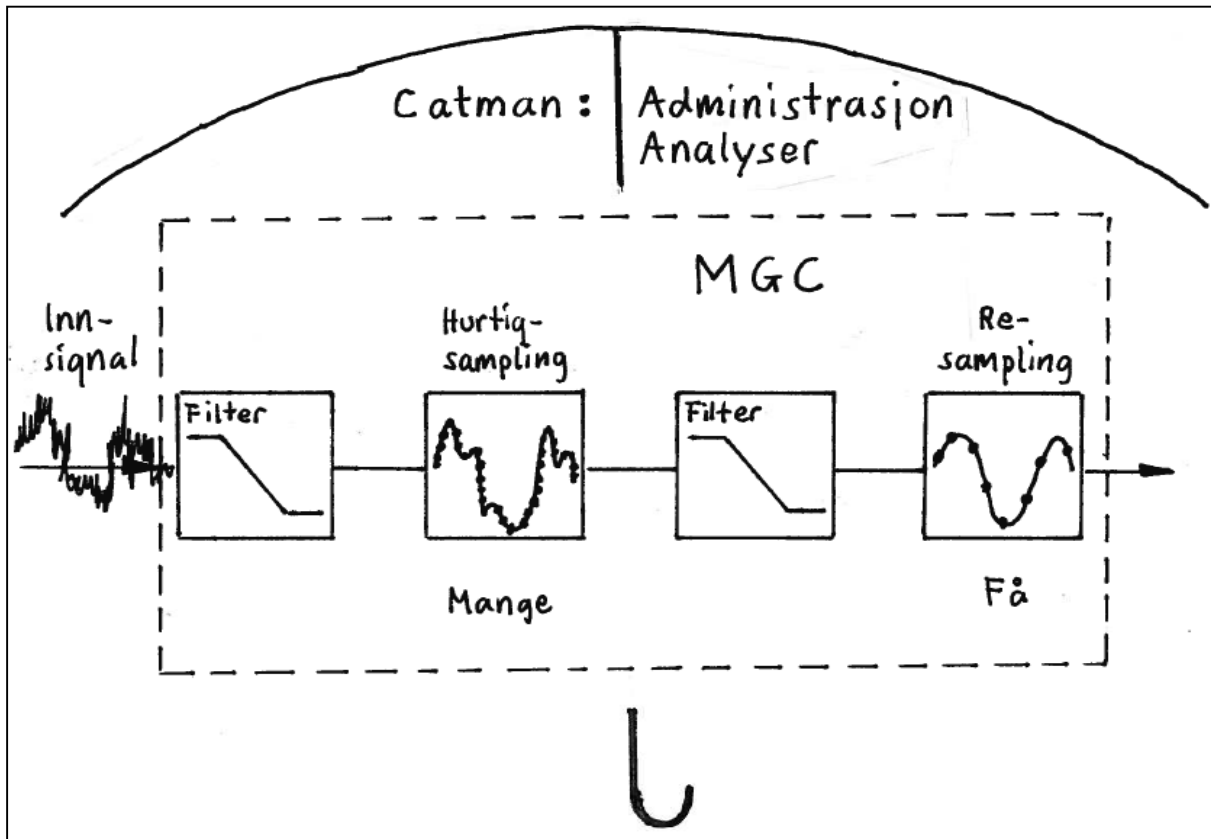
Accelerometer curves for one cycle of severe slugging in L-riser. (Top position = 179 cm, Middle position = 311 cm and Bottom position = 443 cm from the load cell along riser).



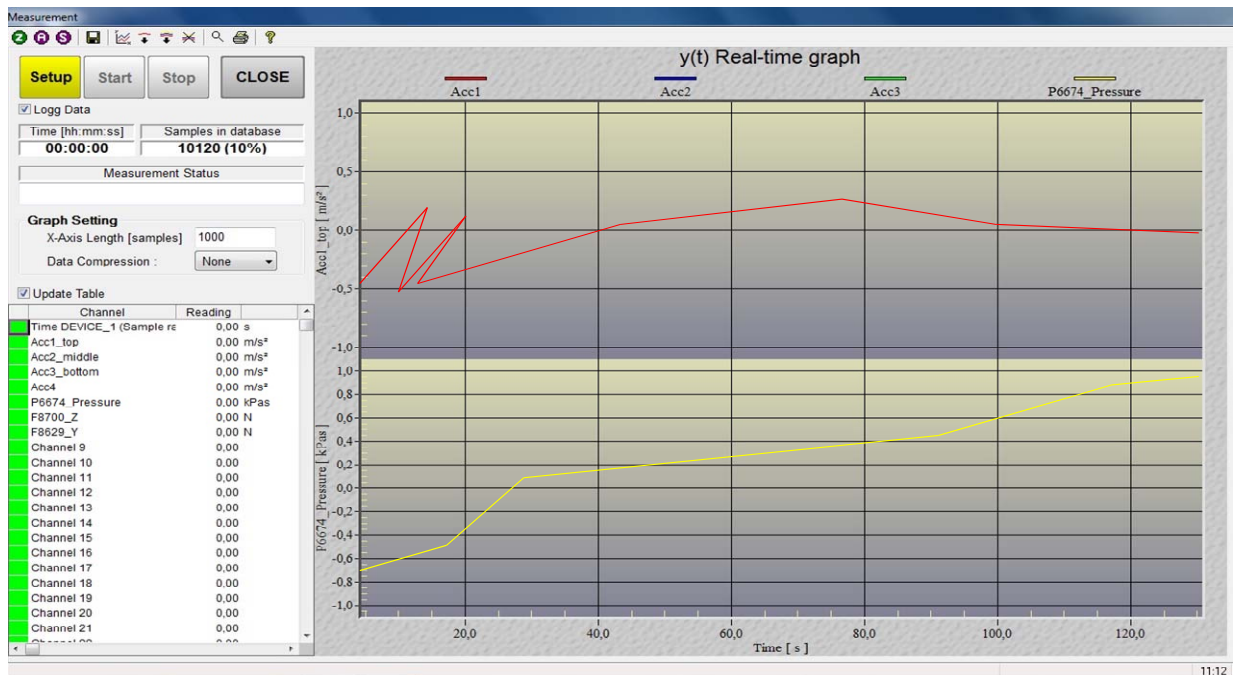
Accelerometer curves for one cycle of severe slugging in S-riser. (Top position = 147.5 cm, Middle position = 348.5 cm and Bottom position = 546.5 cm from the load cell along riser).



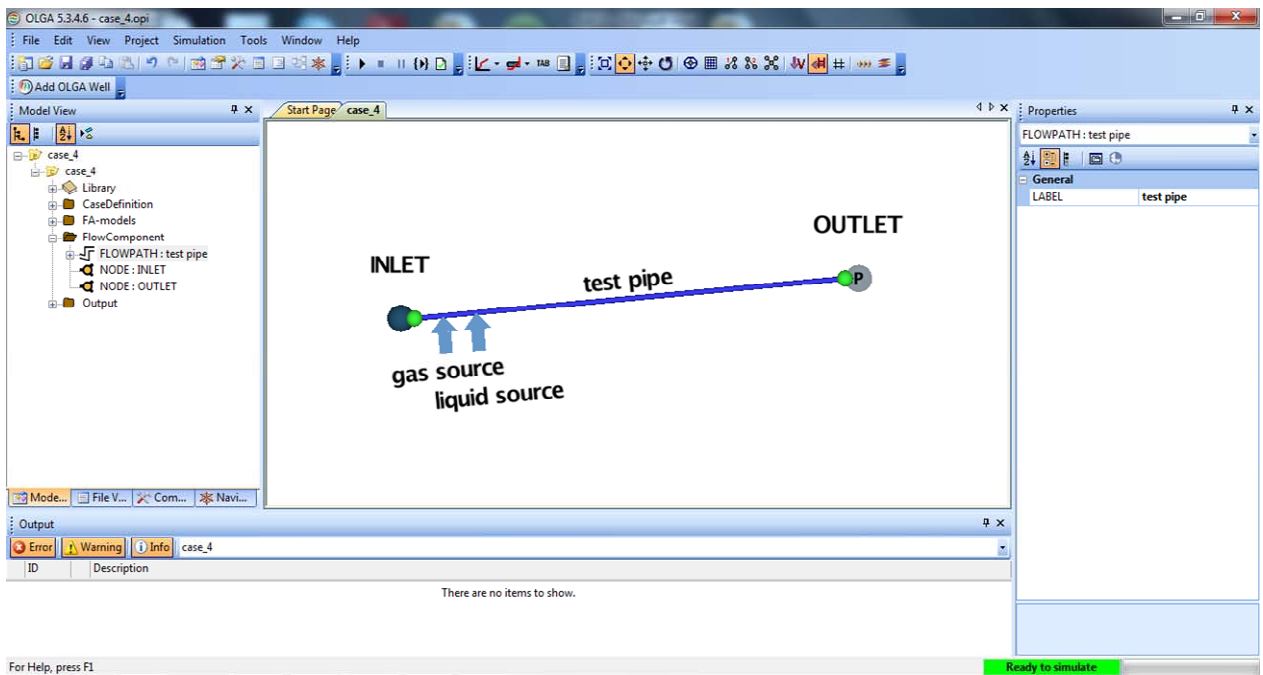
APPENDIX B



Principle for filtering and sampling with MGC plus (Source: Erik Lehn, *Tidserier, Sampling, filtering and analyse*. MarinTek. SINTEF)

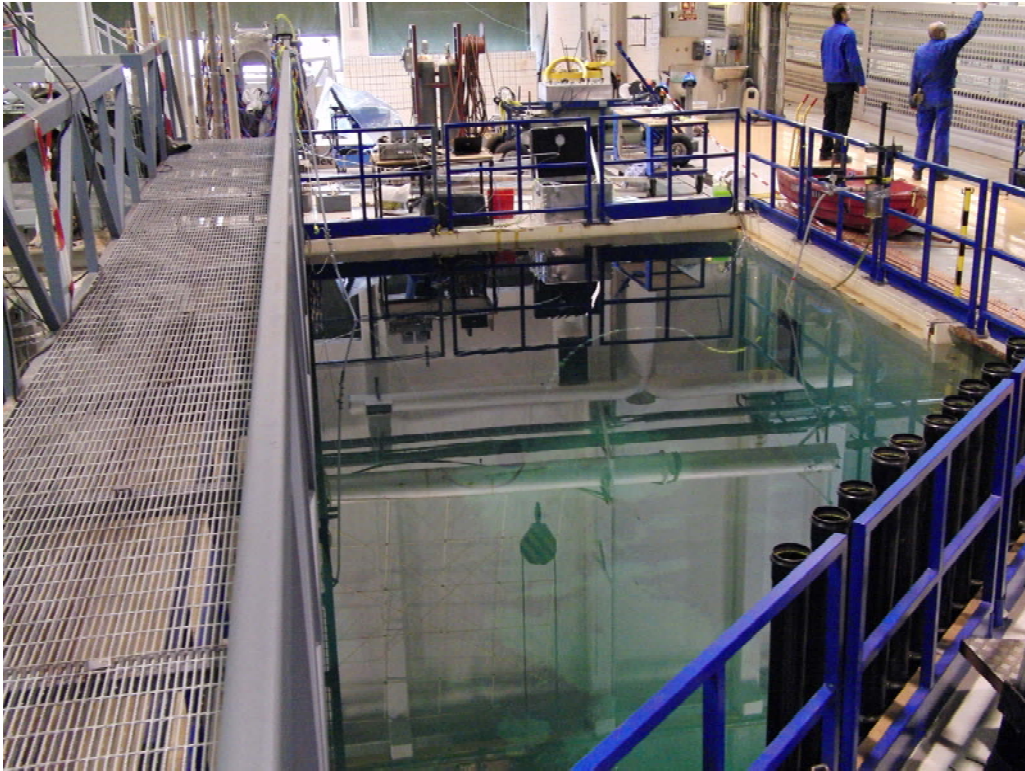


Catman Program graphic user interface (GUI)

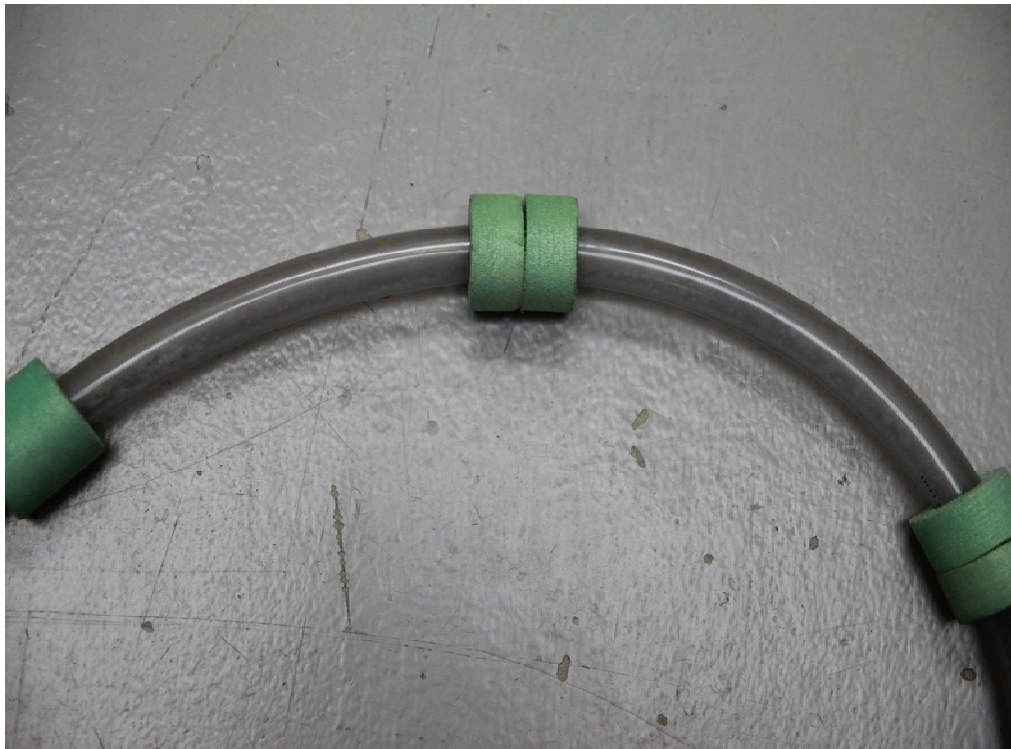


OLGA simulation tool graphic user interface (GUI)

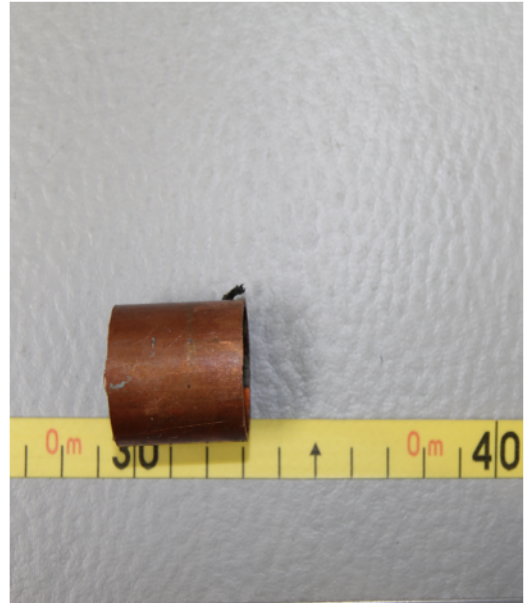
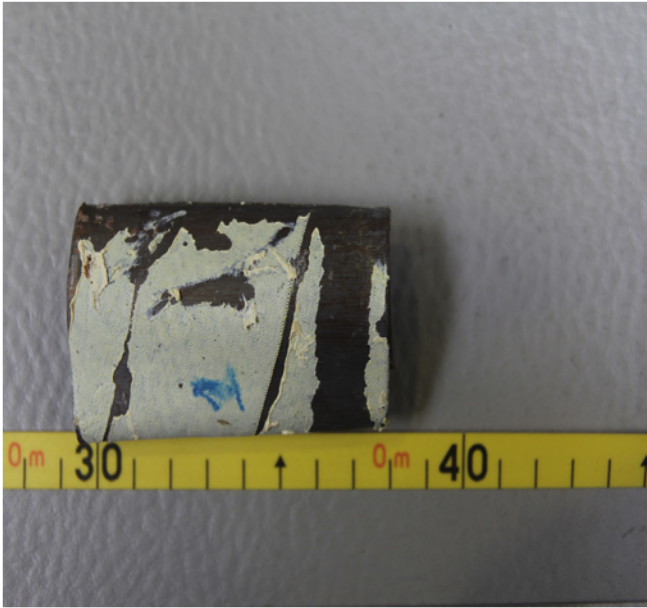
APPENDIX C



Experiment pool at MARINTEK.



Divinycell foam (buoyancy elements) on riser



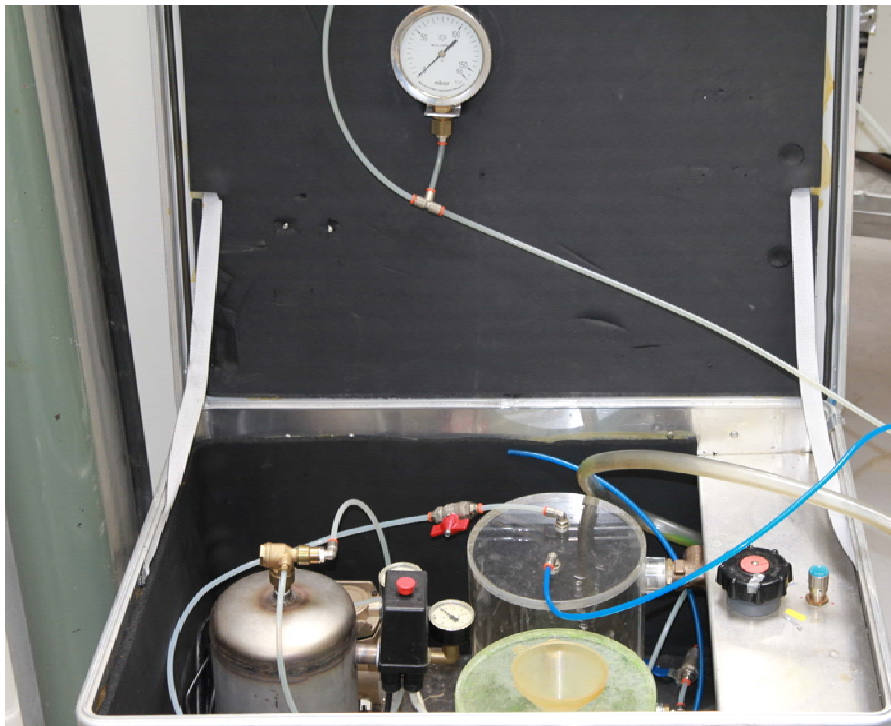
Lead and brass rings used to submerge riser



Digital (Mass Stream) and analogue (Platon) gas meter



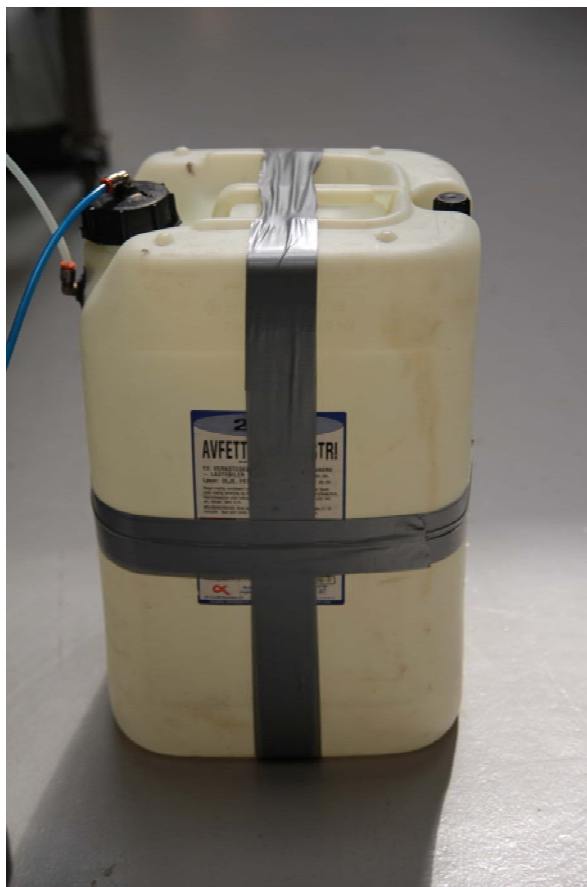
Liquid flow meter*



Mobile Two-phase flow mini loop



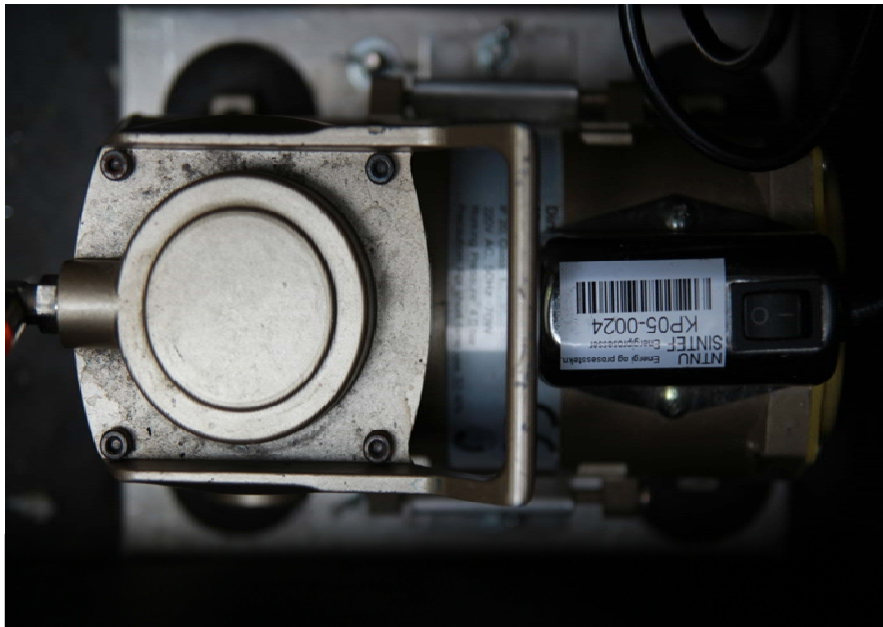
Flexible light emitting diode (LED) strip.



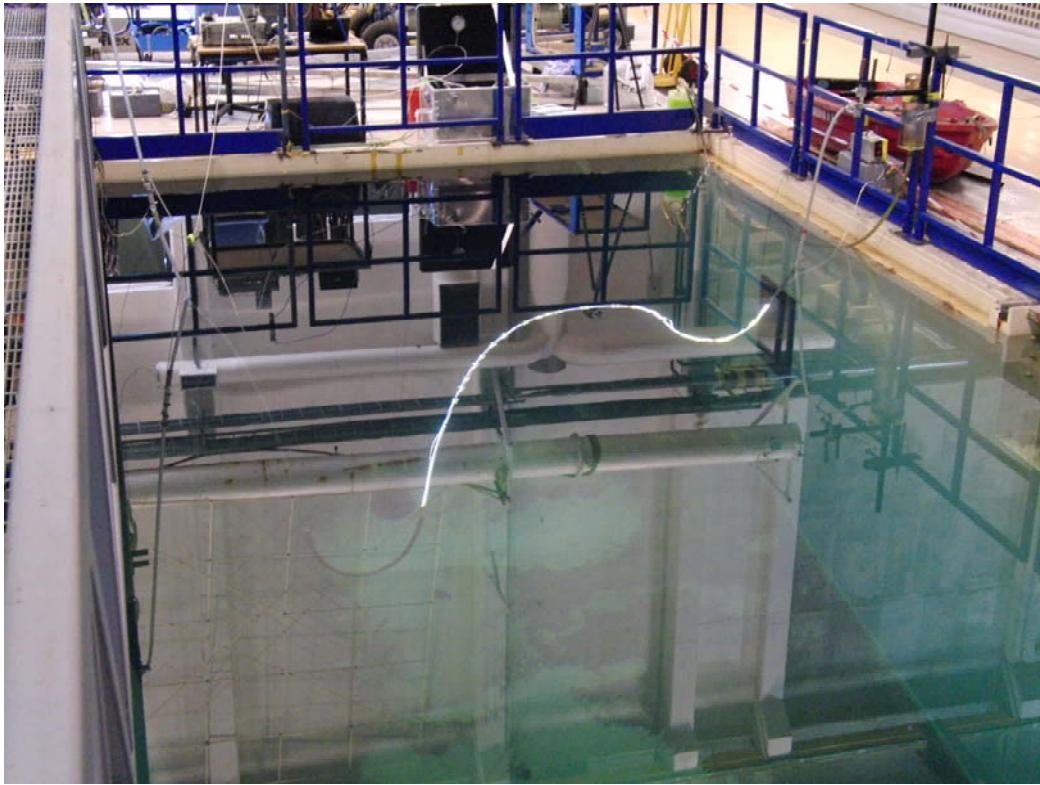
Additional compressible volume.



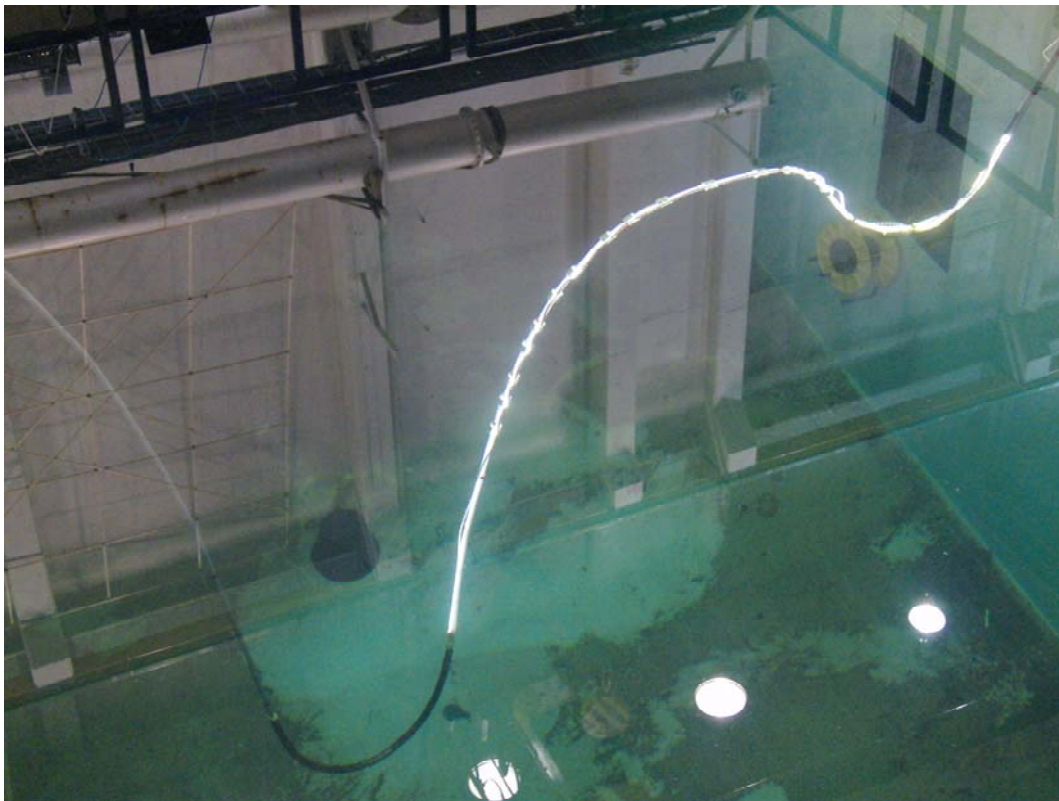
Grundfos Liquid centrifugal pump



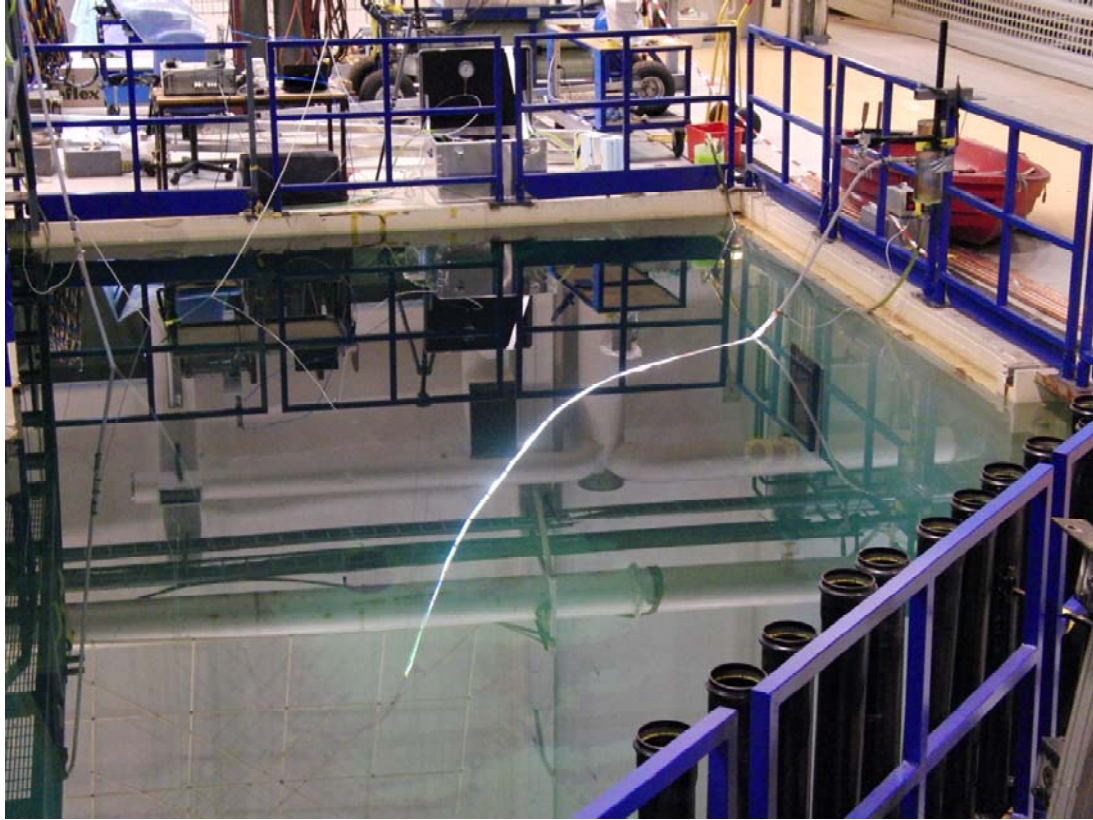
Air compressor



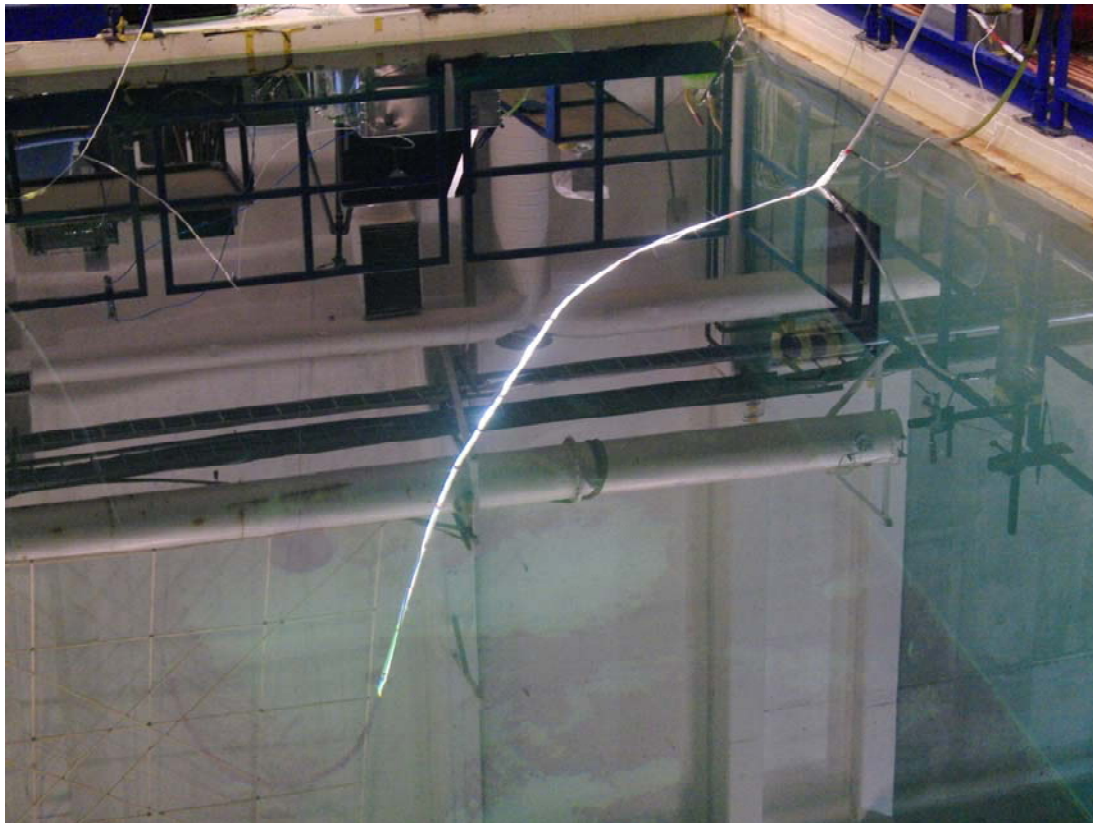
S- Riser in experiment pool.



Close Up of S-riser in experiment pool.



L-riser in experiment pool



Close up of L-riser in experiment pool.

APPENDIX D

```
!*****
!   CASE
!*****
CASE AUTHOR="ITA", \
PROJECT="L-riser"
!
!*****
!   OPTIONS
!*****
OPTIONS DEBUG=ON, SLUGVOID=AIR, TEMPERATURE=OFF, STEADYSTATE=ON
!
!*****
!   FILES
!*****
FILES PVTFILE="./air_water_15C.tab"
!
!*****
!   INTEGRATION
!*****
INTEGRATION DTSTART=1 s, ENDTIME=1000 s, MAXDT=10 s, MINDT=3.24e-005 s, STARTTIME=0 S
!
!*****
!   GEOMETRY
!*****
GEOMETRY LABEL=case_4, XSTART=0 M, YSTART=0 M, ZSTART=0 M
PIPE LABEL=PIPE-1, ROUGHNESS=1E-05 M, XEND=0.989949 M, YEND=-0.98995 M, DIAMETER=0.2
M,\
NSEGMENT=50, LSEGMENT=(0.028, 0.028, 0.028, 0.028, 0.028, 0.028, 0.028, 0.028, 0.028,\
0.028, 0.028, 0.028, 0.028, 0.028, 0.028, 0.028, 0.028, 0.028, 0.028, 0.028, 0.028,\
```



```

! TABLE
|*****
TABLE LABEL=TABLE-1, XVARIABLE=OPEN, YVARIABLE=CV
TABLE POINT=(1, 12)
!
|*****
! SLUGTRACKING
|*****
SLUGTRACKING HYDRODYNAMIC=OFF, LEVEL=OFF
!
|*****
! BOUNDARY
|*****
BOUNDARY NODE=INLET, TYPE=CLOSED
BOUNDARY NODE=OUTLET, TYPE=PRESSURE, TEMPERATURE=15 C, PRESSURE=101300 Pa
!
|*****
! INITIALCONDITIONS
|*****
INITIALCONDITIONS BRANCH=test pipe, INTEMPERATURE=15 C, OUTTEMPERATURE=15 C
!
|*****
! CONTROLLER
|*****
!
|*****
! SOURCE
|*****
SOURCE LABEL=gas source, TIME=0 s, TEMPERATURE=15 C, BRANCH=test pipe, PIPE=PIPE-1,\
SECTION=1, MASSFLOW=0.00013175 kg/s, GASFRACTION=1

```

SOURCE LABEL=liquid source, TIME=0 s, TEMPERATURE=20 C, BRANCH=test pipe, PIPE=PIPE-2,\

SECTION=1, MASSFLOW=0.08 kg/s, GASFRACTION=0, PRESSURE=0 bara

!

!*****

! OUTPUT

!*****

OUTPUT DTOUT=1 s

!

!*****

! TREND

!*****

TREND DTPLOT=1 s

TREND BRANCH=test pipe, VARIABLE=PT, PIPE=PIPE-1, SECTION=1

!

!*****

! PROFILE

!*****

PROFILE DTPLOT=1 s

PROFILE BRANCH=test pipe, VARIABLE=PT

ENDCASE

```

|*****
!
!   CASE
|*****

CASE AUTHOR="ITA", \
PROJECT="S-riser"
!
|*****

!   OPTIONS
|*****

OPTIONS DEBUG=ON, SLUGVOID=AIR, TEMPERATURE=OFF, STEADYSTATE=ON
!
|*****

!   FILES
|*****

FILES PVTFILE="./air_water_15C.tab"
!
|*****

!   INTEGRATION
|*****

INTEGRATION DTSTART=1 s, ENDTIME=1000 s, MAXDT=10 s, MINDT=3.24e-005 s, STARTTIME=0 S
!
|*****

!   GEOMETRY
|*****

GEOMETRY LABEL=case_4, XSTART=0 M, YSTART=0 M, ZSTART=0 M

PIPE LABEL=PIPE-1, ROUGHNESS=1E-05 M, XEND=0.989949 M, YEND=-0.98995 M, DIAMETER=0.2
M,\

    NSEGMENT=10, LSEGMENT=(0.14, 0.14, 0.14, 0.14, 0.14, 0.14, 0.14, 0.14, 0.14, 0.14) M

PIPE LABEL=PIPE-2, ROUGHNESS=1E-05 M, XEND=1.9866 M, YEND=-6.6429 M, DIAMETER=0.016 M,\

    NSEGMENT=70, LSEGMENT=(0.0820019, 0.0820019, 0.0820019, 0.0820019, 0.0820019,
0.0820019,\

```

0.0820019, 0.0820019, 0.0820019, 0.0820019, 0.0820019, 0.0820019, 0.0820019, 0.0820019, \
 0.0820019, 0.0820019, 0.0820019, 0.0820019, 0.0820019, 0.0820019, 0.0820019, 0.0820019, \
 0.0820019, 0.0820019, 0.0820019, 0.0820019, 0.0820019, 0.0820019, 0.0820019, 0.0820019, \
 0.0820019, 0.0820019, 0.0820019, 0.0820019, 0.0820019, 0.0820019, 0.0820019, 0.0820019, \
 0.0820019, 0.0820019, 0.0820019, 0.0820019, 0.0820019, 0.0820019, 0.0820019, 0.0820019, \
 0.0820019, 0.0820019, 0.0820019, 0.0820019, 0.0820019, 0.0820019, 0.0820019, 0.0820019, \
 0.0820019, 0.0820019, 0.0820019, 0.0820019, 0.0820019, 0.0820019, 0.0820019, 0.0820019, \
 0.0820019, 0.0820019, 0.0820019, 0.0820019, 0.0820019, 0.0820019, 0.0820019, 0.0820019) M

PIPE LABEL=PIPE-3, ROUGHNESS=1E-05 M, XEND=2.18035 M, YEND=-6.978 M, DIAMETER=0.016 M, \
 NSEGMENT=5, LSEGMENT=(0.07741603774412667, 0.077416037744126559, \
 0.077416037744126559, \
 0.077416037744126559, 0.077416037744126559) M

PIPE LABEL=PIPE-4, ROUGHNESS=1E-05 M, XEND=2.95535 M, YEND=-6.978 M, DIAMETER=0.016 M, \
 NSEGMENT=10, LSEGMENT=(0.077500000000000124, 0.077500000000000124, \
 0.077500000000000124, \
 0.077500000000000124, 0.077500000000000124, 0.077500000000000124, \
 0.077500000000000124, \
 0.077500000000000124, 0.077500000000000124, 0.077500000000000124) M

PIPE LABEL=PIPE-5, ROUGHNESS=1E-05 M, XEND=3.1491 M, YEND=-6.6424 M, DIAMETER=0.016 M, \
 NSEGMENT=5, LSEGMENT=(0.0775026251168307, 0.0775026251168307, 0.0775026251168307, \
 0.0775026251168307, 0.0775026251168307) M

PIPE LABEL=PIPE-6, ROUGHNESS=1E-05 M, XEND=3.5085 M, YEND=-4.604 M, DIAMETER=0.016 M, \
 NSEGMENT=20, LSEGMENT=(0.10349206394695179, 0.10349206394695179, \
 0.10349206394695179, \
 0.10349206394695179, 0.10349206394695179, 0.10349206394695179, 0.10349206394695179, \
 0.10349206394695179, \
 0.10349206394695179, 0.10349206394695179, 0.10349206394695179, 0.10349206394695179, \
 0.10349206394695179, \
 0.10349206394695179, 0.10349206394695179, 0.10349206394695179, 0.10349206394695179, \
 0.10349206394695179) M

PIPE LABEL=PIPE-7, ROUGHNESS=1E-05 M, XEND=3.7385 M, YEND=-4.2056 M, DIAMETER=0.016 M, \
 NSEGMENT=25, LSEGMENT=(0.018401, 0.018401, 0.018401, 0.018401, 0.018401, 0.018401, \
 0.018401, \
 0.018401, 0.018401, 0.018401, 0.018401, 0.018401, 0.018401, 0.018401, 0.018401, \
 0.018401, \
 0.018401, 0.018401, 0.018401, 0.018401, 0.018401, 0.018401, 0.018401, 0.018401, \
 0.018401) M

0.018401, 0.018401, 0.018401, 0.018401, 0.018401, 0.018401, 0.018401, 0.018401, 0.018401, \

0.018401) M

PIPE LABEL=PIPE-8, ROUGHNESS=1E-05 M, XEND=4.1985 M, YEND=-4.2056 M, DIAMETER=0.016 M, \

NSEGMENT=20, LSEGMENT=(0.023, 0.023, 0.023, 0.023, 0.023, 0.023, 0.023, 0.023, 0.023, \

0.023, 0.023, 0.023, 0.023, 0.023, 0.023, 0.023, 0.023, 0.023, 0.023) M

PIPE LABEL=PIPE-9, ROUGHNESS=1E-05 M, XEND=4.6585 M, YEND=-5 M, DIAMETER=0.016 M, \

NSEGMENT=20, \

LSEGMENT=(0.045898566426414496, 0.045898566426414496, 0.045898566426414496, \

0.045898566426414496, \

0.045898566426414496, 0.045898566426414496, 0.045898566426414496, \

0.045898566426414496, \

0.045898566426414496, 0.045898566426414496, 0.045898566426414496, \

0.045898566426414496, \

0.045898566426414496, 0.045898566426414496, 0.045898566426414496, \

0.045898566426414496, \

0.045898566426414496, 0.045898566426414496, 0.045898566426414496, \

0.045898566426414496) M

PIPE LABEL=PIPE-10, ROUGHNESS=1E-05 M, XEND=4.7285 M, YEND=-5.1212 M, DIAMETER=0.016 \

M, \

NSEGMENT=5, LSEGMENT=(0.027992456126606641, 0.027992456126606641, \

0.027992456126606641, \

0.027992456126606641, 0.027992456126606641) M

PIPE LABEL=PIPE-11, ROUGHNESS=1E-05 M, XEND=5.0085 M, YEND=-5.1212 M, DIAMETER=0.016 \

M, \

NSEGMENT=10, LSEGMENT=(0.02799999999999581, 0.02799999999999581, \

0.02799999999999581, \

0.02799999999999581, 0.02799999999999581, 0.02799999999999581, \

0.02799999999999581, \

0.02799999999999581, 0.02799999999999581, 0.02799999999999581) M

PIPE LABEL=PIPE-12, ROUGHNESS=1E-05 M, XEND=5.0785 M, YEND=-5 M, DIAMETER=0.016 M, \

NSEGMENT=10, LSEGMENT=(0.0139962, 0.0139962, 0.0139962, 0.0139962, 0.0139962, 0.0139962, \

0.0139962, 0.0139962, 0.0139962, 0.0139962) M

PIPE LABEL=PIPE-13, ROUGHNESS=1E-05 M, XEND=5.4266 M, YEND=-3.0254 M, DIAMETER=0.016 \

M, \

NSEGMENT=60, LSEGMENT=(0.033417472018558284, 0.033417472018558284, \

0.033417472018558284, \

0.033417472018558284, 0.033417472018558284, 0.033417472018558284,
0.033417472018558284,\

0.033417472018558284, 0.033417472018558284, 0.033417472018558284,
0.033417472018558284,\

0.033417472018558284, 0.033417472018558284, 0.033417472018558284,
0.033417472018558284,\

0.033417472018558284, 0.033417472018558284, 0.033417472018558284,
0.033417472018558284,\

0.033417472018558284, 0.033417472018558284, 0.033417472018558284,
0.033417472018558284,\

0.033417472018558284, 0.033417472018558284, 0.033417472018558284,
0.033417472018558284,\

0.033417472018558284, 0.033417472018558284, 0.033417472018558284,
0.033417472018558284,\

0.033417472018558284, 0.033417472018558284, 0.033417472018558284,
0.033417472018558284,\

0.033417472018558284, 0.033417472018558284, 0.033417472018558284,
0.033417472018558284,\

0.033417472018558284, 0.033417472018558284, 0.033417472018558284,
0.033417472018558284,\

0.033417472018558284, 0.033417472018558284, 0.033417472018558284,
0.033417472018558284,\

0.033417472018558284, 0.033417472018558284, 0.033417472018558284,
0.033417472018558284,\

0.033417472018558284, 0.033417472018558284, 0.033417472018558284,
0.033417472018558284,\

0.033417472018558284, 0.033417472018558284, 0.033417472018558284,
0.033417472018558284,\

0.033417472018558284) M

PIPE LABEL=PIPE-14, ROUGHNESS=1E-05 M, XEND=5.4266 M, YEND=-2.8354 M, DIAMETER=0.016
M,\

NSEGMENT=10, LSEGMENT=(0.019, 0.019, 0.019, 0.019, 0.019, 0.019, 0.019, 0.019, 0.019,\

0.019) M

PIPE LABEL=PIPE-15, ROUGHNESS=1E-05 M, XEND=5.6266 M, YEND=-2.8354 M, DIAMETER=0.016
M,\

NSEGMENT=10, LSEGMENT=(0.02000000000000462, 0.01999999999999574,
0.01999999999999574,\

0.019999999999999574, 0.019999999999999574, 0.019999999999999574,
0.019999999999999574,\

0.019999999999999574, 0.019999999999999574, 0.019999999999999574) M

!*****

! NODE

!*****

NODE LABEL=INLET, TYPE=TERMINAL

NODE LABEL=OUTLET, TYPE=TERMINAL

!

!*****

! BRANCH

!*****

BRANCH LABEL=test pipe, FROM=INLET, TO=OUTLET, GEOMETRY=case_4, FLUID="luft_vann"

!

!*****

! TABLE

!*****

TABLE LABEL=TABLE-1, XVARIABLE=OPEN, YVARIABLE=CV

TABLE POINT=(1, 12)

!

!*****

! SLUGTRACKING

!*****

SLUGTRACKING HYDRODYNAMIC=OFF, LEVEL=OFF

!

!*****

! BOUNDARY

!*****

BOUNDARY NODE=INLET, TYPE=CLOSED

BOUNDARY NODE=OUTLET, TYPE=PRESSURE, TEMPERATURE=15 C, PRESSURE=101300 Pa

!

```

|*****
!  INITIALCONDITIONS
|*****

INITIALCONDITIONS BRANCH=test pipe, INTEMPERATURE=15 C, OUTTEMPERATURE=15 C

!

|*****

!  CONTROLLER
|*****

!

|*****

!  SOURCE
|*****

SOURCE LABEL=gas source, TIME=0 s, TEMPERATURE=15 C, BRANCH=test pipe, PIPE=PIPE-1,\
SECTION=1, MASSFLOW=0.000135 kg/s, GASFRACTION=1

SOURCE LABEL=liquid source, TIME=0 s, TEMPERATURE=20 C, BRANCH=test pipe, PIPE=PIPE-2,\
SECTION=1, MASSFLOW=0.05675 kg/s, GASFRACTION=0, PRESSURE=0 bara

!

|*****

!  OUTPUT
|*****

OUTPUT DTOUT=1 s

!

|*****

!  TREND
|*****

TREND DTPLOT=1 s

TREND BRANCH=test pipe, VARIABLE=PT, PIPE=PIPE-1, SECTION=1

!

|*****

!  PROFILE

```

|*****

PROFILE DTPLT=1 s

PROFILE BRANCH=test pipe, VARIABLE=PT

ENDCASE

```

PVTTABLE LABEL = "luft_vann",PHASE = TWO,\
COMPONENTS = ("H2O","AIR"),\
MOLWEIGHT = (18.02,28,97) g/mol,\
STDPRESSURE = 1.0 ATM,\
STDTEMPERATURE = 293.16 K,\
GOR = -999 Sm3/Sm3,\
GLR = -999 Sm3/Sm3,\
STDGASDENSITY = 1.204 kg/m3,\
STDOILDENSITY = 998 kg/m3,\
MESHTYPE = STANDARD,\
PRESSURE = ( 1.00E+01 , 1.00E+06) Pa,\
TEMPERATURE = ( 13 , 17 ) C,\
COLUMNS = ( PT , TM , ROG , ROHL , DROGDP , DROHLDP , DROGDT , DROHLDT ,
RS , VISG , VISHL , CPG , CPHL , HG , HHL , TCG , TCHL , SIGGHL , SEG , SEHL )
PVTTABLE POINT = ( 1.00E+01 , 13 , 1.21767E-04 , 998.78 , 1.21767E-05 , 0.0 , -4.25521E-07 , 0.0
, 100 , 1.7965E-05 , 1.108E-03 , 1.0059E+03 , 4.0819E+03 , 0 , 0 , 2.5219E-02 , 5.9678E-01 , 7.35E-
02 , 0 , 0 )
PVTTABLE POINT = ( 1.00E+01 , 17 , 1.20088E-04 , 998.78 , 1.20088E-05 , 0.0 , -4.13869E-07 , 0.0
, 100 , 1.7965E-05 , 1.108E-03 , 1.0059E+03 , 4.0819E+03 , 0 , 0 , 2.5219E-02 , 5.9678E-01 , 7.35E-
02 , 0 , 0 )
PVTTABLE POINT = ( 1.00E+06 , 13 , 1.21767E+01 , 998.78 , 1.21767E-05 , 0.0 , -4.25521E-02 , 0.0
, 100 , 1.7965E-05 , 1.108E-03 , 1.0059E+03 , 4.0819E+03 , 0 , 0 , 2.5219E-02 , 5.9678E-01 , 7.35E-
02 , 0 , 0 )
PVTTABLE POINT = ( 1.00E+06 , 17 , 1.20088E+01 , 998.78 , 1.20088E-05 , 0.0 , -4.13869E-02 , 0.0
, 100 , 1.7965E-05 , 1.108E-03 , 1.0059E+03 , 4.0819E+03 , 0 , 0 , 2.5219E-02 , 5.9678E-01 , 7.35E-
02 , 0 , 0 )

```

APPENDIX E

Microsoft Excel sheets of the logged data and video recordings have been attached on a digital video disc (DVD).